63-3-3

REIC Report No. 26
April 19, 1963

TRANSIENT RADIATION EFFECTS ON ELECTRONIC COMPONENTS AND SEMICONDUCTOR DEVICES

734 000

RADIATION EFFECTS INFORMATION CENTER
Battelle Memorial Institute
Columbus 1, Ohio

(4)
$4.60

The Radiation Effects Information Center has been established at Battelle Memorial Institute by the United States Air Force to provide a means of placing radiation-effects data in the hands of designers and those involved in research and development. Access to the Center and to its reports is obtained through the Air Force. This report has been prepared pursuant to the provisions of Contract No. AF 33(657)-10085, Task No. 738103, Project Nos. 7381 and 7634.

REIC Report No. 26
April 1963

Report on

TRANSIENT RADIATION EFFECTS ON ELECTRONIC COMPONENTS AND SEMICONDUCTOR DEVICES

by

D. C. Jones, F. J. Reid, W. E. Chapin,
D. J. Hamman, and E. N. Wyler

AERONAUTICAL SYSTEMS DIVISION

AIR FORCE SYSTEMS COMMAND

RADIATION EFFECTS INFORMATION CENTER
Battelle Memorial Institute
Columbus 1, Ohio

ABSTRACT

This report summarizes the information that was available before 1962 concerning the effects of nuclear-weapon-burst and simulated-burst radiation on electronic components and semiconductor devices. This work reports only the effects observed in components that are due to gamma rays and/or neutrons of a transient radiation environment.

A

TABLE OF CONTENTS

LIST OF FIGURES

TABLE OF CONTENTS

LIST OF FIGURES

LIST OF FIGURES
(Continued)

LIST OF TABLES

LIST OF TABLES
(Continued)

Report on

TRANSIENT RADIATION EFFECTS ON ELECTRONIC COMPONENTS AND SEMICONDUCTOR DEVICES

SUMMARY AND CONCLUSIONS

This report summarizes the information that was available before 1962 concerning the effects of nuclear-weapon-burst and simulated-burst radiation on electronic components and semiconductor devices. Most of the data in this report were obtained from simulation facilities.

The effects observed in electronic components exposed to a transient radiation environment are primarily due to the gamma-ray exposure rate or integrated neutron flux. The effect caused by the gamma exposure rate can be considered as transient, though some component parameter changes may take hours for recovery. Permanent damage that is observed in semiconductor devices is attributed to the integrated neutron flux and is not considered in this report.

The results of studies on semiconductor devices have shown that the production of excess electrons and holes in semiconductor materials is particularly important because the p-n junction can separate the pairs, thus allowing an excess current to flow. Hence in a reverse-biased diode, a larger-than-normal current will be produced when it is exposed to ionizing radiation. In fact, a leakage current will be observed in a passive diode upon bombardment with ionizing radiation. Similarly, a transistor, which normally exhibits a small collector current (I_{CO}) when the collector junction is reverse biased and the emitter is open circuited, can experience large I_{CO} values when exposed to ionizing radiation.

The description and prediction of the radiation-generated currents in semiconductors induced by ionizing radiation are essentially the same for all types of junction devices regardless of whether they are audio, high-frequency, power, or switching transistors; audio, microwave, Esaki, or switching diodes; rectifiers; infrared detectors; or solar, photovoltaic, or photoconductive cells. The degree to which these excess currents affect the operation of the junction device will depend on the function of the device.

The differences reported concerning the transient radiation effects on cables have indicated that much more study and research are needed before cable effects can be adequately predicted. Because of the lack of understanding of cable effects, data generated on components, such as resistors, are somewhat masked since the effects in the measuring cable cannot be separated from the total effect to obtain the component effect.

The transient radiation effect on electron tubes is of a transient nature. The seriousness of the effect depends on the type of tube and its application. The observed effect of transient radiation in many types of electron tubes could be considered insignificant when compared to the tolerances of the circuit and the magnitude of the radiation effects on other components in the same circuit. Because of the small sample size (in most cases) and inaccurate data, there is little evidence to support any hypothesis regarding transient radiation effects on electron tubes. However, it seems reasonable to assume that the effects commonly induced in vacuum tubes by transient radiation are those arising from (1) induced grid charge,(2) gas evolution from elements and walls, (3) decrease in conductivity of insulators, and/or (4) ionization of residual gases.

Two types of thyratron tubes are exceptions to the general case for electron tubes in that there is a considerable amount of transient-radiation-effects data of relatively recent origin (1960, 1961). These transient-radiation-effect data on thyratron tubes support the hypothesis that the gamma exposure rate necessary to fire a thyratron is a function of the negative excess bias, E_{cgx}. This negative excess bias is simply

$$E_{cgx} = E_{cc} - E_{cg} \quad ,$$

where E_{cc} is the applied grid bias and E_{cg} is the critical grid bias for the plate voltage used when the screen grid is tied to the cathode. For 2D21 thyratron the E_{cgx} is approximately equal to (1.55×10^{-9}) (gamma exposure rate in ergs g-1(C)).

The transient radiation effects on resistors are still not fully understood, partially because of the inability to separate the cable and resistor effects. However, the available data give some insight into the transient radiation effects on resistors.

The cause of the effect observed when a resistor is exposed to a pulse of radiation is generally explained in two ways:

(1) A shunt leakage path is produced by the radiation-induced ionization, and/or

(2) An ejection current that is caused by electrons flowing from ground to replace the electrons ejected by radiation (Compton scattering effect).

Neither of the two hypotheses dictate that the observed change results in an actual resistance change.

Most of the research on capacitors has been concerned with the transient current flow through a capacitor when exposed to a pulse of radiation. Generally, the current pulse is considered to result from a decreased leakage resistance which is believed to result from an increase in dielectric conductivity. This increase in the dielectric conductivity is the transient radiation effect of greatest consequence observed in capacitors.

In order to present the effects of transient radiation on capacitors in a form suitable for analysis, two methods have been developed. IBM has assumed that the radiation effect can be considered as a current generator such that this current is proportional, for a given capacitor and applied voltage, to the radiation exposure. The Boeing Company assumes that the radiation effect can be considered as a change in shunt resistance.

Quartz crystals, when exposed to the various gamma-radiation burst levels, do not change systematically, and the manufacturing processes and crystal cuts influence the results. The data show that the crystals of the type studied are susceptible to radiation damage since approximately 20 per cent were rendered inoperable.

Magnetic devices appear not to be significantly affected when exposed to a nuclear environment that is equivalent to that produced by the Sandia Pulsed Reactor.

Data on other components and subsystems exposed to transient radiation are extremely limited and should be considered questionable.

INTRODUCTION

An attempt has been made to present the information contained in this report in a concise fashion that lends itself to maximum use by the design engineer. Data concerning exposure rates and total exposure have been converted to common units for ease of comparison. Neutron fields and exposure rates are described as nv_o for thermal neutrons and n cm^{-2} sec^{-1} for fast neutrons. The corresponding time-integrated exposures are described by $(nv_o)t$ and n cm^{-2}. Where information is available, an additional statement defining the energy or energy distribution of the flux is presented. All gamma exposures are reported in terms of the field, with units being ergs per gram referenced to carbon [ergs $g^{-1}(C)$]. Factors used in converting reported gamma exposures to ergs $g^{-1}(C)$ are as follows:

To Convert	To	Multiply By
Ev g^{-1}	ergs $g^{-1}(C)$	1.6×10^{12}
Roentgen	ergs $g^{-1}(C)$	87.7
Rep	ergs $g^{-1}(C)$	84.6
Rad (tissue)	ergs $g^{-1}(C)$	90.9
Rad (water)	ergs $g^{-1}(C)$	90.0
*Mev cm^{-2}	ergs $g^{-1}(C)$	4.5×10^{8}
*Photons cm^{-2}	ergs $g^{-1}(C)$	4.5×10^{8}

*Assumed average energy of 1 Mev.

INTERACTIONS OF RADIATION WITH MATTER

Effects on Solids

Transient radiation effects on solids will, in this discussion on solids and the following discussions on electronic components, be considered as phenomena associated with the excitation and de-excitation of electrons in solids. Transient effects, therefore, will not include displacement radiation effects, in which atoms are displaced from their normal lattice sites in crystals or their normal position in molecules.

Particle radiation, such as by neutrons, protons, and electrons, which produces displacement effects is a serious source of damage in semiconductors and in other materials having electrical properties which depend critically on atomic structure. Displacement effects are also important in the structural damage produced in metals. Ionizing radiation, such as by gamma rays, protons, and electrons, can deposit energy through a large volume of a solid, producing changes in the chemical bonding of the material, and thus leading to changes in the physical properties of materials. This type of damage is most common in organic materials such as those used in dielectrics and

chemical binders for various electronic components. On the other hand, when ionizing radiation is present in high intensities, free electrons resulting from the ionization can temporarily produce substantial changes in the electrical properties of solids, or transient radiation effects. Therefore, in general, the study of transient radiation effects is taken to be a study of ionization phenomena or, in the language of solid-state physics, carrier generation.

For charged-particle irradiations, most of the energy loss appears as ionization in the target material. Nuclear-physics research has shown that the number of electrons ionized is a function of the total amount of energy deposited. In gases, ionization efficiencies of 25 to 45 ev per electron-ion pair have been measured. In semiconductors this efficiency appears to be between 3 and 4 ev per electron-hole pair. On the basis of the relative ionization potentials, the energy lost per electron ionized in any material can be approximated as 2 to 4 times the ionization potential of the material. In applying this rule of thumb to a solid-state material, the ionization potential is interpreted to be the forbidden energy gap.[1]*

For gamma irradiations almost all of the energy of the incident gamma rays is converted into electrons by photoelectric, Compton, or pair-production events. Hence, the gamma-ray energy is dissipated via ionization and results in electron-ion production similar to that produced by electrons having energies somewhat less than the gamma-ray energy.

Fast neutrons, on the other hand, interact with matter primarily via elastic scattering from nuclei in the short-range nuclear force field. On the average, a neutron imparts to a target atom an energy equal to 1/A times the neutron energy, where A is the atomic-mass number of the atom. For medium- or heavy-mass elements and typical reactor fast neutrons, the resulting atom moves at a velocity which is considerably less than that of the outermost orbital electrons. Hence, the atom is not expected to be ionized and should lose energy primarily via elastic collisions with other atoms in the solid. As a result, only a small fraction of a neutron's energy eventually appears as ionization, and a neutron is therefore relatively inefficient in producing transient radiation effects.[1] This conclusion is invalid in case the target material contains hydrogen, since a large fraction of the neutron's energy is imparted to the hydrogen atoms and they dissipate it via ionization.

A calculation has been performed[1] on the relative energy deposition by neutrons and gamma rays in a typical mixed field from a nuclear reactor or a nuclear burst. One example of this calculation is the biological dose which represents the relative energy deposition for a hydrogen containing tissue-equivalent material. Typical neutron-to-gamma dose ratios in biological material of 0.1 to 10 are encountered in practice. In this case the relative ionization effectiveness is approximately proportional to the tissue dose. On the other hand, in material not containing an appreciable amount of hydrogen, it has been shown that the total energy deposition by neutrons is usually less than that by gamma rays, and hence the ionization production by neutrons is almost always negligible compared with that produced by the gamma-ray component of a mixed field. Exceptions to this rule are some unusual materials, such as B^{10} and Li^6, in which inelastic neutron reactions occur, (n,α) in these cases, which result in a large amount of ionization energy deposition.

*References appear on page 102.

Semiconductors and Semiconductor Junctions

In a metal the electrons, which are produced as a result of ionization, temporarily occupy high-energy states in the conduction band at the expense of some of the lower energy states. Since the excess energy can be distributed quickly among a large number of conduction electrons in a metal, relaxation times are extremely short as compared with those of semiconductors. Hence, the conductivity and other bulk electrical properties of a metal are not expected to be affected appreciably by available ionization intensities.[1]

In the case of a semiconductor, electrons may be excited from filled states in the valence band into originally empty states in the conduction band, leaving behind a hole. Hence, the process is described as the generation of electron-hole pairs, producing a nonequilibrium state which is eliminated when the excess electrons and holes recombine. Most excess carriers, or electron-hole pairs, recombine at defects in the crystalline lattice. These defects are referred to as recombination centers and are associated with various energy levels within the forbidden energy band gap. The time required for the excess carriers to come to equilibrium by recombining is the excess carrier lifetime which is primarily dependent on the density and recombination cross section of these recombination centers.

In many semiconductor devices which require long minority-carrier lifetimes for efficient operation, ultrapure materials are used which have relatively few recombination centers. Recombination times in excess of 1 microsecond are common, and times as long as 1 millisecond have been observed. Hence, relatively long relaxation times associated with transient radiation phenomena are observed. By purposely adding impurities to semiconductors or by producing displacement defects by prolonged irradiation, lifetimes much shorter than these can be obtained. In certain cases, shorter lifetimes are desired for the particular device application. In other cases, particularly when a high-lifetime device is irradiated for a long-enough period to decrease the lifetime, the operating parameters of the device are affected.

As in a gas, the excess electrons and holes temporarily created in a semiconductor by exposure to ionizing radiation enhance the conductivity of the media. However, a more sensitive manifestation of the radiation effects is observed in semiconductor junctions. The reverse current of a semiconductor junction is primarily dependent upon the minority-carrier density near the junction. The conductivity, on the other hand, is a function of the majority carriers. An ionization density capable of increasing the majority-carrier concentration, and hence the conductivity, by a negligibly small amount may increase the minority-carrier density by orders of magnitude. For example, if the base region of a junction device contains ultrapure silicon, having a majority-carrier concentration of $2 \times 10^{13}/cm^3$, there are about 1×10^7 minority carriers/cm^3 at room temperature. If this material is exposed to ionizing radiation which produces a 0.1 of 1 per cent increase in the majority-carrier concentration, the minority-carrier concentration is increased to $2 \times 10^{10}/cm^3$, or by a factor of 2000. In this case, the reverse current of the junction would be greatly increased and the normal operation of a semiconductor device incorporating this junction would be affected adversely.

Easley and Blair[2] and Brown and Easley[3] have presented formulations regarding the ionization current produced in a semiconductor junction exposed to ionizing radiation. These formulations and the authors' discussions are given in the following paragraphs.

In semiconductor devices the generation of hole-electron pairs produces excess junction currents, since the junction separates those pairs which are generated in its vicinity. In addition to this current in the volume of the device, there may be an additional current component from surface conduction, or conduction to some other element of an encapsulating or supporting structure.

If the latter current component is assumed to be negligible, the current from radiation-generated hole-electron pairs separated by the junction is given by

$$I(t) = qgA(x_1 + x_2) = \frac{q\dot{R}(t)\rho A}{\underline{e}} (x_1 + x_2) \quad , \tag{1}$$

where q is the electronic change, g is the generation rate of hole-electron pairs per unit time and volume, A is the area of the junction, and x_1 and x_2 are the widths of the regions on each side of the junction in which, on the average, generated hole-electron pairs will be separated at the junction. In the second form, $\dot{R}$ is the exposure rate in ergs g^{-1} sec^{-1}, ρ is the density of the semiconductor, and $\underline{e}$ is the average energy, expressed in ergs, required to produce a hole-electron pair. The value of $\underline{e}$ is approximately 3.0 ev or 4.8×10^{-12} ergs in germanium, and 3.5 ev or 5.6×10^{-12} ergs in silicon. The values of x_1 and x_2 are determined by the characteristics of any given device and the time history of its exposure. Three cases will be considered. The first two require a radiation pulse of sufficient duration so that a steady-state equilibrium exists in the processes of generation, annihilation, and junction collection of hole-electron pairs. The third applies to situations in which the pulse duration is short compared to the time for the establishment of steady-state equilibrium.

Case I. If the width, perpendicular to the plane of the junction of semiconductor material on both sides of the junction, is greater than a minority-carrier diffusion length, and if the radiation intensity does not change appreciably during a minority-carrier lifetime, then x = L and the instantaneous value of current is given by

$$I(t) = qgA(L_1 + L_2) = \frac{q\dot{R}(t)\rho A}{\underline{e}} (L_1 + L_2) \quad . \tag{2}$$

Generally, one of the two diffusion lengths can be neglected.

Case II. If a contact surface or other junction is within a distance B of the junction, and if B is less than the diffusion length, then the corresponding x is equal to B/n, where $1<n<2$, depending on the nature of the adjacent interface. In the latter case the condition of steady-state equilibrium requires that the radiation intensity must not change appreciably during a time $t \approx (B/n)^2/D$, where D is the diffusion constant for minority carriers in the region of width W.

Case III. If the radiation-pulse duration is sufficiently short, steady-state equilibrium will not exist. If we consider a rectangular pulse of amplitude $\dot{R}$ and width t_1 so that

$$t' < t_1 < \left(\frac{B}{n}\right) / D < L^2/D \quad , \tag{3}$$

where t' is the time for carriers to be swept out of the junction space charge region (W_{sc} = width of space charge region) (t'≈10^{-10} second), then for $t_1 \geq t$,

$$I(t) \approx \frac{q\dot{R}\rho A}{e} (W_{sc} + \sqrt{D_1 t} + \sqrt{D_2 t}) \quad , \tag{4}$$

where D_1 and D_2 are the diffusion constants for minority carriers on eigher side of the junction. The value of Equation (4) when $t_1 = t$ yields the maximum current amplitude, since when $t_1 < t$ the current decays at a rate determined primarily by the diffusion constant.

For the Godiva exposures, in which the radiation pulse width is approximately 80 microseconds, the pulse width is long compared with the minority-carrier lifetimes generally encountered in semiconductor devices (of the order of 1 microsecond or less). Consequently, Equations (1) and (2) are applicable.

Account must also be taken of another effect which will be encountered for many semiconductors devices when samples are exposed to simultaneous fast neutron and gamma-ray fluxes. This occurs at Godiva and also for any fission source when samples are positioned near enough to the source so that the difference in velocities of the neutrons and gamma rays does not result in a time separation of the two flux components. This simultaneous exposure can produce a difference in the observed effect form the reduction in difference in the observed effect from the reduction in diffusion length by the fast-neutron bombardment reduction of carrier lifetime during the irradiation pulse. In the Godiva exposure case, the diffusion length is not a constant during the exposure for devices with initial carrier lifetimes greater than the order of 1 microsecond for germanium and 0.1 microsecond for silicon, these being the approximate minimum values of lifetime produced by the neutrons in a single Godiva burst.

In a device in which the junctions are located at a distance from an interface greater than the initial diffusion length, Brown and Easley[3] have shown that the observed current at any time during a Godiva pulse is somewhat less than would be observed for equal ionizing-radiation intensity in the absence of the fast-neutron component. Also, the current peak occurs earlier than the peak intensity of irradiation. This is primarily caused by the fast-neutron reduction in carrier lifetime, and therefore diffusion lengths, during the pulse of radiation.

Insulators

An insulator exposed to ionizing radiation behaves in a manner similar to the behavior of a semiconductor, in that electrons are excited from bound states in the valence band, across the forbidden energy gap, into conducting states in the normally empty conduction band. The rate of excitation of these electrons is proportional to the ionization dose rate. The resulting conducting charge carriers then recombine, usually with the assistance of impurity states in the forbidden gap. However, unlike the case

for semiconductors, impurity states in the forbidden energy gap of insulators frequently act not as recombination centers, but as trapping centers. In this role a center readily captures one type of charge carrier but does not annihilate it by allowing the other type of carrier to be captured. For typical insulators the recombination time is extremely short, probably of the order of 10^{-10} seconds.[4] However, electronic perturbations in an insulator can frequently last much longer than the extremely short carrier recombination times because of the occurrence of trapping. Electronic changes lasting minutes or hours are frequently encountered.[1] One difficulty in the study of insulator materials is that they are not available as controlled pure specimens, such as are provided by modern semiconductor technology. Hence, the concentration and nature of the impurities are frequently unknown, and it is much more difficult to deduce a consistent description of the recombination processes.

Observations of radiation-induced electrical conductivity in insulators have, for the most part, been made by investigating the irradiation behavior of electronic piece parts which contain dielectric materials as a major part of their structure. Such electronic parts include capacitors, wiring and cables, switches, and transformers. In addition to what may be ascribed to bulk conductivity changes during irradiation, the emission or insertion of secondary electrons appears to be important.

Since ionizing radiation interacts primarily with atomic electrons, it can impart sufficient energy to these electrons to eject them from the material. This is primarily a surface effect, although the range of the more energetic secondary electrons may be enough to eject them from distances of the order of millimeters inside a solid sample.[1] In metals and semiconductors the net space charge left behind by the emitted electrons is easily compensated by an opposite charge flowing through an attached circuit. In an insulator the phenomena may be more complicated because the conductivity of the insulator material itself may be so low that a compensating charge cannot arrive promptly. In actual observations, electrons may be emitted by the material under study or they may be inserted into it after emission from nearby materials.

Gamma rays produce high-energy secondary electrons directly by the photoelectric, Compton, or pair production processes. In the case of typical reactor or nuclear-detonation gamma rays, the Compton process is predominant. In this case, the secondary electrons are almost uniformly distributed in energy between a low value and a value almost equal to the energy of the gamma ray.

Contrasting the two radiation-induced effects[1], for low-value capacitors, the emission of secondary electrons is probably the predominant effect. In high-value capacitors, the conductivity induced in the insulating material becomes important. Similarly, it is suggested that the predominant radiation effect on the insulating materials in cables operated at low voltages is the insertion or emission of secondary electrons.

EFFECTS OF PULSED RADIATION ON ELECTRONIC COMPONENTS

Semiconductor Devices

The production of excess electrons and holes in semiconductor materials is particularly important in the case of semiconductor devices because the p-n junction can

separate the pairs, thus allowing an excess current to flow. Hence in a reverse-biased diode, a larger-than-normal current will be produced when it is exposed to ionizing radiation. In fact, a leakage current will be observed in a passive diode upon bombardment with ionizing radiation. Similarly, a transistor, which normally exhibits a small collector current I_{CO} when the collector junction is reverse biased and the emitter is open circuited, can experience large I_{CO} values when exposed to ionizing radiation.

As indicated in Equation (1), the excess current generated in the volume of a junction device may be expressed as

$$I(t) = \frac{q\dot{R}(t)\rho Ax}{e} \quad , \tag{5}$$

where $\dot{R}$ is expressed in ergs $g^{-1}(C)\ sec^{-1}$ and x assumes various forms depending on a combination of conditions including minority-carrier lifetime, the rate of change of the ionizing radiation, and the width of the region of high-lifetime material. Hence the magnitude of the radiation-generated current is directly proportional to the exposure rate $\dot{R}$ and depends on the geometry of the device. The dependence on exposure rate has been demonstrated by van Lint[5] and others who showed that the radiation-induced leakage current in a reverse-biased semiconductor junction increases linearly with increasing gamma-radiation rates. With respect to the geometry of the device, the radiation-generated current is directly proportional to the area A of the junction regardless of the form of x.

In discussing the form of x, it will be assumed that the current contribution from the region on only one side of the junction need be considered. This is nearly always a justifiable simplification for practical junction devices. If the width B (perpendicular to the plane of the junction) of this region is greater than a minority-carrier diffusion length L and if the radiation intensity does not change appreciably during a minority-carrier lifetime ($\tau = L^2/D$), then x may be replaced by L in Equation (5). Charge carriers are swept out of the junction space charge region (of width W_{SC}) in times in the range 10^{-9} to 10^{-10} sec. The current, arising from the diffusion of hole-electron pairs to the junction from distances the order of a diffusion length away, rises and saturates in times the order of the lifetime (generally on the order of 10^{-6} to 10^{-5} sec).

If $B < L$ and if the radiation intensity does not change appreciably during a time $t = (B/n)^2/D$, then B/n may be substituted for x in Equation (5), where $1 < n < 2$, depending on the nature of the adjacent interface. For example, considering a p-type region of germanium with a diffusion constant D of 100 cm^2/sec and a lifetime of 10^{-6} sec, the diffusion length would be equal to 0.01 cm. Therefore, if the distance B to the nearest contact or other junction is less than 0.01 cm or 4 mils, B/n should be used in Equation (5). Similarly, with n-type silicon having D = 12 cm^2/sec and $\tau = 10^{-6}$ sec, L would be 0.0035 cm or 1.4 mils

For a moment, consider irradiation pulse durations appreciably longer than either $\tau = L^2/D$ or $t = (B/n)^2/D$. The radiation-generated current can be minimized by adjusting various parameters, as follows:

(1) In all cases, minimize the area of the junction.

(2) For a given B, and small enough values of τ so that $L < B$, minimize τ.

(3) For $B < L$, minimize B.

If the radiation pulse duration is sufficiently short, steady-state equilibrium will not exist. The maximum current induced by a rectangular irradiation pulse of amplitude $\dot{R}$ and width t_1 will be

$$I_m = \frac{q\dot{R}\rho A}{e}(W_{sc} + \sqrt{Dt_1}) \quad . \tag{6}$$

Equation (6) implies that t_1 is short compared to $(B/n)^2/D$ and L^2/D, but is long compared to the time required for a carrier to transit across the space charge region.

The description and prediction of the radiation-generated currents induced by ionizing radiation are essentially the same for all types of junction devices regardless of whether they are audio, high-frequency, power, or switching transistors; audio, microwave, Esaki, or switching diodes; rectifiers; infrared detectors; or solar, photovoltaic, or photoconductive cells. The degree to which these excess currents affect the operation of the junction device will depend on the function of the device. It is reassuring that an estimate of the magnitude of the radiation-generated current can be obtained for a junction device by knowing the geometry of the device and the electrical characteristics of the high-lifetime region. Various workers have reported data on transient leakage currents in transistors and diodes, but the effective junction volumes [i.e., AL, AB/n, or $A(W_{sc} + \sqrt{Dt})$ as the case may be] were not known. Where this information was available, as in the case of Easley and Blair's work[2], the peak transient currents in a junction device exposed to a Godiva burst were observed to be approximately proportional to the effective volume.

Transistors

In-pile measurements on transistors exposed to pulsed radiation have consisted of monitoring the transistor collector-to-base leakage current (I_{CO}) and the gain of the transistor. Figure 1 shows typical test circuits for the measurement of transient leakage current and gain.[6] The circuit in Figure 1a is for measuring the transient leakage current by monitoring the voltage across a 75-ohm resistor connected in series with a 3- or 6-volt battery and the collector and base leads. The emitter is open circuited. The circuit in Figure 1b permits a gain test during the irradiation pulse. For an I_{CO} test using this circuit, there is no voltage applied to the 75-ohm emitter resistor and the base current is monitored.

There is a transient increase in the I_{CO} of both germanium and silicon transistors during a radiation pulse. Figure 2 shows a typical I_{CO} transient, in this case an IBM Type 51 NPN germanium transistor.[6-8] In general, all types of transistors tested show this behavior in which the transient leakage current follows approximately the radiation pulse. Sauer[9] indicates that three distinct effects are observed in the I_{CO} response, as follows: (1) an "instantaneous" response faithfully following the dose-rate curve (presumably due to hole-electron pairs produced by the gamma flux), (2) a

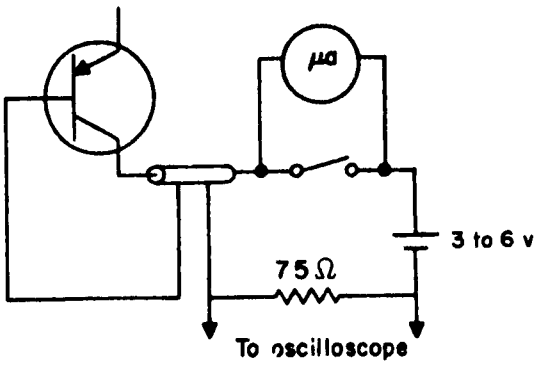

a. I_{co} Test

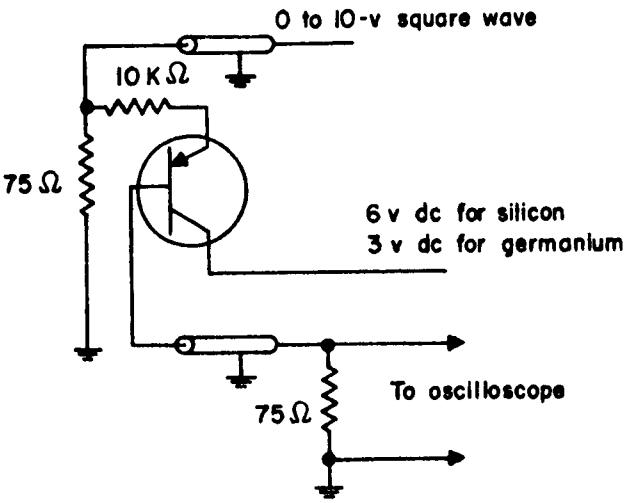

b. Gain and I_{co} Test

FIGURE 1. TEST CIRCUITS FOR TRANSIENT EFFECTS IN TRANSISTORS

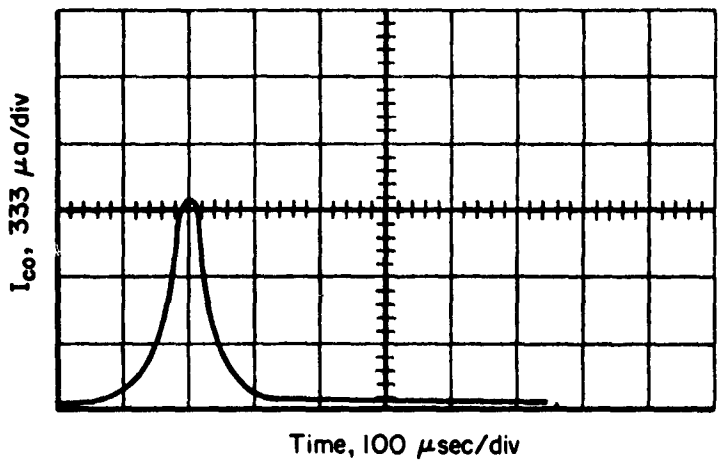

FIGURE 2. I_{CO} VERSUS TIME DURING A GODIVA BURST FOR AN IBM TYPE 51 TRANSISTOR

"permanent" damage level, proportional to the integrated dose (presumably due to the production of defects by fast neutrons), and (3) relatively small, rapidly decaying contribution (may be due to recombination of close vacancy-interstitial pairs, electron-hole recombination, short-lived radioactive species, surface or ionization effects, or several of these).

Table 1 shows values of I_{co} for a variety of transistors exposed to transient radiation. Most of the information comes from Godiva exposures (designated as G) in which the time rate of change of the gamma exposure rate is such that Equation (5) with x replaced by either L or B/n is applicable to predict the transient I_{co} value. The same is true for TRIGA exposures (designated as τ).

Some experiments have been performed using a linear accelerator as a radiation source (designated as L), in which the bremsstrahlung produced from stopping electrons in a target material provides the ionizing radiation.[12] The 6-Mev linear accelerator provided either single or multiple pulses of radiation of variable duration up to 1.8×10^{-6} sec. In this case, one may be required to use Equation (6) to describe the peak transient I_{co} values. For recording changes in I_{co}, a single pulse or radiation was emitted by the accelerator, and the change in reverse current of the transistor was almost completely transient in nature. Figure 3 shows the variation in the magnitude of these transient pulses as a function of the exposure rate for the transistors tested. The output voltage (measured across a 75-ohm resistor) is a linear function of the exposure rate for each sample, as predicted from Equation (5), where I is proportional to $\dot{R}Ax$. The rate of change with exposure rate varies from one sample to another, the different slopes presumably resulting from different values of Ax. The transient I_{co} values of the transistors exposed to ionizing radiation was of the same order of magnitude with and without an applied potential, suggesting that photocurrents were created during the pulse.

A column is provided in Table 1 to show values of effective junction volume Ax calculated from Equation (5). One would expect some variation in the Ax values, for a given transistor type, due simply to manufacturing variations. Also, if it is appropriate to use L in place of x, variations will occur due to differences in the material property τ. However, somewhat larger variations may be evident in Table 1 because of uncertainties in measured values of $\dot{R}$ and the peak transient values of I_{co}. For example, results of Godiva exposures for 6 samples of transistor Type 2N123 give a spread in Ax of 2 to 10×10^{-5} cm^3, and for 2 samples of Type 2N389 an order of magnitude spread is observed. More consistent results were obtained for 6 samples of transistor Type IBM 51 for which the Ax values were in the range 6 to 12×10^{-5} cm^3.

For the transistor types shown in Table 1, the transient I_{co} values are, in general, smaller for silicon devices than for germanium devices. For devices of the two materials having the same initial characteristics (particularly with respect to Ax), theory predicts that the transient I_{co} values for germanium should be about a factor of 2.5 larger than those for silicon. However, without a great deal of information about the devices shown in Table 1, one would suspect that the major differences between I_{co} values for devices of the two materials are reflections of differences in fabrication techniques affecting the device geometry and the properties of the base materials.

There should be a difference in the transient current traversing the base-collector junction of a transistor for an open emitter (as used in all the tests reported) and for a grounded emitter. That is, the base-to-collector current can include the effects of transistor action if the external connections are appropriate, as would be the case for a

TABLE 1. TRANSIENT I_{co} MEASUREMENTS

Transistor	Type	Sample	Irradiation Source[a]	Integrated Neutron Flux, n cm^{-2}	Gamma Exposure Rate R, ergs g^{-1} (C) sec^{-1}	I_{co} Pretest Value, μa	I_{co} Peak Transient Value, μa	I_{co} Posttest Value, μa	Calculated Effective Junction Volume[b], cm^3	Reference
2N123	Ge PNP	13	G	9.7×10^{10}	1×10^{7}	0.4	3.6	0.5	2×10^{-5}	6
		12	G	7.3×10^{11}	7×10^{7}	0.4	153	0.8	1×10^{-4}	
		8	G	1.4×10^{13}	1.4×10^{9}	0.5	680	2.8	3×10^{-5}	
		11	G	1.5×10^{13}	1.5×10^{9}	0.2	1,200	3.9	4×10^{-5}	
		20	G	1.2×10^{13}	1.2×10^{9}	0.4	2,800	3.7	1×10^{-4}	
		29	G	1.2×10^{13}	1.2×10^{9}	0.5	3,200	6.4	1×10^{-4}	
IBM 01	Ge PNP	37	G	1.5×10^{13}	1.5×10^{9}	3.5	175	5.5	7×10^{-6}	6
2N395	Ge PNP	A	G		1×10^{9}		100		6×10^{-6}	10
2N167	Ge NPN	12	G	1.4×10^{13}	1.4×10^{9}	1.0	250	1.4	1×10^{-5}	6
IBM 51	Ge NPN	15	G	1.5×10^{10}	1.5×10^{6}	2.1	<1.5	2.5	$<6 \times 10^{-5}$	6
		13	G	9.4×10^{10}	1×10^{7}	1.4	10		6×10^{-5}	
		14	G	1.0×10^{11}	1×10^{7}	1.0	9	1.2	6×10^{-5}	
		12	G	7.7×10^{11}	8×10^{7}	0.7	105	1.0	7×10^{-5}	
		8	G	1.3×10^{13}	1.3×10^{13}	2.5	3,000	5.3	1.2×10^{-4}	
		17	G	1.4×10^{13}	1.4×10^{9}	0.5	3,000	3.3	1.2×10^{-4}	
1275	Si PNP	A	G	1.1×10^{13}	1.1×10^{9}		55		7×10^{-6}	6
		B	G	1.5×10^{13}	1.5×10^{9}		66		7×10^{-6}	
2N495 (Philco)	Si PNP	A	G		1×10^{10}		60		1×10^{-6}	11
		B	G		1×10^{10}		170		3×10^{-6}	11
		C	L	None	2×10^{9}		13		1×10^{-6}	12
2N389	Si NPN	7	G	9.9×10^{12}	1×10^{9}		12,000		2×10^{-3}	6
		3	G	1.1×10^{13}	1.1×10^{9}	0.034	1,600		2×10^{-4}	
2N338	Si NPN	Z	G	1.0×10^{13}	1×10^{9}		70		1×10^{-5}	6
		Y	G	1.1×10^{13}	1×10^{9}		130		2×10^{-5}	
		X	G	9.5×10^{12}	1×10^{9}		540		8×10^{-5}	
2N338 (TI)	Si NPN	W	L	None	1×10^{9}		17		3×10^{-6}	12
		W	L	None	2×10^{9}		35		3×10^{-6}	
2N335 (TI)	Si NPN	A	G		4×10^{8}		100		4×10^{-5}	8
		B	G		4×10^{9}		800		3×10^{-5}	
		C	L	None	1×10^{9}		40		6×10^{-6}	6
		C	L	None	2×10^{9}		80		6×10^{-6}	
		D	L	None	1×10^{9}		220		3×10^{-5}	
		D	L	None	2×10^{9}		490		4×10^{-5}	
2N335 (GE)	Si NPN	A	G		4×10^{8}		60		2×10^{-5}	8
		B	G		4×10^{9}		300		1×10^{-5}	
		C	L	None	1×10^{9}		90		1.3×10^{-5}	6
		C	L	None	2×10^{9}		200		1.5×10^{-5}	
		D	L	None	1×10^{9}		200		3×10^{-5}	
		D	L	None	2×10^{9}		490		4×10^{-5}	

(a) G = Godiva; L = linear accelerator.

(b) Calculated from Equation (5) as $Ax = CI_{co}/\dot{R}$, where $C = 5.6 \times 10^{7}$ and 1.5×10^{8} $\frac{cm^3\ ergs}{g\ coulomb}$ for germanium and silicon, respectively.

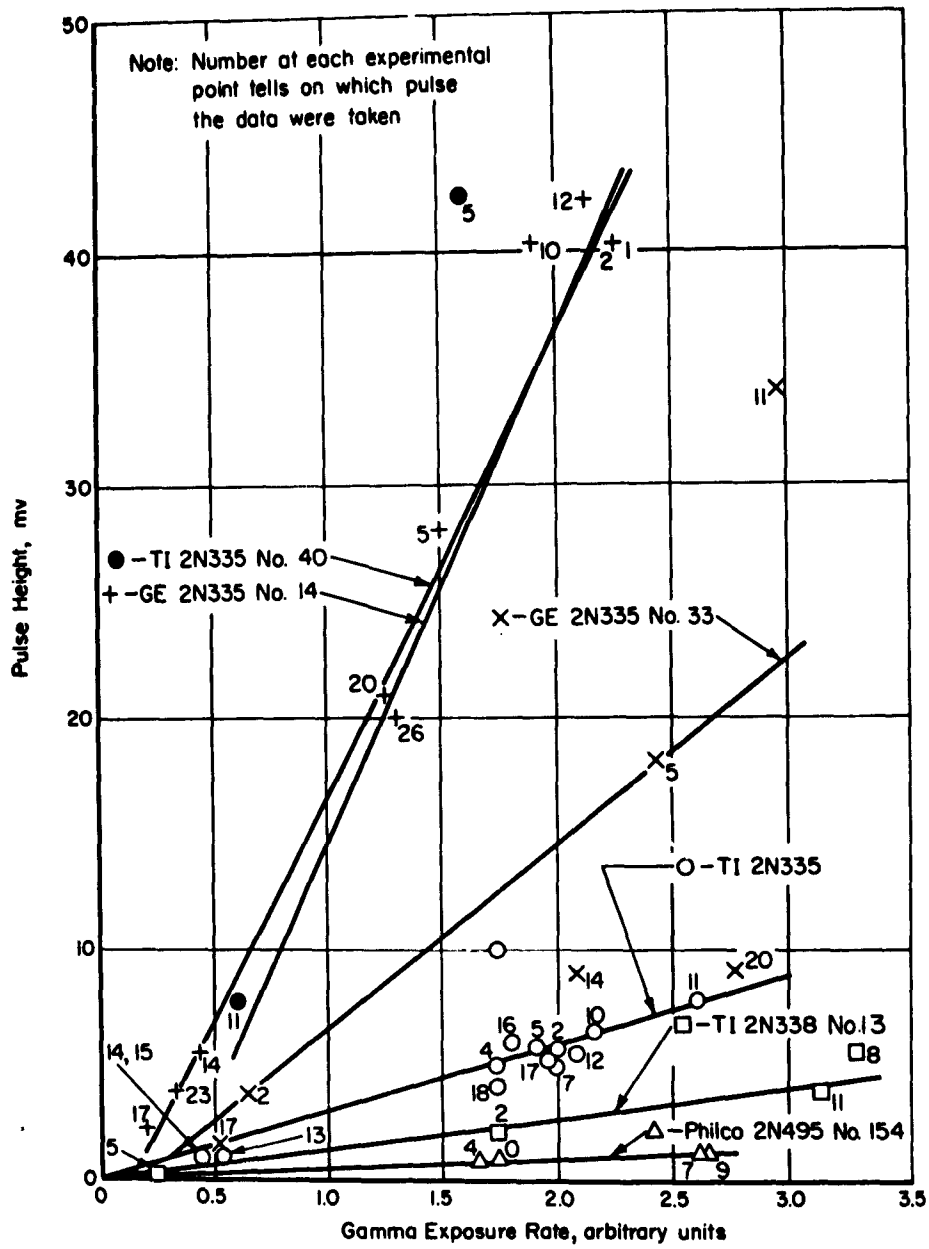

FIGURE 3. PULSE HEIGHT VERSUS X-RADIATION EXPOSURE RATE (VOLTAGE APPLIED)

grounded emitter. Hence, it is extremely important to indicate the test configuration when reporting excess leakage currents produced in devices exposed to ionizing radiation. In addition, to evaluate properly the electrical behavior of any given transistor subjected to a radiation pulse, it will be necessary to obtain more accurate information on the individual junction volumes.

One additional word should be said about the effect of short-duration pulses compared with those obtained by testing at Godiva facilities. For example, if the values of the important parameters for a silicon transistor, include $\tau = 1 \times 10^{-6}$ sec, $L = 5.5 \times 10^{-3}$ cm, $A = 2 \times 10^{-3}$ cm^2, $B = 10^{-2}$ cm, and $W_{sc} = 10^{-5}$ cm, then a peak transient I_{co} value of about 100 μa would be predicted for a Godiva-type burst having a peak radiation exposure rate of 1.4×10^{9} ergs g^{-1}(C) sec^{-1}. However, for the same peak gamma exposure rate but for a nearly rectangular pulse 10^{-8} sec wide, the predicted peak transient I_{co} value would be about 10 μa. It is quite clear that the value of current per unit exposure rate ($I/\dot{R}$) for any given device may be quite different for short-duration pulses from that which is observed at Godiva or TRIGA facilities.

Diodes

In general, the transient leakage currents induced in diodes by radiation are smaller than those induced in transistors. This is reasonable, since the leakage current without radiation is also generally much smaller, which implies a smaller initial Ax product for diodes than for transistors. Oscilloscope traces of the leakage current induced in diodes are similar in shape to that shown in Figure 2 for a transistor.

Steele[13] of Boeing exposed diodes to a Godiva pulse of about 3×10^{5} r sec^{-1} peak gamma exposure rate and observed a transient leakage current of about 7 microamperes. The circuit used is shown in Figure 4. No pulse was obtained when the cable was open circuited, and the pulse was the same magnitude with or without the applied voltage. Thus, it was concluded that the transient leakage current observed was a photocurrent.

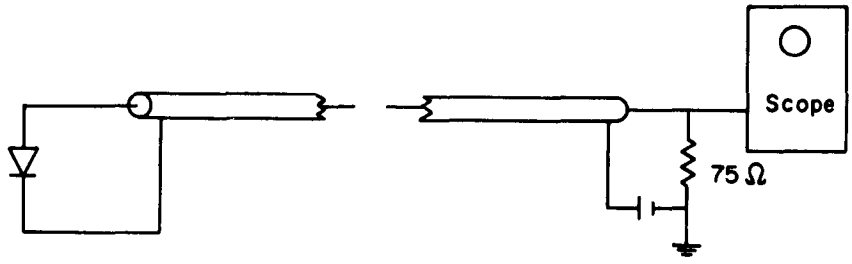

FIGURE 4. DIODE TEST CIRCUIT

Junction diodes of various areas were exposed to a Godiva pulse, and the transient leakage current was measured. To get the larger areas, power diodes and the diode section of transistors were used. The results showed that the transient leakage current is approximately proportional to the area of the junction of the diodes.[13]

The reverse leakage current of silicon diodes was measured across a 75-ohm load with a 6-volt supply during a Godiva pulse.[11] Transient leakage currents of about 33, 420, and 320 microamperes were observed at a peak gamma exposure rate of

7×10^9 ergs $g^{-1}(C)$ sec^{-1} for Diodes 1N251 - Transitron, 1N643 - Pacific Semiconductor, and 1N658 - Radio Receptor, respectively. The remarks made previously on the I_{CO} of the collector-to-base diode of a transistor as a function of flux also apply to the reverse currents of the diodes tested. In particular, the units with smaller diffusion volumes (Ax product) (e.g., the 1N251) experienced less transient reverse current than those with larger diffusion volumes (e.g., the 1N643).

A number of diodes have been exposed to gamma-radiation bursts obtained when high-energy electrons produced by a linear accelerator strike a heavy metal target.[14] The gamma-radiation pulse was about 2×10^8 ergs $g^{-1}(C)$ sec^{-1} for a time of 10 microseconds. Table 2 shows the initial amplitude of the transient diode current pulse. Measurements on two dummy diodes consisting only of the glass diode body with the leads sealed in each end, in the radiation field, and on two silicon diodes outside of the radiation field gave currents during the radiation pulse of 2 microamperes and 1 microampere, respectively. These are negligible in comparison with other signals and gave assurance that electrical pickup and air ionization within the diode envelope were not significant at the exposure rates used. Reverse diode currents ranging between 10 and 100 microamperes were observed during the radiation pulse. These currents decayed to zero within a few microseconds following the radiation pulse. No permanent change in diode characteristics was observed as a result of irradiation. It is noteworthy that the single HD6008 diode selected for short recovery time had a pulse amplitude similar to that for the 1N629 fast-recovery diode.

Two diode types shown in Table 2 were also tested in the Godiva facility.[15] The peak transient reverse currents were 16 and 38 microamperes for a HD6008 diode, with applied voltages of 0 and 100 volts, respectively. A 1N76A diode with an applied voltage of 50 volts had a peak reverse current of 38 microamperes during the pulse.

Transient reverse currents from 2500 to 4000 microamperes were obtained in the large-area silicon power diode Type 1N1128 exposed to a Godiva pulse.[16] These current pulses are two orders of magnitude larger than the pulses observed with low-level silicon diodes. This observation supports the findings of Steele[13] that the transient leakage current is proportional to the area of the junction of the diode.

Radiation-induced reverse currents were monitored for a number of germanium gold-bonded diodes exposed to a KUKLA source.[17] In Table 3 the change in diode reverse current at 12 volts for KUKLA Bursts 5 and 9 are tabulated together with the cable and dummy-diode leakage information from Burst 4. The diode currents ΔI_d are also given after some correction from cable and diode-dummy leakage normalized to the peak gamma rates for Bursts 5 and 9. The rather large differences between the currents of the individual diodes irradiated on the same bursts, and the failure to scale from one burst to the other were taken to be caused by differences in some diode parameter which controls the current.[17] Actually, if one calculates the effective junction volumes, Ax that these diodes would have according to Equation (5), the volumes of the six devices are in the rather narrow range of 5 to 10×10^{-6} cm^3.[18]

The ability of a Zener diode to maintain a constant voltage during a Godiva pulse has been measured.[11] Output voltages were recorded in only three cases. In four other cases, no change was observed because of the lack of sensitivity of the oscilloscope. Peak transient changes in Zener diode voltage of 108 and 29 millivolts (Transitron Diode SV-6) and of 14 millivolts (U.S. Semiconductor Diode Z3.9) were observed for gamma exposure rates of 3×10^9, 7×10^8, and 7×10^9 ergs $g^{-1}(C)$ sec^{-1}, respectively.

TABLE 2. INITIAL AMPLITUDE OF DIODE CURRENT PULSE

Radiation pulse = 2×10^8 ergs g^{-1} (C) sec^{-1}

Diode Type	Diode No.	Recovery Time	Current, μa, at Indicated Applied Voltage						
			Forward		Reverse				
			1 v	0 v	15 v	30 v	50 v	100 v	150 v
HD6008 (Si)	230	Not measured	--	--	--	--	--	38	--
HD6008 (Si)	229	Not measured	--	--	--	--	--	75	--
HD6008 (Si)	214	Not measured	--	--	--	--	--	64	--
HD6008 (Si)	166	Long	--	--	--	--	--	75	--
HD6008 (Si)	182	Short	--	--	--	--	--	14	--
1N629 (Si)	18	Short	1	11	--	--	15	18	20
1N629 (Si)	22	Short	1	10	--	--	17	20	--
1N629 (Si)	23	Short	1	4	--	--	11	13	--
1N76A (Ge)	62	--	--	--	38	48	50	--	--
1N76A (Ge)	39	--	--	--	50	52	62	--	--
1N76A (Ge)	52	--	--	--	40	44	50	--	--

TABLE 3. SUMMARY OF IN277 DIODE RADIATION-INDUCED CURRENT CHANGES AT 12 VOLTS REVERSE

Case	$\dot{R}$	ΔI_t	ΔI_{dd}	ΔI_d	Diode
9-3-4	6.11	14.9 ± 0.3	14.9 ± 0.3	--	Dummy
10-1-5	7.28	100 ± 10	17.8 ± 0.4	82 ± 10	H12
10-2-5	7.28	114.0 ± 1.0	17.8 ± 0.4	96.2 ± 1.1	H14
10-4-5	7.28	132 ± 8	17.8 ± 0.4	114 ± 8	H19
11-1-9	2.35	21 4 ± 0.3	5.8 ± 0.1	15.6 ± 0.3	T6
11-2-9	2.35	26.3 ± 0.3	5.8 ± 0.1	20.5 ± 0.3	H9
11-3-9	2.35	30.0 ± 0.3	5.8 ± 0.1	24.2 ± 0.3	T7

Notes:

Case = Setup No. - Channel No. - Burst No.

$\dot{R}$ = 10^{-6} x peak gamma rate during a burst, in r/sec (±10%).

ΔI_t = peak increase in current through the terminating resistor, in microamperes.

ΔI_{dd} = the contribution to ΔI_t from leakage in microamperes, as measured with the diode dummy.

ΔI_d = $\Delta I_t - \Delta I_{dd}$, in microamperes.

Diode = diode identifying number.

In a later test, the complete reverse characteristics of Zener diodes were determined during the Godiva pulse.[14] In order to observe the knee of a Zener breakdown during a radiation test, it was necessary to plot several current-voltage curves during the Godiva pulse. Two Zener diodes were tested, a Hoffman 1N1313A and a Texas Instrument 651C4. Both diodes exhibited no change in the knee of the reverse characteristics during the Godiva pulse of about 10^9 ergs $g^{-1}(C)$ sec^{-1}. However, it was observed that the minimum diode voltage did not return to zero and varied as the shape of the burst. This rise was attributed to a cable effect.

Esaki diodes of germanium (IBM 1-ma diode) and GaAs (TI 1N652 5-ma diode) have been exposed to nominal Godiva pulses.[14] An oscilloscope trace was taken which plots several I-V characteristics of the diodes during the burst. This was accomplished by impressing a 400-millivolt, 25-kilocycle, linear sawtooth voltage across the diode and observing on the oscilloscope a time plot of diode current. Both diodes exhibited no transient or permanent change in the peak or valley currents. These observations and theoretical considerations indicate that Esaki diodes of germanium or GaAs will not be affected in the Godiva environment. Effective junction volumes for these devices will be on the order of 10^{-9} to 10^{-8} cm^3; hence, radiation-induced currents are predicted to be less than 1 μa at gamma exposure rates on the order of 10^9 ergs $g^{-1}(C)$ sec^{-1}.

Electronic Devices

Coaxial Cables

Many of the present-day concepts concerning the effects of transient nuclear radiation on cable insulations were derived from early studies performed with the various component parts subjected to steady-state conditions of the radiation environment. In these research programs, three main effects were observed to occur when the organic insulations were exposed to nuclear radiation: (1) crosslinking, (2) chain cleavage, and (3) ionization. Crosslinking and chain cleavage usually occur together, and the combined effect is dependent upon the relative rates of the two processes. In general, plastic and elastomeric materials tend to become more brittle under the influence of radiation, and the tensile strength increases. Ionization effects which are transient in nature are responsible for the increase in electrical conductivity which correspondingly increases the surface leakage current during irradiation of the insulation material. Results from many studies on cables have led to conclusions that all insulation materials are extremely sensitive to gamma exposure rate. The substantial changes in leakage current and insulation resistance are primarily attributed to ionization effects. Thus, ionization effects can be expected to be an important factor in the selection of coaxial and other types of cables for application in an environment involving transient radiation conditions.

Studies have indicated that polystyrene and polyethylene, both dielectric materials that are used in the manufacture of coaxial cables, are the most radiation resistant of the organic insulations. Polystyrene has been found to be the most radiation resistant of the two dielectric materials; however, its use for coaxial cables is limited to bead-type construction because it lacks flexibility. Therefore, polyethylene, because it is more flexible than polystyrene and nearly as radiation resistant, is frequently used where the nuclear-radiation environment is encountered.

A limited amount of information which would describe the magnitude of transient radiation effects to coaxial cables has been gleaned from research experiments which require the use of cables for instrumentation purposes. The results of these experiments have pointed out that a large number of factors must be considered by the designer and component engineer in the application and selection of coaxial cables which might be subjected to transient-type radiation. Some of these factors are (1) construction (solid or partial dielectrics), (2) cable length and thickness, (3) termination configuration, (4) potential between center conductor and shield, and (5) circuit and line impedances.

Radiation-effects researchers have concluded that the solid dielectric is less affected[15] than the partial-dielectric-type coaxial cable. This conclusion was derived by empirical means from experiments conducted with the RG-59/U (solid dielectric) and the RG-62/U (partial dielectric) in which it was found that a voltage pulse, ten times greater for the partial-dielectric than for the solid-dielectric cable, was observed at the Godiva II critical assembly. The explanation offered for the pulse occurrence was that it might be caused by the differences between Compton charge scattering into and out of the dielectric region. This appears to have a strong dependence on the dielectric geometry of the cables. Although these effects are relatively small, they may be of major importance in small-signal and high-impedance circuits. In solid-dielectric cables, when no potential is applied between conductors, the net effect leaves the cable with a positive charge on the center conductor with a net scattering of electrons outward. In a partial-air-dielectric such as that of the RG-62/U cable, the net effect is the opposite; that is, a negative charge on the center conductor results in a greater negative voltage pulse at the instant of peak radiation during the nuclear pulse.

Unfortunately, a major portion of the knowledge gained thus far concerning transient radiation effects on coaxial cables is related only to instrumentation requirements found necessary in determining radiation effects on various electronic parts connected to the cable ends. Information that would be useful to applications where long coaxial lines are of prime consideration is not available. The question may often arise as to whether a high-intensity radiation burst occurring at a midway point of a coaxial transmission line would affect its function and whether the effects might cause malfunctioning of electronic equipment at either end of the line. It has been hypothesized that three physical factors might be considered as contributing to the magnitude of induced currents and voltages caused by ionization effects of both neutron fluxes and gamma radiation. These physical factors are (1) length of entire line, (2) thickness of dielectric, and (3) length of exposed portion of line. It has been found that the dielectric thickness for a short line (approximately 75 feet) is independent of an induced voltage pulse for studies[15] made with RG-59/U (1/4 inch in diameter) and the "Microdot" (1/8 inch in diameter) cables. However, when considering longer lines and the possibility that a large portion may be exposed, the dielectric thickness might become a more dependent factor and should not be discounted.

A large portion of the transient radiation effects measured for coaxial cables has been attributed to a state of intense air ionization that exists at the cable termination or radiation source during the instant of peak neutron flux build-up. To counteract these undesirable influences, most experimenters have used acrylic insulating sprays, and others have potted the terminal ends with paraffin. Some of the advantages gained through paraffin applications to terminations are shown in Table 4. Prohibitive values of induced voltages were measured when coaxial connectors were used to terminate the line

TABLE 4. SUMMARY OF TRANSIENT RADIATION EFFECTS ON COAXIAL CABLES

Type of Coaxial Cable	Test Circuit Conditions			Radiation Environment					Effects of Radiation		Reference Numbers	Comments
	Cable Termination, KΩ	Termination Treatment	Voltage Between Cable Conductors, v	Radiation Facility	Gamma Exposure Rate, ergs $g^{-1}(C)\ sec^{-1}$	Total Gamma Exposure, ergs $g^{-1}(C)$	Neutron Flux Rate, n cm^{-2} sec^{-1}	Total Neutron Flux, n cm^{-2}	Parameter Observation Units	Observed Pulse Effects		
RG-59/U	10	None	0	Godiva	--	2.73×10^4	10^{16}	10^{12}	Volts	+0.10	(9)	10 KΩ resistor located 25 feet from exposed cable end
RG-59/U	10	None	+120.0	Godiva	--	2.73×10^4	10^{16}	10^{12}	Volts	-.21	(9)	10 KΩ resistor located 25 feet from exposed cable end
RG-59/U	10	None	+120.0	Godiva	--	2.73×10^4	10^{16}	10^{12}	Volts	-.17	(9)	10 KΩ resistor located 25 feet from exposed cable end
RG-59/U	5	None	+100.0	Godiva	--	2.73×10^4	10^{16}	10^{12}	Volts	-0.10	(9)	5 KΩ resistor located 25 feet from exposed end
RG-62/U	Open	None	0	Godiva II	--	--	10^{17}	10^{13}	Capacity, $\mu\mu f$	-15.0 Pct.	(19)	Cables recovered after 3 milliseconds; no permanent effects reported
RG-59/U	Open	None	0	Godiva II	--	2.73×10^4	10^{16}	10^{12}	Volts	-0.10	(15)	
RG-62/U	Open	None	0	Godiva II	--	2.73×10^4	10^{16}	10^{12}	Volts	-0.90	(15)	Solid dielectric cable
Microdot	Open	None	0	Godiva II	--	2.73×10^4	10^{16}	10^{12}	Volts	-0.10	(15)	Solid dielectric cable
RG-59/U	10	None	0	Godiva II	--	2.73×10^4	10^{16}	6.5×10^{11}	Microamp	+11.3	(16)	Neutron flux rate stated within 20 per cent accuracy
RG-59/U	10	None	+6.0	Godiva II	--	2.73×10^4	10^{16}	6.5×10^{11}	Microamp	+6.1	(16)	Solid dielectric cable
RG-59/U	10	One	+23.0	Godiva II	--	2.73×10^4	10^{16}	6.5×10^{11}	Microamp	0.0	(16)	Near crossover point
RG-59/U	10	One	+45.0	Godiva II	--	2.73×10^4	10^{16}	6.5×10^{11}	Microamp	-6.4	(16)	Approaching saturation with respect to applied voltage

TABLE 4. (Continued)

Type of Coaxial Cable	Test Circuit Conditions: Cable Termination, KΩ	Termination Treatment	Voltage Between Cable Conductors, v	Radiation Environment: Radiation Facility	Gamma Exposure Rate, erg $g^{-1}(C)$ sec^{-1}	Total Gamma Exposure, erg $g^{-1}(C)$	Neutron Flux Rate, n cm^{-2} sec^{-1}	Total Neutron Flux, n cm^{-2}	Effects of Radiation: Parameter Observation Units	Observed Pulse Effects	Reference Number	Comments
RG-59/U	Open	None	0.0	Godiva II	--	2.73×10^4	10^{16}	10^{12}	Volts	-0.13	(20)	Approximately 50 feet of cable; shield grounded
RG-59/U	Open	Waxed	0.0	Godiva II	--	2.73×10^4	10^{16}	10^{12}	Volts	-0.07	(20)	Approximately 50 feet of cable; shield grounded
RG-59/U	Open	None	+45.0	Godiva II	--	2.73×10^4	10^{16}	10^{12}	Volts	-0.03	(20)	Voltage applied between shield and ground
RG-59/U	Open	Waxed	-45.0	Godiva II	--	2.73	10^{16}	10^{12}	Volts	-0.40	(20)	Induced voltage estimated
RG-59/U	Open	Connector	-45.0	Godiva II	--	2.73×10^4	10^{16}	10^{12}	Volts	-1.0	(20)	Induced voltage estimated
RG-59/U	Open	Wax potting	0.0	Godiva II	2.1×10^9	2.9×10^5	--	--	Microamp	+5.3	(21)	Shield grounded
RG-59/U	Open	Wax potting	4.52	Godiva II	1.3×10^9	2.8×10^5	--	--	Microamp	-18.7	(21)	75-ohm input to test cable; shield grounded
RG-59/U	Open	Wax potting	23.5	Godiva II	1.4×10^9	2.65×10^5	--	--	Microamp	+45.3	(21)	75-ohm input to test cable; shield grounded
RG-59/U	Open	Wax potting	34.5	Godiva II	1.4×10^9	3×10^5	--	--	Microamp	+28.2	(21)	75-ohm input to test cable; shield grounded
RG-59/U	Open	Wax potting	94.0	Godiva II	1.6×10^9	3×10^5	--	--	Microamp	-5.3	(21)	75-ohm input to test cable; shield grounded
RG-59/U	Open	Wax potting	185.0	Godiva II	1.6×10^9	3×10^5	--	--	Microamp	+40.8	(21)	75-ohm input to test cable; shield grounded
RG-59/U	Open	Wax potting	380.0	Godiva II	1.3×10^9	2.9×10^5	--	--	Microamp	+87.1	(21)	75-ohm input to test cable; shield grounded
RG-59/U	Open	Wax potting	645.0	Godiva II	1.4×10^9	3.1×10^5	--	--	Microamp	+110.98	(21)	75-ohm input to test cable; shield grounded
RG-59/U	Open	Wax potting	940.0	Godiva II	1.2×10^9	2.8×10^5	--	--	Microamp	+98.47	(21)	75-ohm input to test cable; shield grounded

in an experiment at the Godiva II critical assembly[20]. Thus, it would appear that the effects of air ionization caused by the sudden intense flux build-up on cable terminations can be greatly reduced by proper treatment in the form of potting and by avoiding the use of coaxial cable connectors wherever possible. When it becomes imperative that coaxial cable connectors be used, some steps should be taken to coat the metal outer surface.

It has been mentioned that coaxial cables tend to exhibit charge scattering and increased internal leakage when they are subjected to neutron and gamma pulses. It has been found that when no potential was applied between the center conductor and the shield, the end result was in the form of negative current or voltage pulses[20] which closely resembled the general shape of the time versus radiation flux curve. It was theorized that the negative pulse observed was caused by free electrons produced in the dielectric by both the neutron and gamma pulse, directly from primary interactions, and by secondary reactions on the hydrogenous plastic. These reactions are thought to occur quickly, charging the insulation of the cable positive, and the conductor negative. Some values of these negative pulses are shown in Table 4 for various studies at the Godiva II critical assembly.

Experiments have shown that the application of a negative voltage to the outer shield of a cable during a radiation pulse caused further increases in the observed effects. In contrast, a positive potential applied to the outer shield decreased the effect. Of further interest may be the finding that the first pulse to which the cable was exposed caused the greatest effect. Subsequent exposure to transient radiation pulses displayed tendencies for lesser effects. This has been explained from the standpoint that the insulation becomes positively charged during the pulse, and as such the charge reverts to a residual state. Thus, under further irradiations, electrons leaving the plastic dielectric require greater energies. Therefore, after each irradiation fewer electrons are ejected into the conductors. A second explanation of the decrease in the effect with subsequent irradiation might be that the radiation causes an increase in the resistivity of the organic dielectric. This change in resistivity is considered as a damage mechanism because it has been known for some time that the dielectric properties of some plastic insulators undergo permanent changes at relatively low doses. One of these changes, the increase in resistivity, has been frequently observed. This second explanation should not be construed to indicate that transient radiation exposures tend to improve insulation qualities of the dielectric in comparison with the nonirradiated item.

Radiation-effects researchers who have studied transient effects on coaxial cables have seldom agreed on the exact nature and magnitude of the effects. General agreement has been reached over the possibility that most of the results obtained from past radiation-effects experiments on various component parts may truly have been biased by cable effects. With this consideration in mind, comprehensive studies and experiments were initiated recently to determine dependency of (1) potential between conductor and outer shield, (2) polarity of applied potential, (3) manufacturing processes, (4) peak gamma exposure rate, (5) coil configurations, and (6) spacing between conductors on the magnitude and pulse current shape of radiation-induced currents. These studies were conducted at the Sandia Pulse Reactor facility[22].

The above-mentioned research experiments to determine dependency of voltage and voltage polarity were conducted by exposing 40 Type RG-59/U coaxial cables to single bursts of gamma radiation. The cable end configuration consisted of a termination of two wires approximately 1 inch long and spaced 1/4 inch apart. A typical arrangement

and test circuit are shown in Figures 5 and 6. The magnitude of applied potentials and their polarity with respect to the center conductor and shield for the experiment are listed in Table 5. A positive voltage value indicates that the shield is positive with respect to the center conductor. Table 5 also includes information concerning the peak gamma rate, the observed radiation-induced current, and an approximate shape of the current pulse for each cable tested. Contrary to some previous theories expounded on the effects of voltages and polarity, the magnitude of the induced currents appears to increase with voltage, and the dependency of polarity on these current values is not clearly indicated. It is believed that the inconsistencies or disagreement between results from this experiment and previous studies could be attributed to possible differences in cable impedance, positioning of cable ends with respect to the radiation source, and the paraffin coating of the open ends of the cable. Since there are some differences in the peak gamma rate for the various cables, some indication exists in the data that might explain dissimilarities between the measured current pulses. For example, Cable 13 (with +140.55 volts) can be compared with Cable 36 (with -140.63 volts) where it can be seen that the peak gamma rates are reasonably close in value with correspondingly similar induced-current pulses. In a number of instances where cables are subjected to successively higher voltages, a decrease in induced peak current occurred. In a majority of instances, the general trend is established where greater effects were measured for each successive increase in voltage. In this latter instance, it would appear that the dielectric has become more conductive, and with higher voltages more leakage current flows through the dielectric. The approximate shapes of the pulse current during the radiation pulse are given also in Table 5 for the purpose of showing their general trends. Distinct oscillations were observed for voltages up to 50 volts. These oscillations contained both positive and negative segments. At the higher voltages, some of the oscilloscope traces showing the voltage pulse contained fluctuations and others exhibited plateaus. Over the entire voltage range, there were traces that were approximately proportional to the radiation pulse. For a few negative voltage conditions, the polarity of the trace was in question, and these are indicated by the + sign shown on the trace.

Differences in manufacturing techniques for the same cable types have been considered as a possibility for some disagreement among various researchers, in observed effects caused by transitory radiation. To resolve this question, a study[22] was made with RG-59/U coaxial cables of three manufacturers. The cables were prepared in the manner shown in Figure 6. The results from the experimental work for the three manufacturers' cables are shown in Table 6. It can be seen that the RG-59/U coaxial cables of Manufacturers A and B did not differ appreciably. The coaxial cable from Manufacturer C exhibited fewer effects than those from Manufacturers A and B. The other cables shown in Table 3, listed as twinax and triax cables (Amphenol RG-108A/U and RG-59A/U, respectively) were irradiated for comparison purposes. It can be seen that the triax cable appears to be less affected than the twinax cable. The triax cable in this experiment is identical to the Type RG-59A/U cable with the exception of the added outer shield. The twinax cable is essentially a twisted pair of insulated wires with an outer shield, and its poor performance might be attributed to the proximity of the positive and negative wires in the encasment.

The question often arises as to whether a coaxial cable used for experimentation can be re-used in subsequent studies. An exploratory study for the solution of this problem was made by exposing a Type RG-59A/U coaxial cable to ten successive radiation pulses[22] at the Sandia Pulsed Reactor facility. The results of this study are presented in Table 7. In examining the results, two observations can be made. The

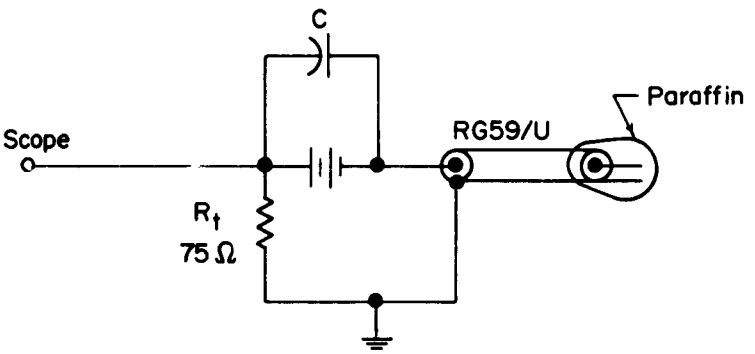

FIGURE 5. TEST CIRCUIT FOR OPEN CABLES

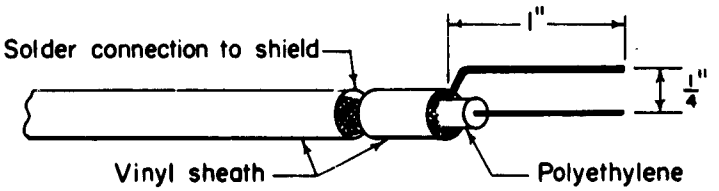

FIGURE 6. END CONFIGURATION FOR COAXIAL-CABLE TESTS

TABLE 5. TRANSIENT RADIATION EFFECTS ON RG-59/U COAXIAL CABLES AS A FUNCTION OF D-C POTENTIAL AND GAMMA EXPOSURE RATE

Cable Number	Potential Applied	Peak Gamma Rate, 10^9 ergs $g^{-1}(C)$ sec^{-1}	Observed Peak Current Pulse Value, 10^{-4} amp	Approximate Shape of Pulse
1	0	3.327	0.0723	
2	3.098	3.33	--	
3	9.366	3.202	0.1079	
4	17.11	3.654	0.2194	
5	23.487	3.77	0.1394	
6	27.87	2.970	0.2160	
7	34.07	2.722	0.1370	
8	47.007	2.996	--	
9	58.54	2.685	0.2710	
10	81.94	2.816	0.3100	
11	94.18	4.090	0.4780	
12	117.15	3.920	0.3470	
13	140.55	3.189	0.3685	
14	164.96	2.820	0.3270	
15	187.60	2.893	0.3550	
16	236.48	4.770	0.7190	
17	282.84	3.747	0.550	
18	331.90	3.560	0.9450	
19	375.13	2.665	0.7980	
20	426.75	2.771	0.8440	

TABLE 5. (Continued)

Cable Number	Potential Applied	Peak Gamma Rate, 10^9 ergs $g^{-1}(C)$ sec^{-1}	Observed Peak Current Pulse Value, 10^{-4} amp	Approximate Shape of Pulse
21	490.00	2.762	0.8650	
22	598.0	2.782	0.8190	
23	628.0	2.6460	2.2050	
24	690.0	2.646	0.8140	
25	786.9	3.551	0.8670	
26	915.0	2.594	0.9640	
27	0	5.121	0.1097	
28	-3.0763	2.802	0.0621	
29	-6.30	5.896	0.1177	
30	-9.04	3.088	0.0954	
31	-17.13	3.576	--	
32	-23.371	3.910	0.1440	
33	-23.371	3.057	0.2090	
34	-46.80	2.735	0.3370	
35	-94.33	3.635	0.0953	
36	-140.63	3.309	0.3070	
37	-235.74	4.887	0.9100	
38	-426.37	2.782	2.610	
39	-643.0	2.646	0.8140	
40	-920.0	2.547	2.950	

TABLE 6. TRANSIENT RADIATION EFFECTS ON RG-59/U COAXIAL CABLES OF VARIOUS MAKES AND MANUFACTURE AS A FUNCTION OF D-C POTENTIAL AND GAMMA EXPOSURE RATE

Manufacturer or Make	Potential Applied	Peak Gamma Rate, 10^9 ergs $g^{-1}(C)$ sec^{-1}	Observed Peak Current Pulse Value, 10^{-4} amp	Approximate Shape of Current Pulse
Mfr. A RG-59/U	376.19	3.4	1.16	
Mfr. A RG-59/U	376.17	2.77	1.094	
Mfr. B RG-59/U	369.1	3.33	1.186	
Mfr. E RG-59/U	376.2	4.84	1.389	
Mfr. C RG-59/U	370.03	2.91	0.6422	
Mfr. C RG-59/U	370.20	4.66	0.7622	
Twinax	46.65	2.954	1.13	
RG-108A/U	6.3	4.494	--	
RG-108A/U	280.98	3.298	81.0	
Triax	46.808	3.037	0.195	
RG-59A/U	6.25	4.339	--	
RG-59A/U	281.0	3.77	1.370	

TABLE 7. TRANSIENT RADIATION EFFECTS ON RG-59A/U COAXIAL CABLES AS A FUNCTION OF PEAK GAMMA EXPOSURE RATE

Shot Number	Potential Applied	Peak Gamma Rate, 10^9 ergs $g^{-1}(C)$ sec^{-1}	Observed Peak Current Pulse Value, 10^4 amp	Approximate Shape of Current Pulse
1	376.0	6.067	1.159	
2	116.8	6.570	0.160	
3	360.0	3.59	--	
4	370.0	5.596	--	
5	369.78	5.32	0.586	
6	369.7	2.747	0.863	
8	375.2	3.863	1.014	
9	375.0	3.63	0.480	
10	375.33	1.076	0.48	

first is that there is a tendency for the peak current pulse to decrease during the series of pulses by radiation exposure. The second is concerned with the influence of exposure rate shown between radiation pulse Number 1 and Number 10. It would appear that the earlier theory in which it was mentioned that the plastic dielectric tends to become less conductive with prolonged radiation exposure might be valid.

It was hypothesized that the charges produced within the dielectric of the coaxial cable are collected by the conductors, suggesting that the radiation-induced current is dependent on the length of cable exposed to radiation. To test this hypothesis, an experiment was performed in which cables were coiled around the reactor safety screen with 1, 2, and 4 turns. Three different voltage conditions - 0, 9, and 280 volts – were applied. The results of this study are shown in Table 8. The effects of the radiation pulses are shown in both negative and positive values of pulse current to aid in evaluation of the approximate wave shapes given in the tabulations. It can be seen that when no voltage is applied to the cables, the net effects for the 4-turn arrangement are greater than for the 1-turn and 2-turn configurations. When the applied voltage is increased to approximately 9 and 280 volts, the dependency of the number of turns diminishes. These results tend to negate the assumption of a simple relationship between magnitude of induced current and the length of cable irradiated; however, they also indicate that the applied voltage must be considered as a cause for the inconsistency.

The exploration study conducted to determine the dependency[22] of distance between conductors of an open transmission line to the radiation-induced current was performed by exposing two transmission lines to radiation pulses. The first open transmission line consisted of Number 14 wires spaced 4 inches apart. The second transmission line consisted of Number 18 wires spaced 1 inch apart. Although the second transmission line was subjected to a less intense radiation pulse, the effects (shown in Table 9) were much greater. It was concluded that the increased separation between the conductors should and did result in lower leakage current. However, the current in each case was high in comparison with results shown for the various coaxial cables, which would indicate that the coaxial cables are superior to the open transmission lines. In direct comparisons between coaxial lines and open transmission lines it was postulated, on the basis of the studies, that an open transmission line would require a spacing of approximately 8 inches between conductors before they can compare favorably. The study of transient radiation effects for twisted wires (see Table 9) indicated that the radiation effects were extremely high and approximately 20 times the effects measured for the RG-59/U cable.

In conclusion, the insight gained through research by various organizations serves to point to vital areas of concern. Much more study and research are needed to correctly identify conditions of cable configurations, termination treatment, construction, impedance, and potential conditions which will tend to minimize the effects of transient radiation. The information made available to this point has emphasized that:

(1) The first radiation pulse can be expected to produce the greatest effect.

(2) The use of solid dielectrics such as polyethylene and polystyrene seems to reduce the undesirable effects.

(3) Partial-air-dielectric coaxial cables and open or twisted transmission lines can be expected to exhibit appreciable transitory effects.

TABLE 8. TRANSIENT RADIATION EFFECTS ON COILED RG-59/U COAXIAL CABLES AS A FUNCTION OF APPLIED POTENTIAL

Number of Turns in Coil	Potential Applied	Peak Gamma Rate, 10^9 ergs $g^{-1}(C)$ sec^{-1}	Peak-Current Values, 10^{-6} amp		Approximate Shape of Current Pulse
			Positive	Negative	
1	0	2.81	5.25	7.88	
1	9.288	2.647	12.93	3.88	
1	278.9	2.06	100.40	--	
2	0	2.445	8.41	14.23	
2	9.34	2.019	12.28	7.76	
2	279.02	1.638	56.67	--	
4	0	3.389	11.64	35.60	
4	9.289	1.930	6.40	7.76	
4	279.0	2.121	63.5	--	

TABLE 9. TRANSIENT RADIATION EFFECTS ON OPEN-TRANSMISSION AND TWISTED-WIRE LINES AS A FUNCTION OF PHYSICAL CONFIGURATIONS

Type of Line	Potential Applied, v	Peak Gamma Rate, 10^9 ergs g^{-1}(C) sec^{-1}	Observed Peak-Current Pulse, Value, milliamp
Open transmission line, No. 14 wire, spaced 4 inches apart	472.8	2.20	0.213 ± 0.05
Open transmission line, No. 18 wire, spaced 1 inch apart	468.7	0.89	1.20 ± 0.27
Twisted pair, No. 22 wires, vinyl-thermoplastic wire	3.08	4.08	0.105 ± 0.02
Ditto	6.00	2.60	0.125 ± 0.025

(4) Some treatment of coaxial-cable terminations such as paraffin coatings or acrylic sprays reduces air ionization effects.

(5) The use of coaxial connectors should be avoided.

(6) The magnitude of induced pulse current is dependent under certain conditions on the length of the line.

(7) The d-c potential between the center conductor and shield, and its polarity can add to or detract from the over-all effects under certain physical conditions.

Electron Tubes

The transient radiation effect on electron tubes is of a transient nature. The seriousness of the effect depends on the type of tube and its application. The observed effect of transient radiation in many types of electron tubes could be considered insignificant when compared to the tolerances of the circuit and the magnitude of the radiation effects of other components in the same circuit.

In most cases the sample size for radiation-effects studies on a special type of electron tube has been small. In early transient radiation experiments, 1957-1958, the dosimetry and instrumentation techniques were relatively poor, and hence the accuracy of the data generated during this time must be considered questionable. As can be seen from Table 10, a considerable amount of the electron-tube data was obtained during this "early" period. Because of the small sample size (in most cases) and inaccurate data, there is little evidence to support any hypothesis. However, it seems reasonable to assume the effects commonly induced in vacuum tubes by transient radiation are those arising from (1) induced grid charge (2) gas evolution from elements and walls, (3) decrease in conductivity of insulators, and/or (4) ionization of residual gases.

Image orthicon tubes (television pickup tubes) were exposed at two different transient radiation facilities. No effects were observable in the video response of a Z-5358 image orthicon tube during a gamma exposure of 4.4×10^6 ergs $g^{-1}(C)$ sec^{-1} in a 1-Mev Cockroft-Walton electron accelerator.[33] One Z-5358 and three GL-7629 image orthicon tubes were exposed to a pulse of radiation from a Mark F reactor. No transient measurements were made. However, all tubes performed satisfactorily following the exposure. Browning of the glass envelopes was detectable for tubes receiving over two exposures of transient radiation.[33]

In another test a vidicon camera head with preamplifier, and an image orthicon camera head were subjected to several pulses of radiation from a Triga Mark F pulse reactor.[36] As a result of the vidicon camera head being subjected to a pulse of radiation, there was a loss of video information at the monitor screen for approximately 1/10 second. Most of the resistors above 600 kilohms in the vidicon subsystem were found to be outside their per cent tolerance limits but within 11 per cent of the nominal value after being exposed to the transient radiation environment. The permanent change observed in the image orthicon subsystem was caused by faceplate browning and/or electrical characteristic change (i.e., beam and photocathode current).

TABLE 10. SUMMARY OF TRANSIENT RADIATION EFFECTS ON ELECTRON TUBES

Type of Tube	Tube Type Number	Plate Voltage, v	Bias Voltage, v	Filament Voltage, v	Preburst Current, ma	Sample Size	Maximum Gamma Exposure Rate, ergs $g^{-1}(C)$ $sec^{-1} \times 10^8$	Current Change, μa	Voltage Change, v	Manufacturer	Reactor	Experiment	Date of Test	Reference
Voltage regulator	OB2		+110			1		(a)	-5		Godiva	Hughes	1958	9
Voltage regulator						1			-3.3		Godiva	Hughes	1958	9
Voltage regulator						1					Godiva	Hughes	1958	9
Voltage regulator	OB2					1		90		Westinghouse	Godiva	IBM	Jan 59	24
Voltage regulator	OB2					1		1360			Godiva	IBM	Jan 59	24
Voltage regulator						1		170(b)			Godiva	IBM	May 59	26
Voltage regulator						1		390(b)			Godiva	IBM	May 59	26
Photomultiplier	1P28					1	9×10^{-7}	<8		RCA	Godiva	IBM	Apr 60	29
Photomultiplier	1P28						2.7×10^{-5}	2290 ± 60		RCA	Godiva	IBM	Apr 60	29
Photomultiplier	1P28					1	1.8	8900 ± 500		RCA	Godiva	IBM	Apr 60	29
Beam power amplifier	829B					2		(d)			Nuclear burst	DOFL	1958	34
Receiving	1724G					1		(e)		Sylvania	Godiva	USASRDL	Oct 58	35
Receiving	1724G					1		(e)		Sylvania	Godiva	USASRDL	Oct 58	35
Receiving	1724G					1		(e)		Sylvania	Godiva	USASRDL	Oct 58	35
Receiving	1724G					1		(f)		Sylvania	Godiva	USASRDL	Oct 58	35
Receiving	1724G					1		(f)		Sylvania	Godiva	USASRDL	Oct 58	35
Receiving	2146B					1		(g)		Sylvania	Godiva	USASRDL	Oct 58	35
Receiving	2146B					1		(g)		Sylvania	Godiva	USASRDL	Oct 58	35
Receiving	2146B					1		(g)		Sylvania	Godiva	USASRDL	Oct 58	35

TABLE 10. (Continued)

Type of Tube	Tube Type Number	Plate Voltage, v	Bias Voltage, v	Filament Voltage, v	Preburst Current, ma	Sample Size	Maximum Gamma Exposure Rate, ergs g^{-1}(C) sec^{-1} x 10^8	Current Change, μa	Voltage Change, v	Manufacturer	Reactor	Experiment	Date of Test	Reference
Receiving	2146B					1		(g)		Sylvania	USA	USASRDL	Oct 58	35
Receiving	2146B					1		(f)		Sylvania	Godiva	USASRDL	Oct 58	35
Receiving	2146B					1		(f)		Sylvania	Godiva	USASRDL	Oct 58	35
Receiving	2225A					1		(h)		Sylvania	Godiva	USASRDL	Oct 58	35
Receiving	2225A					1		(h)		Sylvania	Godiva	USASRDL	Oct 58	35
Receiving	2225A					1		(h)		Sylvania	Godiva	USASRDL	Oct 58	35
Receiving	2225A					1		(f)		Sylvania	Godiva	USASRDL	Oct 58	35
Receiving	2225A					1		(f)		Sylvania	Godiva	USASRDL	Oct 58	35
Ceramic dual triode	SN2225A					100		(d)			Nuclear burst	DOFL	1958	34
Ceramic triode	Z2389					99		(d)			Nuclear burst	DOFL	1958	34
Glass	5636					4	34.5(c)	300		Sylvania	Godiva	IBM	Aug 58	11
Glass	5636					5	58.1(c)	900		Sylvania	Godiva	IBM	Aug 58	11
Glass	5636					10	36.4(c)	650		Sylvania	Godiva	IBM	Aug 58	11
Glass	6111					1	6.2(c)	1010		Sylvania	Godiva	IBM	Aug 58	11
Glass	6111					5	3.5(c)	630		Sylvania	Godiva	IBM	Aug 58	11
T-3 guided-missile-type	6947					32		(d)			Nuclear burst	DOFL	1953	34
Dual triode	6948					68		(d)			Nuclear burst	DOFL	1958	34
Ceramic	7077					1	0.9(c)	2450		GE	Godiva	IBM	Aug 58	11
Ceramic	7077					6	71.8(c)	1500		GE	Godiva	IBM	Aug 58	11
Ceramic	7077					7	43.6(c)	750		GE	Godiva	IBM	Aug 58	11
Ceramic	7077					10	82.7(c)	1500		GE	Godiva	IBM	Aug 58	11

TABLE 10. (Continued)

Type of Tube	Tube Type Number	Plate Voltage, v	Bias Voltage, v	Filament Voltage, v	Preburst Current, ma	Sample Size	Maximum Gamma Exposure Rate, ergs $g^{-1}(C)$ $sec^{-1} \times 10^8$	Current Change, μa	Voltage Change, v	Manufacturer	Reactor	Experiment	Date of Test	Reference
Image orthicon	Z5358						3.6	(d)		GE	Mark F	GE	Aug 58	33
Image orthicon	GL7629						2.6	(d)		GE	Mark F	GE		33
Image orthicon	GL7629						2.6	(d)		GE	Mark F	GE		33
Image orthicon	GL7629						2.6	(d)		GE	Mark F	GE		33
Image orthicon	GL7629						2.6	(d)		GE	Mark F	GE		33
Image orthicon							5.87				Mark F	FA	Mar 61	36
Vidicon						1	5.87				Mark F	FA	Oct 61	36
Gas diode	GEXD400						12.7	(j)			Godiva	IBM	Apr 60	29
Gas diode	GEXD400						2.5	(j)			Godiva	IBM	Apr 60	29
Gas diode	GEXD400						13.6	(j)			Godiva	IBM	Apr 60	29
Pentode subminiature	5702	120	-0.8	Hot		1			2.4					9
Pentode subminiature	5702	120	-0.8	Cold		1			0.89		Godiva	Hughes	1958	9
T-3 pentode triode	5702WA					100		(d)			Godiva	Hughes	1958	34
Subminiature	5703	120	0			1		70	0.66		Nuclear burst	DOFL	1958	9
T-3 triode	5718					100		(d)			Godiva	Hughes	1958	34

TABLE 10. (Continued)

Type of Tube	Tube Type Number	Plate Voltage, v	Bias Voltage, v	Filament Voltage, v	Preburst Current, ma	Sample Size	Maximum Gamma Exposure Rate, ergs g^{-1}(C) sec^{-1} x 10^{8}	Current Change, μa	Voltage Change, v	Manufacturer	Reactor	Experiment	Date of Test	Reference
Pentode	5840					100		(d)			Nuclear burst	DOFL	1958	34
Glass	5840					5	100.0[c]	820		RCA	Nuclear burst	DOFL	1958	11
Glass	5840					7	(c)	800		RCA	Godiva	IBM	Aug 58	11
Glass	5840					10	27.3[c]	360		RCA	Godiva	IBM	Aug 58	11
Duo-diodes	5896	90		6.3	4.050	1	0.6[i]	117		Sylvania	Godiva	IBM	Aug 58	24
Duo-diodes	5896	90		6.3	4.200	1	5.2[i]	141		Sylvania	Godiva	IBM	Aug 58	24
Duo-diodes	5896	90		6.3	4.050	1	5.1[i]	141		Sylvania	Godiva	IBM	Jan 59	24
Duo-diodes	5896	90		6.3	4.270	1	7.1[c]	257		Sylvania	Godiva	IBM	Jan 59	24
Duo-diodes	5896	90		0	0	1	7.0[c]	414		Sylvania	Godiva	IBM	Jan 59	24
Duo-diodes	5896	90		0	0	1	6.9[c]	331		Sylvania	Godiva	IBM	Jan 59	24
Duo-diodes	5896	-86		6.3	0	1	4.1[i]	412		Sylvania	Godiva	IBM	Jan 59	24
											Godiva	IBM	Jan 59	24
Gas diode	GEXD400						2.2	(j)			Godiva	IBM	Apr 60	29
Gas diode	GEXD400						17.3	(j)			Godiva	IBM	Apr 60	29
Gas diode	GEXD 400						2.5	(j)			Godiva	IBM	Apr 60	29
Ceramic triode	RO171					200		(d)			Nuclear burst	DOFL	1958	34
VT fuze	SN891B					88		(d)			Nuclear burst	DOFL	1958	34
VT fuze	QF826					130		(d)			Nuclear burst	DOFL	1958	34
VT fuze	QF826					130		(d)			Nuclear burst	DOFL	1958	34
VT fuze	BL-102					31		(d)			Nuclear burst	DOFL	1958	34

TABLE 10. (Continued)

Type of Tube	Tube Type Number	Plate Voltage, v	Bias Voltage, v	Filament Voltage, v	Preburst Current, ma	Sample Size	Maximum Gamma Exposure Rate, ergs g^{-1}(C) sec^{-1} x 10^{8}	Current Change, μa	Voltage Change, v	Manufacturer	Reactor	Experiment	Date of Test	Reference
VT fuze	N-67				100		(d)				Nuclear burst	DOFL	1958	34
Low power klystron	R-1B				12		(d)				Nuclear burst	DOFL	1958	34

(a) Became conducting during pulse.
(b) Change may be due to exposed resistor.
(c) Overestimates of actual exposure rates.
(d) No measurements made during burst.
(e) Signal was attenuated to about 2/3 of its original value.
(f) Signal was only slightly affected.
(g) Signal was completely attenuated.
(h) Signal was attenuated to almost zero.
(i) Value is known to be in error.
(j) Tube fitted.

The dark current of a photomultiplier tube, as might be expected, was significantly increased even at very low gamma exposure rates, as can be seen in Table 10. The relationship between the change in dark current and gamma exposure rate is not known because of the limited data.[29]

A large sample of electron tubes was exposed to the radiation environment of a nuclear burst. Pre- and postirradiation measurements indicated that the electron tubes experienced no permanent damage due to radiation. No transient measurements were made.[34]

All the transient-radiation-effects data on electron tubes, with the exception of thyratron tubes, are presented in Table 10. The data for thyratron tubes are presented in Tables 11 and 12. Two types of thyratron tubes are exceptions to the general case for electron tubes in that there is a considerable amount of transient-radiation-effects data of relatively recent origin (1960, 1961). These transient-radiation-effects data on thyratron tubes support the hypothesis that the gamma exposure rate necessary to fire a thyratron is a function of the negative excell bias, E_{cgx}. This negative excell bias is simply

$$E_{cgx} = E_{cc} - E_{cg} \quad ,$$

where E_{cc} is the applied grid bias and E_{cg} is the critical grid bias for the plate voltage used when the screen grid is tied to the cathode.[22] Figure 7 is a plot of the E_{cgx} versus gamma exposure rate for Type 2D21 thyratron tubes. The demarcation between the fired and not fired tubes, though not absolute, gives an indication of what one could expect from a 2D21 thyratron tube exposed to a pulse of radiation. The equation of the line implying the demarcation between the fired and not fired 2D21 thyratron tubes in Figure 7 is $E_{cgx} = 1.55 \times 10^{-9}$ times the gamma exposure rate in ergs $g^{-1}(C)\ sec^{-1}$.[22] This line of demarcation should be considered to have a questionable firing region of 10 per cent on either side.

The data available on the 5643 thyratron tubes are insufficient to state that the relationship between the gamma exposure rate and the excess critical grid voltage is linear. However, it does not preclude this as a possibility. The data for Type 5643 thyratron tubes are presented in Figure 8.[21] Since most of the data on thyratron tubes were generated by the same experimenter and in the same simulation facility, some factors concerning radiation effects may not have become apparent.

Resistors

The transient radiation effects on resistors are still not fully understood. Because of the variety of resistor types investigated, it is difficult to obtain a statistically significant sample size for any given type. Obtaining accurate measurements of the transient radiation environment is also a problem. However, the available data give some insight to the transient radiation effects on resistors.

The cause of the effect observed when a resistor is exposed to a pulse of radiation is generally explained in two ways:

TABLE 11. SUMMARY OF TRANSIENT RADIATION EFFECTS ON 2D21 THYRATRON TUBES

Plate Voltage, v	Grid Bias, v	Critical Grid Bias, v	Negative Excess Bias, v	Maximum Gamma Exposure Rate for Tubes Not Fired, ergs g^{-1} (C) $sec^{-1} \times 10^8$	Maximum Gamma Exposure Rate for Tubes Fired, ergs g^{-1} (C) $sec^{-1} \times 10^8$	Reactor	Experimenter	Date of Test	Reference
350	-3			1.73[a]	3.55[b]	Godiva	IBM	Jul 60	21
250	-2.7			4.29[a]	8.58[b]	Godiva	IBM	Jul 60	21
350	-2.8			--	--	Godiva	IBM	Jul 60	21
250	-2.4			2.18[a]	4.27[b]	Godiva	IBM	Jul 60	21
350	-2.9			1.55[a]	3.18[b]	Godiva	IBM	Jul 60	21
400	-2.6			3.00[a]	6.00[b]	Godiva	IBM	Jul 60	21
138	-2	-1.75	0.25		22.6	Godiva	IBM	Nov 59	26
185	-4	-0.75	3.25	3.73		Godiva	IBM	Nov 59	26
185	-4	-1.8	2.2		42.77	Godiva	IBM	Nov 59	26
133				7.54		Godiva	IBM	Jan 59	24
132				5.36		Godiva	IBM	Jan 59	24
			1.398	6.37		SPRF	IBM	Jan 61	22
			0.682	4.26		SPRF	IBM	Jan 61	22
			0.586	2.06		SPRF	IBM	Jun 61	22
			0.537	2.97		SPRF	IBM	Jun 61	22
			0.509	0.70		SPRF	IBM	Jun 61	22
			0.454	1.14		SPRF	IBM	Jun 61	22
			0.169	0.79		SPRF	IBM	Jun 61	22
			0.464	3.06		SPRF	IBM	Jun 61	22
			0.368	1.88		SPRF	IBM	Jun 61	22
			0.292	1.40		SPRF	IBM	Jun 61	22
			0.237	1.71		SPRF	IBM	Jun 61	22
			0.104	0.67		SPRF	IBM	Jun 61	22
			0.414	2.01		SPRF	IBM	Jun 61	22
			0.354	1.10		SPRF	IBM	Jun 61	22
			0.847	1.35		SPRF	IBM	Jun 61	22
			0.828	1.31		SPRF	IBM	Jun 61	22
			0.792	3.39		SPRF	IBM	Jun 61	22
			0.586	2.87		SPRF	IBM	Jun 61	22
			0.477	1.75		SPRF	IBM	Jun 61	22
			0.524	0.419		SPRF	IBM	Jun 61	22
			0.506	0.446		SPRF	IBM	Jun 61	22
			0.469	1.28		SPRF	IBM	Jun 61	22
			0.263	1.09		SPRF	IBM	Jun 61	22
			0.716	0.490		SPRF	IBM	Jun 61	22
			0.656	0.527		SPRF	IBM	Jun 61	22
			0.484	1.50		SPRF	IBM	Jun 61	22

TABLE 11. (Continued)

Plate Voltage, v	Grid Bias, v	Critical Grid Bias, V	Negative Excess Bias, v	Maximum Gamma Exposure Rate for Tubes Not Fired, ergs g^{-1} (C) sec^{-1} x 10^8	Maximum Gamma Exposure Rate for Tubes Fired, ergs g^{-1} (C) sec^{-1} x 10^8	Reactor	Experimenter	Date of Test	Reference
			1.61	0.758		SPRF	IBM	Jun 61	22
			1.55	0.815		SPRF	IBM	Jun 61	22
			1.38	2.32		SPRF	IBM	Jun 61	22
			1.27	3.10		SPRF	IBM	Jun 61	22
			1.24	4.94		SPRF	IBM	Jun 61	22
			1.17	1.77		SPRF	IBM	Jun 61	22
			0.963	1.19		SPRF	IBM	Jun 61	22
			0.627	0.624		SPRF	IBM	Jun 61	22
			0.568	0.671		SPRF	IBM	Jun 61	22
			0.931	0.818		SPRF	IBM	Jun 61	22
			0.758	4.96		SPRF	IBM	Jun 61	22
			0.686	0.761		SPRF	IBM	Jun 61	22
			0.648	1.83		SPRF	IBM	Jun 61	22
			0.614	3.12		SPRF	IBM	Jun 61	22
			0.544	2.32		SPRF	IBM	Jun 61	22
			0.340	1.19		SPRF	IBM	Jun 61	22
			1.015		54.0	SPRF	IBM	Jun 61	22
			0.958		41.5	SPRF	IBM	Jun 61	22
			0.958		22.0	SPRF	IBM	Jun 61	22
			0.798		53.5	SPRF	IBM	Jun 61	22
			0.740		36.3	SPRF	IBM	Jun 61	22
			0.740		20.5	SPRF	IBM	Jun 61	22
			0.643		4.82	SPRF	IBM	Jun 61	22
			0.320		2.37	SPRF	IBM	Jun 61	22
			0.672		86.0	SPRF	IBM	Jun 61	22
			0.636		49.3	SPRF	IBM	Jun 61	22
			0.482		6.22	SPRF	IBM	Jun 61	22
			0.463		24.9	SPRF	IBM	Jun 61	22
			0.427		3.27	SPRF	IBM	Jun 61	22
			0.220		1.45	SPRF	IBM	Jun 61	22
			0.056		3.03	SPRF	IBM	Jun 61	22
			1.04		90.5	SPRF	IBM	Jun 61	22
			1.00		35.4	SPRF	IBM	Jun 61	22
			0.779		49.7	SPRF	IBM	Jun 61	22
			0.721		4.66	SPRF	IBM	Jun 61	22
			0.421		7.49	SPRF	IBM	Jun 61	22

TABLE 11. (Continued)

Plate Voltage, v	Grid Bias, v	Critical Grid Bias, V	Negative Excess Bias, v	Maximum Gamma Exposure Rate for Tubes Not Fired, ergs g^{-1} (C) sec^{-1} x 10^8	Maximum Gamma Exposure Rate for Tubes Fired, ergs g^{-1} (C) sec^{-1} x 10^8	Reactor	Experimenter	Date of Test	Reference
			0.714		25.3	SPRF	IBM	Jun 61	22
			0.678		12.3	SPRF	IBM	Jun 61	22
			0.456		20.5	SPRF	IBM	Jun 61	22
			0.397		1.87	SPRF	IBM	Jun 61	22
			0.097		2.89	SPRF	IBM	Jun 61	22
			0.690		33.6	SPRF	IBM	Jun 61	22
			0.675		13.1	SPRF	IBM	Jun 61	22
			0.411		22.6	SPRF	IBI	Jun 61	22
			0.374		2.61	SPRF	IBM	Jun 61	22
			0.339		3.17	SPRF	IBM	Jun 61	22
			0.269		0.974	SPRF	IBM	Jun 61	22
			1.59		52.1	SPRF	IBM	Jun 61	22
			1.57		20.3	SPRF	IBM	Jun 61	22
			1.31		34.7	SPRF	IBM	Jun 61	22
			0.602		42.8	SPRF	IBM	Jun 61	22
			0.591		16.7	SPRF	IBM	Jun 61	22
			0.395		1.91	SPRF	IBM	Jun 61	22
			0.323		28.9	SPRF	IBM	Jun 61	22
			0.286		2.56	SPRF	IBM	Jun 61	22
			0.251		4.07	SPRF	IBM	Jun 61	22
			0.181		1.37	SPRF	IBM	Jun 61	22
			0.990		20.3	SPRF	IBM	Jun 61	22
			0.965		52.1	SPRF	IBM	Jun 61	22
			0.949		34.7	SPRF	IBM	Jun 61	22
	4.0	2.3910	1.6090		12.0	SPRF	IBM	Jun 61	22
	87.0	2.7116	84.288	23.59					
	87.0	2.3910	84.6090	25.31					
	4.0	2.7116	1.2884		8.4				

TABLE 12. SUMMARY OF TRANSIENT RADIATION EFFECTS ON 5643 THYRATRON TUBES

Plate Voltage, v	Grid Bias, v	Critical Grid Bias, v	Negative Excess Bias, v	Maximum Gamma Exposure Rate for Tubes Not Fired, ergs g^{-1} (C) $sec^{-1} \times 10^8$	Maximum Gamma Exposure Rate for Tubes Fired, ergs g^{-1} (C) $sec^{-1} \times 10^8$	Reactor	Experimenter	Date of Test	Reference
300		-2.0				Godiva	Hughes	1958	9
						Godiva	Hughes	1959	16
						Godiva	Hughes	1959	16
						Godiva	Hughes	1959	16
450		-2.5		1 to 10		Kukla	Boeing	Jun 60	31
			1.16	5.46		SPRF	IBM	Jun 61	22
			1.00	2.56		SPRF	IBM	Jun 61	22
			0.968	3.43		SPRF	IBM	Jun 61	22
			0.947	0.900		SPRF	IBM	Jun 61	22
			0.918	1.62		SPRF	IBM	Jun 61	22
			0.825	1.31		SPRF	IBM	Jun 61	22
			0.506	0.837		SPRF	IBM	Jun 61	22
			0.522	2.43		SPRF	IBM	Jun 61	22
			0.306	0.401		SPRF	IBM	Jun 61	22
			0.807	1.92		SPRF	IBM	Jun 61	22
			0.695	0.674		SPRF	IBM	Jun 61	22
			0.644	1.11		SPRF	IBM	Jun 61	22
			0.591	2.57		SPRF	IBM	Jun 61	22
			0.562	0.983		SPRF	IBM	Jun 61	22
			0.406	4.09		SPRF	IBM	Jun 61	22
			1.24		57.3	SPRF	IBM	Jun 61	22
			1.12		38.7	SPRF	IBM	Jun 61	22
			1.05		22.4	SPRF	IBM	Jun 61	22
			0.443		41.0	SPRF	IBM	Jun 61	22
			0.365		3.91	SPRF	IBM	Jun 61	22
			0.320		27.7	SPRF	IBM	Jun 61	22
			0.254		16.0	SPRF	IBM	Jun 61	22
			0.202		1.83	SPRF	IBM	Jun 61	22
			0.170		2.45	SPRF	IBM	Jun 61	22
			0.150		0.644	SPRF	IBM	Jun 61	22
			0.121		1.19	SPRF	IBM	Jun 61	22
			0.600		25.6	SPRF	IBM	Jun 61	22
			0.476		17.3	SPRF	IBM	Jun 61	22
			0.410		10.0	SPRF	IBM	Jun 61	22
			0.359		1.14	SPRF	IBM	Jun 61	22
			0.327		1.53	SPRF	IBM	Jun 61	22
			0.277		0.743	SPRF	IBM	Jun 61	22
			0.118		0.586	SPRF	IBM	Jun 61	22
			0.885		42.9	SPRF	IBM	Jun 61	22
			0.761		16.8	SPRF	IBM	Jun 61	22
			0.611		29.0	SPRF	IBM	Jun 61	22

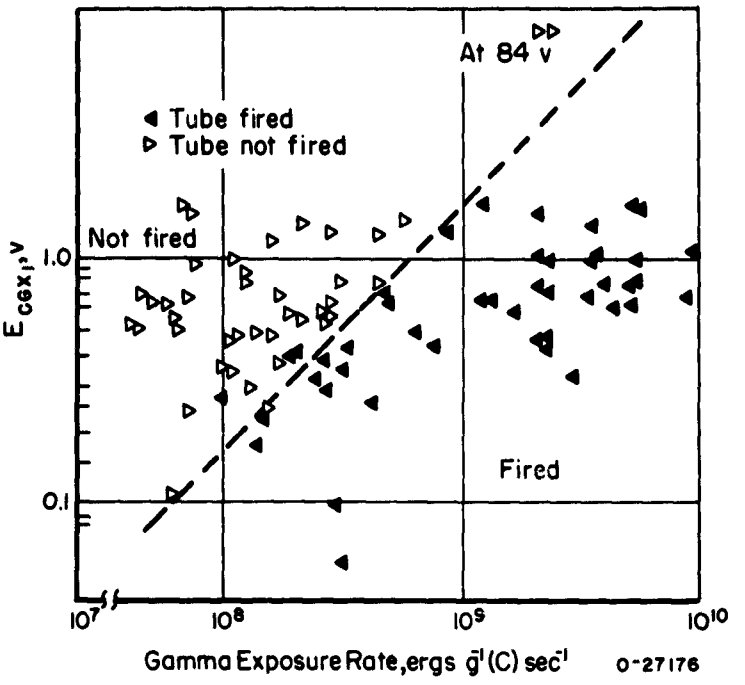

FIGURE 7. E_{cgx} VERSUS GAMMA EXPOSURE RATE FOR 2D21 THYRATRON TUBES(22)

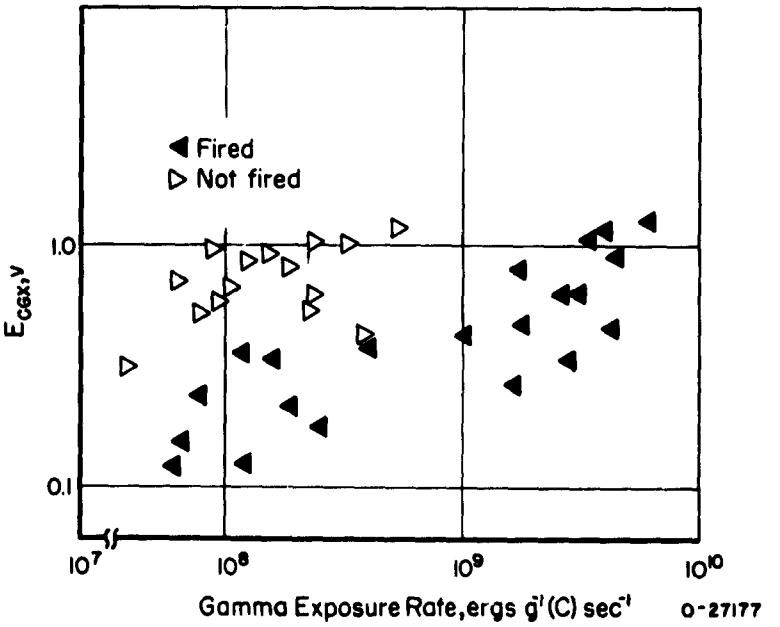

FIGURE 8. E_{cgx} VERSUS GAMMA EXPOSURE RATE FOR 5643 THYRATRON TUBES(22)

(1) A shunt leakage path that is produced by the radiation-induced ionization, and/or

(2) An ejection current that is caused by electrons flowing from ground to replace the electrons ejected by radiation (Compton scattering effect).[23]

Neither of the two hypotheses dictate that the observed change results in an actual resistance change.

The leakage current observed can be represented by an equivalent circuit in which there is a shunt resistor in parallel with the sample resistor. The value of this shunt resistance for an unpotted resistor is a combination of the resistance of the ionized air and other ionized material between the leads. When these materials are ionized by radiation, the value of the shunt resistance drops and a change in current flow results. This effect can be reduced by potting the resistor to reduce the air ionization with a subsequent increase in the shunt resistance.

When no voltage is applied across an irradiated resistor, a current flow is still observed through the resistor. This current flow cannot be explained as a resistance change resulting from ionization shunting, so another mechanism must be involved. Experiments have indicated that an ejection current caused by electrons flowing from ground to replace the electrons ejected by radiation is apparently the explanation.

The radiation effects of circuit cables must be disassociated from the test sample to obtain the actual radiation effects of the test sample. In earlier experiments (1957, 1958), cable effects were generally not considered. In later experiments, attempts have been made to correct for the cable effects to study the mechanism of damage to the resistors. However, because of the lack of understanding of cable effects, it seems unreasonable to assume that a technique for complete correction has been achieved.

The magnitude of the effects observed in resistors is generally considered to be a function of the gamma exposure rate. Data for 2-watt, potted resistors are presented in Figure 9. From this figure, one could hypothesize that for a given gamma exposure rate the value of the per cent change of apparent resistance increases with the nominal value of the resistor. Because of the small sample size, it is undesirable to rate the types of resistors with respect to their ability to resist being affected when exposed to a transient radiation environment.

Tables 13, 14, and 15 are a compilation of the data available on the effects of transient radiation on resistors. Results that were not expressed in per cent change of apparent resistance $\left(\frac{\Delta R}{100R}\right)$ were converted to this common measure when it was possible. When no voltage was applied to the test circuit, no means could be found to convert the results to the common measure using the reported data. Data that were not expressible in apparent resistance change are not presented in Tables 13, 14, 15.

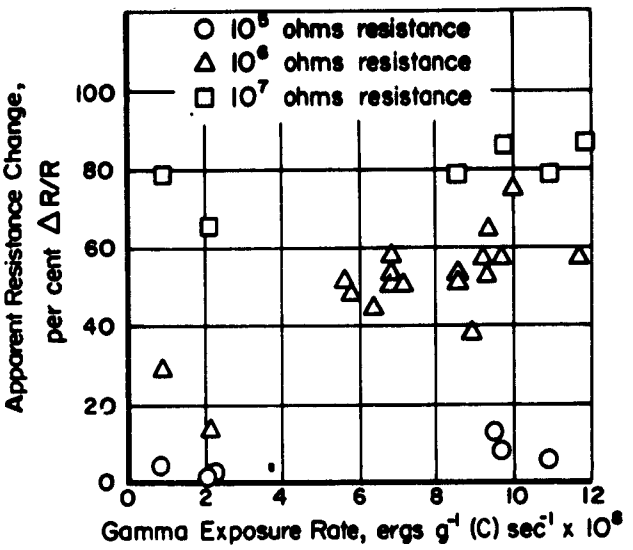

FIGURE 9. TRANSIENT RADIATION EFFECTS ON 2-WATT POTTED RESISTORS

It was not always obvious from the reported data whether the apparent resistance change was an increase or a decrease. For this reason no indication is given in Tables 13 through 15 of the direction of apparent resistance change. However, the uncertainty in direction of change exists only at the lower values of apparent resistance change (under 5 per cent). The higher values of apparent resistance change were an apparent decrease in resistance.

The classification of the resistors is according to type and initial resistance. When the initial resistance was not reported, the nominal value was used. The nominal values for resistors are shown as powers of ten only, while the initial resistance is given by the measured value and a power of ten. Further classification is according to power rating and potting compound.

The entries in Tables 13, 14, and 15 are intended to be for one resistor; however, it is suspected that some of the entries are averages of two or more resistors.

The transient-radiation-effects data on resistors are not of sufficient quantity to make quantitative conclusions. However, many hypotheses have been generated on the basis of data presently available. These hypotheses should aid the engineer in designing a system which will function in a transient-radiation environment. For this reason, the following hypotheses are presented:

(1) The apparent change in resistance of a resistor exposed to transient radiation is mainly a transient change. The permanent damage that has been observed has been under 2.5 per cent and may have been caused by aging through circuit use as well as through exposure. (11,24,25)

TABLE 13. SUMMARY OF TRANSIENT RADIATION EFFECTS ON CARBON COMPOSITION RESISTORS

Nominal or Initial Resistance, ohms	Power Rating, watts	Potting Compound	Test Voltage, v	Gamma Exposure, erg g^{-1} (C) x 10^4	Maximum Gamma Exposure Rate, ergs g^{-1} (C) sec^{-1} x 10^8	Apparent Resistance Change, per cent	Manufacturer	Reactor	Experiment	Date of Test	Reference
10^2	2	None	9			0	Allen Bradley	Godiva	IBM	Aug 58	11
1.0170 x 10^2	2			54.5[a]	4.09[c]	0.1	Allen Bradley	Godiva	IBM	Jan 59	24
1.0215 x 10^2	2			54.5[a]	12.73[c]	0.1	Allen Bradley	Godiva	IBM	Jan 59	24
1.0359 x 10^2	2			54.5[a]	5.91[c]	0.0	Allen Bradley	Godiva	IBM	Jan 59	24
.9988 x 10^3	2			54.5	4.09[c]	0.4	Allen Bradley	Godiva	IBM	Jan 59	24
10^3						2.5[d]	Allen Bradley	Godiva	USASRDL	Aug 59	25
1.021 x 10^3	2	Paraffin	22.5		38.8 [e]	0.3	Allen Bradley	Godiva	IBM	May 59	26
1.0228 x 10^3	2			54.5[a]	12.73[c]	1.2	Allen Bradley	Godiva	IBM	Jan 59	24
1.0236 x 10^3	2			54.5[a]	8.00[c]	0.3	Allen Bradley	Godiva	IBM	Jan 59	24
1.0244 x 10^3	2			54.5[a]	7.36[c]	0.9	Allen Bradley	Godiva	IBM	Jan 59	24
1.0291 x 10^3	2			54.5[a]	14.54[c]	1.7	Allen Bradley	Godiva	IBM	Jan 59	24
10^4	1/2	None	125	2.6		0.2		Godiva	Hughes	1958	9
10^4						1.5[d]	Allen Bradley	Godiva	USASRDL	Aug 59	25
10^4	2	Paraffin	46.5	18.2	10.93	0.6		Godiva	IBM	July 60	14
10^4	2	Paraffin	46.2	3.8	2.10	0.4		Godiva	IBM	July 60	14
10^4	2	Paraffin	46.9	8.3	4.34	1.5		Godiva	IBM	July 60	14
10^4	2	None	250	2.6		0.2		Godiva	Hughes	1958	9
10^4	2	None	250	2.6		0.5		Godiva	Hughes	1958	9
10^4	2	None	200	2.6		0.2		Godiva	Hughes	1958	9
10^4	2	Paraffin	-22.5		41.50	0.9	Allen Bradley	SPRF	IBM	June 61	22
10^4	2	Paraffin	22.5		43.19	0.8		SPRF	IBM	June 61	22
1.0107 x 10^4	2			54.5[a]	9.09[c]	4.8	Allen Bradley	Godiva	IBM	Jan 59	24
1.0234 x 10^4	2			54.5[a]	7.36[c]	2.6	Allen Bradley	Godiva	IBM	Jan 59	24
1.0228 x 10^4	2			54.5[a]	4.82[c]	2.1	Allen Bradley	Godiva	IBM	Jan 59	24
1.033 x 10^4	2	Paraffin	93		45.00[e]	4.3	Allen Bradley	Godiva	IBM	May 59	26

TABLE 13. (Continued)

Nominal or Initial Resistance, ohms	Power Rating, watts	Potting Compound	Test Voltage, v	Gamma Exposure, ergs g^{-1} (C) x 10^4	Maximum Gamma Exposure Rate, ergs g^{-1} (C) sec^{-1} x 10^8	Apparent Resistance Change, per cent	Manufacturer	Reactor	Experiment	Date of Test	Reference
10^5	2	None	100	0. [b]	2.28[b]	1.5	Allen Bradley	Linac	Hughes	1957	27
10^5	2	None	200	0. [b]	2.28[b]	1.7	Allen Bradley	Linac	Hughes	1957	26
10^5	2	None	300	0.2[b]	2.28[b]	1.9	Allen Bradley	Linac	Hughes	1957	27
10^5	2	Acrylic	200	0.2[b]	2.28[b]	.6	Allen Bradley	Linac	Hughes	1957	27
10^5	2	Acrylic	100	0.2[b]	2.28[b]	1.2	Allen Bradley	Linac	Hughes	1957	27
10^5	2	Acrylic	200	0.2[b]	2.28[b]	2.2	Allen Bradley	Linac	Hughes	1957	27
10^5	2	Acrylic	300	0.2[b]	2.28[b]	2.1	Allen Bradley	Linac	Hughes	1957	27
10^5	2	None	200	0.2[b]	2.28[b]	>14.9	Allen Bradley	Linac	Hughes	1957	27
10^5	2	Paraffin	-22.5		42.71	3.1		SPRF	IBM	June 61	22
10^5	2	None	500		62.27[e]	16	Allen Bradley	Godiva	IBM	Aug 58	11
10^5						10 [d]	Allen Bradley	Godiva	USASRDL	Aug 59	25
10^5	2	Paraffin	93	18.2	10.93	5.6		Godiva	IBM	July 60	14
10^5	2	Paraffin	93	3.8	2.10	1.8 ± .3		Godiva	IBM	July 60	14
1.0017 x 10^5	2			54.5[a]	5.91[c]	15.5	Allen Bradley	Godiva	IBM	Jan 59	24
1.007 x 10^5	2	Paraffin	270		30.54	15.1	Allen Bradley	Godiva	IBM	Nov 59	26
1.0079 x 10^5	2			54.5[a]	4.55[c]	19.7	Allen Bradley	Godiva	IBM	Jan 59	24
1.0463 x 10^5	2			54.5[a]	9.09[c]	24.8	Allen Bradley	Godiva	IBM	Jan 59	24
10^6	1/10	Paraffin	185.0	15.0	8.10	30.5		Godiva	IBM	July 60	14
10^6	1/2	Paraffin	186.0	12.0	6.29	50.2		Godiva	IBM	July 60	14
10^6	2	None	200	0.2[b]	2.28[b]	5.6	Allen Bradley	Linac	Hughes	1957	27
10^6	2	None	300	0.2[b]	2.28[b]	0.5	Allen Bradley	Linac	Hughes	1957	27
10^6	2	Paraffin	279.0	15.5	8.49	38.6		Godiva	IBM	July 60	14
10^6	2	Paraffin	278.0	3.8	2.10	13.5		Godiva	IBM	July 60	14
10^6	2	Paraffin	93.0	12.9	6.77	52.7		Godiva	IBM	July 60	14
10^6	2	Paraffin	460.0	12.9	6.77	51.0		Godiva	IBM	July 60	14
10^6	2	Paraffin	282.0	12.9	6.77	58.0		Godiva	IBM	July 60	14

TABLE 13. (Continued)

Nominal or Initial Resistance, ohms	Power Rating, watts	Potting Compound	Test Voltage, v	Gamma Exposure ergs g^{-1} (C) x 10^4	Maximum Gamma Exposure Rate, ergs g^{-1} (C) sec^{-1} x 10^8	Apparent Resistance Change, per cent	Manufacturer	Reactor	Experiment	Date of Test	Reference
10^6	2	Paraffin	185.0	12.0	6.29	44.7		Godiva	IBM	July 60	14
1.0222 x 10^6	2			5.4(a)	5.82(c)	48.1		Godiva	IBM	Jan 59	24
1.0251 x 10^6	2	Paraffin	940		51.63(e)	58.2		Godiva	IBM	Nov 59	26
1.0508 x 10^6	2			5.4(a)	5.64(c)	52.1		Godiva	IBM	Jan 59	24
1.0553 x 10^6	2			5.4(a)	10.00(c)	74.9		Godiva	IBM	Jan 59	24
10^6	2				46.44	73.4	Allen Bradley	SPRF	IBM	June 61	22
10^6	2	Paraffin	22.5		43.07	56.1	Allen Bradley	SPRF	IBM	June 61	22
	-	Paraffin	-22.5								
10^7	2				42.35	96.8	Allen Bradley	SPRF	IBM	June 61	22
10^7	2	Paraffin	22.5		48	85.0	Allen Bradley	SPRF	IBM	June 61	22
10^7	2	Paraffin	-22.5	15.5	8.49	79.0 ± 0.3		Godiva	IBM	July 60	14
10^7	2	Paraffin	935.0	3.8	2.10	66.1 ± 3.0		Godiva	IBM	July 60	14
10^7	2	Paraffin	935.0	18.2	10.93	78.6 ± 5.1		Godiva	IBM	July 60	14
10^7	2	Paraffin	935.0	5.4(a)	11.82(c)	86.8		Godiva	IBM	Jan 59	24

(a) Theoretical value.
(b) Average value per pulse.
(c) Value is known to be in error.
(d) Cable effects known to be neglected.
(e) Overestimates of actual exposure rates.

TABLE 14. SUMMARY OF TRANSIENT RADIATION EFFECT ON METAL FILM RESISTORS

Nominal or Initial Resistance, ohms	Power Rating, watts	Potting Compound	Test Voltage, v	Gamma Exposure, $ergs\ g^{-1}(C) \times 10^4$	Maximum Gamma Exposure Rate, $ergs\ g^{-1}(C)\ sec^{-1} \times 10^8$	Apparent Resistance Change, per cent	Manufacturer	Reactor	Experiment	Date of Test	Reference
10^4	2	Paraffin	46.5	18.2	9.66	1.2		Godiva	IBM	July 60	14
10^4	2	Paraffin	46.0	1.6	0.85	0.4		Godiva	IBM	July 60	14
10^4						1.0	Weston	KEWB	USASRDL		28
10^5						3.0		KEWB	USASRDL		28
10^5						0.3		Triga	USASRDL		28
k9^5		None	500		53.63(a)	15.0	IRC	Godiva	IBM	Aug 58	11
10^5		None	500		71.81(a)	14.0	IRC	Godiva	IBM	Aug 58	11
10^5	2	Paraffin	93.0	18.2	9.66	8.1 ± 0.5		Godiva	IBM	Jul 60	14
10^5	2	Paraffin	93.0	1.6	0.85	4.4		Godiva	IBM	Jul 60	14
10^6	1/4	Paraffin	185.0	20.9	11.77	37.3		Godiva	IBM	Jul 60	14
10^6	1/2	Paraffin	185.0	20.9	11.77	51.3		Godiva	IBM	Jul 60	14
10^6	2	Paraffin	185.0	20.9	11.77	56.8		Godiva	IBM	Jul 60	14
10^6	2	Paraffin	279.0	18.2	9.66	56.0		Godiva	IBM	Jul 60	14
10^6	2	Paraffin	279.0	1.6	0.85	29.3		Godiva	IBM	Jul 60	14
10^6	2	Paraffin	278.0	15.9	8.58	52.3		Godiva	IBM	Jul 60	14
10^6	2	Paraffin	93.0	16.4	9.22	53.0		Godiva	IBM	Jul 60	14
10^6	2	Paraffin	282.0	16.4	9.22	57.5		Godiva	IBM	Jul 60	14
10^6	2	Paraffin	460.0	16.4	9.22	64.7 ± 1.4		Godiva	IBM	Jul 60	14
10^7	2	Paraffin	935.0	18.2	9.66	85.9		Godiva	IBM	Jul 60	14
10^7	2	Paraffin	935.0	1.6	0.85	78.9		Godiva	IBM	Jul 60	14

TABLE 14. (Continued)

Nominal or Initial Resistance, ohms	Power Rating, watts	Potting Compound	Test Voltage, v	Gamma Exposure, ergs $g^{-1}(C) \times 10^4$	Maximum Gamma Exposure Rate, ergs $g^{-1}(C)$ $sec^{-1} \times 10^8$	Apparent Resistance Change, per cent	Manufacturer	Reactor	Experiment	Date of Test	Reference
Nichrome Film											
10^3						1(b)	Weston	Godiva	USASRDL	Aug 59	25
10^4						1(b)	Weston	Godiva	USASRDL	Aug 59	25
10^4						2(b)	IRC	Godiva	USASRDL	Aug 59	25
10^5						3 to 8(b)	Weston	Godiva	USASRDL	Aug 59	25
10^5						1 to 2(b)	IRC	Godiva	USASRDL	Aug 59	25
10^6						5(b)	Weston	Godiva	USASRDL	Aug 59	25

(a) Overestimates of actual exposure rates.
(b) Cable effects known to be neglected.

TABLE 15. SUMMARY OF TRANSIENT RADIATION EFFECTS ON MISCELLANEOUS RESISTORS

Nominal or Initial Resistance, ohms	Power Rating, watts	Potting Compound	Test Voltage, v	Gamma Exposure, ergs g^{-1}(C) x 10^4	Maximum Gamma Exposure Rate, ergs g^{-1}(C) sec^{-1} x 10^8	Apparent Resistance Change, per cent	Manufacturer	Reactor	Experiment	Date of Test	Reference
Wirewound											
10^2		None	9			0	Mepco	Godiva	IBM	Aug 58	11
10^4	2	Paraffin	46.0	16.3	6.08	1.8 ± 0.1		Godiva	IBM	Jul 60	14
10^5	2	Paraffin	93.0	17.3	9.49	13.2		Godiva	IBM	Jul 60	14
10^5		None	500		79.08	22.0		Godiva	IBM	Aug 58	11
10^6	2	Paraffin	278.0	15.9	8.58	53.6		Godiva	IBM	Jul 60	14
10^6	2	Paraffin	93.0	13.2	7.01	51.2		Godiva	IBM	Jul 60	14
Oxide Film (Tin)											
10^2		None	9			0	Corning Glass	Godiva	IBM	Aug 58	11
10^3						2(a)	Corning Glass	Godiva	USASRDL	Aug 59	25
10^5		None	500		99.99	15	Corning Glass	Godiva	IBM	Aug 58	11
10^5		None	500		79.08	18	Corning Glass	Godiva	IBM	Aug 58	11
Carbon Film											
10^3						0	IRC	KEWB	USASRDL		28
10^3						2(a)	IRC	Godiva	USASRDL	Aug 59	25
10^4						2(a)	IRC	Godiva	USASRDL	Aug 59	25
10^4						1.0		KEWB	USASRDL		28
10^5						1.0		KEWB	USASRDL		28
10^5						7.5 ± 2.5(a)	IRC	Godiva	USASRDL	Aug 59	25
10^5	5			54.5(b)	3.54(c)	11.3	Victoreen	Godiva	IBM	Jan 59	24
10^6						15 ± 5(a)	IRC	Godiva	USASRDL	Aug 59	25

(a) Cable effects known to be neglected.
(b) Theoretical value.
(c) Value is known to be in error.

(2) The apparent resistance change is generally believed to result from ionization and/or an ejection current. The ionization may be of the air or potting compound surrounding the resistor, or of the resistor materials.[11,14,24,25,26] The ejection current is caused by electrons flowing from ground to replace the electrons ejected by radiation (Compton scattering effect).[23,27]

(3) The use of a potting compound will reduce the effect of transient radiation on resistors by reducing the influence of ionized air.[26,14,27]

(4) The higher the resistance value of the sample, the greater will be the apparent per cent change of the resistance when exposed to a pulse of radiation of sufficient magnitude to cause a change. Resistors of 10 kilohms or less show less than 5 per cent change.

(5) For a given resistor, the greater the intensity of the radiation pulse, the greater will be the apparent resistance change.[24]

Capacitors

Research on capacitors has been conducted to study the transient and permanent transient radiation effects on the conductivity, capacitance, and dissipation factor of capacitors. The data obtained from the experiments suffers qualitatively because of inaccurate radiation-environment measurements and difficulties encountered in measuring some parameters of capacitors. However, the information is valuable for providing a better understanding of the effects of transient radiation on capacitors.

Most of the information available on capacitors is concerned with the transient current flow through a capacitor when exposed to a pulse of radiation. This pulse could arise from either a decreased leakage resistance through or around the capacitor or an increase in the capacitance. Generally, the current pulse is considered to result from a decreased leakage resistance, since experiments have given no positive indications of capacitance change during a radiation pulse. The reduction of leakage resistance is believed to result from an increase in dielectric conductivity since effort has been taken to minimize the effects of ionization of matter external to the capacitors. This increase in the dielectric conductivity is the transient radiation effect of greatest consequence observed in capacitors. The magnitude of the effects observed in capacitors is generally considered to be a function of the gamma exposure rate.

The time it takes for a capacitor to regain its preirradiated characteristics is a function of the time constant of the measuring circuit. The leakage current for smaller values of capacitance changes approximately as the intensity of the radiation pulse. For higher values of capacitance, the leakage current does not recover during the radiation pulse but decreases almost exponentially with time.[26]

There has been no positive indication of transient or permanent capacitance change. The capacitance changes measured have either been within the experimental error or of the same magnitude as the control sample. There appears to be no measurable permanent change of the dissipation factor.

In order to present the effects of transient radiation on capacitors in a form suitable for analysis, two methods have been developed. IBM has assumed that the radiation

effect can be considered as a current generator such that this current is proportional, for a given capacitor and applied voltage, to the radiation exposure.[14,21,22,26,29] Using this assumption, IBM has developed an equation which depends on a value "K". The value "K" needs to be determined only once for any capacitor type, and then the equation can be solved uniquely for any given pulse shape or magnitude, provided that the pulse does not differ so greatly from a Godiva pulse that different mechanisms are involved. Using this IBM current generator model, the current flow (i) in the circuit at any time (t) can be estimated by solving the following differential equation:

$$\frac{di}{dt} + \frac{i}{\tau} - \frac{K}{\tau} F(t) = 0 \quad ,$$

where

τ = time constant of circuit

$F(t)$ = function of the radiation exposure rate; $F(t) = e^{\alpha t}/(1 + e^{\alpha t})^2$

α = radiation pulse shape parameter

K = measure of the current producing efficiency of the radiation (see Figures 10 and 11)

$$K = i_{max}/F(t_{i\ max})$$

i_{max} = maximum current during radiation pulse

t_i = time of maximum current.

Though there are data that support this model, IBM is conducting experiments to further determine the validity of the current-generator model.

The Boeing Company assumes that the radiation effect can be considered as a change in shunt resistance.[30,31,32] Consideration was given to the observed radiation effect being due to a change in shunt capacitance or emf generation. However, no capacitance change has been observed, and Boeing assumed negligible emf generation. The Boeing shunt-resistance equation is shown below as calculated from the equation for parallel plate approximation:

$$R_S = \frac{\epsilon\, \epsilon_o}{\sigma C} \quad ,$$

where

R_S = radiation-induced shunt resistance

ϵ = dielectric constant of capacitor dielectric

ϵ_o = electrical permittivity in vacuum

$\sigma = \sigma_1 + \sigma_2$ = radiation-induced electrical conductivity in capacitor dielectric

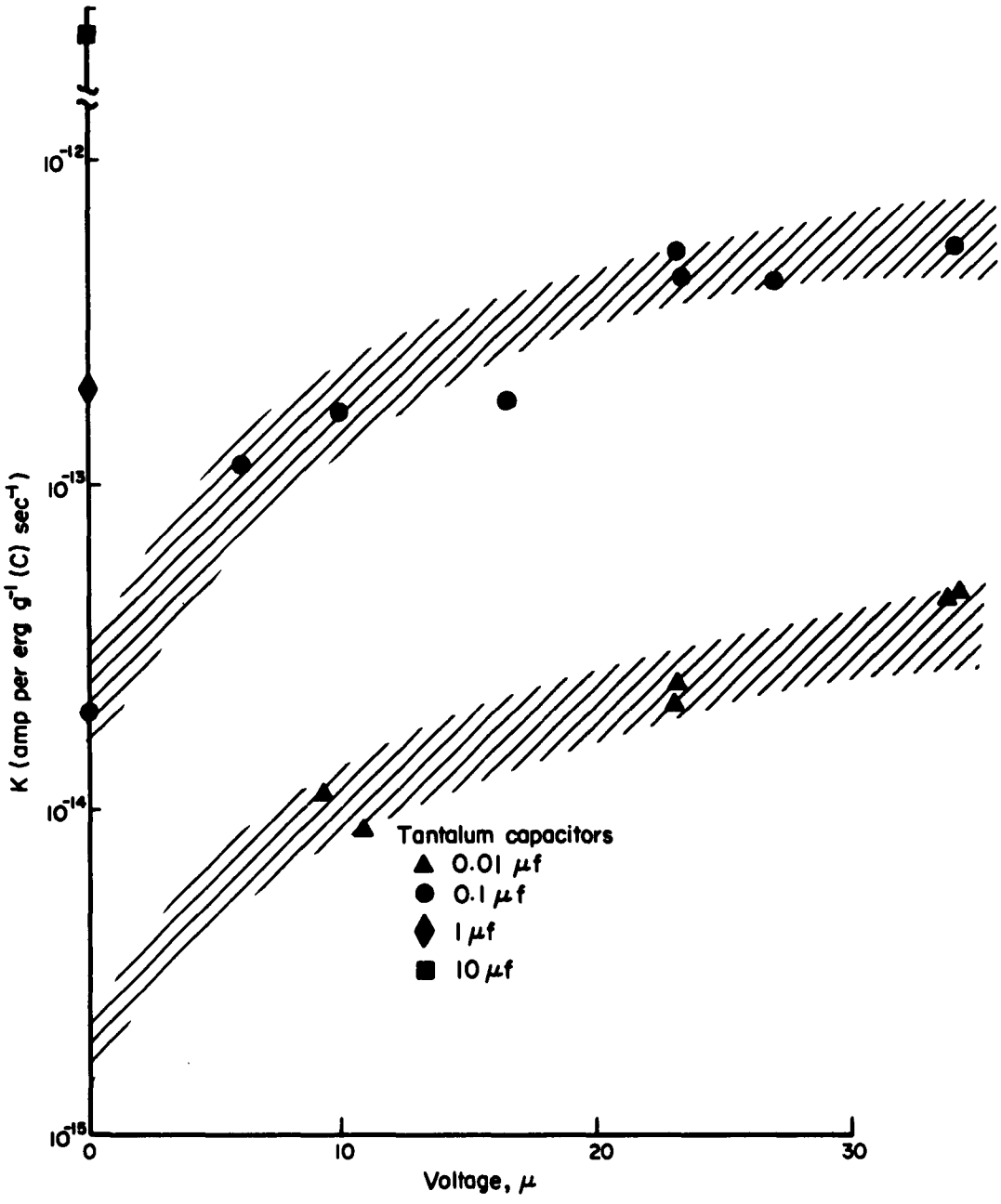

FIGURE 10. K VERSUS APPLIED VOLTAGE FOR TANTALUM CAPACITORS

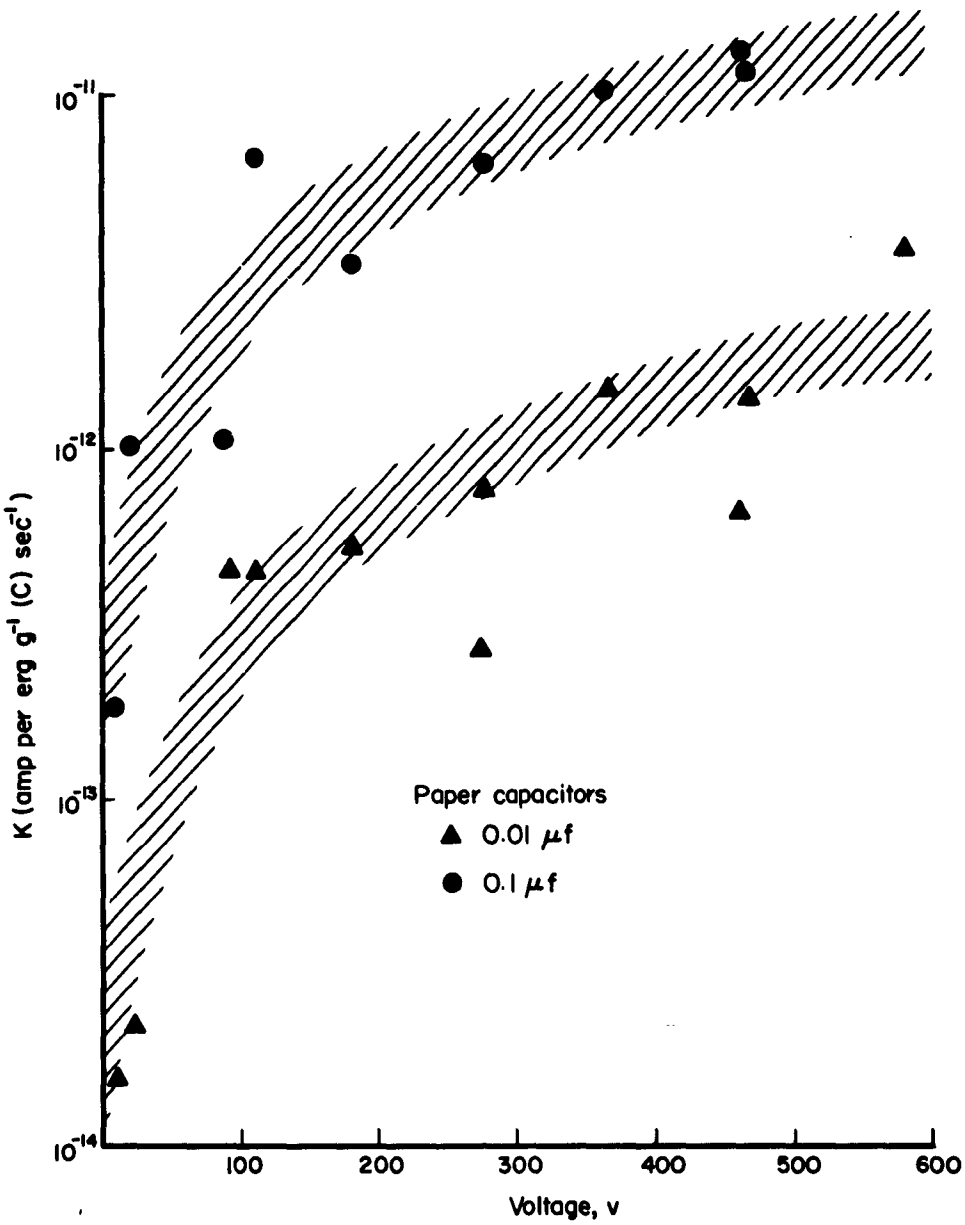

FIGURE 11. K VERSUS APPLIED VOLTAGE FOR PAPER CAPACITORS

$\sigma_1 = K_1 \dot{\gamma}^{\Delta}$ early history component

$\sigma_2 = K_2 \gamma_t - \int_0^t \frac{\sigma_2}{\tau_2}\, dt$ for tantalum oxide capacitors and zero for other capacitors

K_1 = rate-dependent generation constant with units of (roentgen/sec)$^{-1}$ (ohm-centimeter)$^{-1}$

Δ = rate-dependent generation constant

K_2 = exposure-dependent generation constant with units of (ohm-centimeter-roentgen)$^{-1}$

τ_2 = decay constant, seconds

t = time measured from beginning of radiation pulse

$\dot{\gamma}$ = gamma exposure rate

γ_t = the total exposure up to time ϵ.

Values for K_1 and Δ are obtained from experimental data similar to those plotted in Figures 12, 13, and 14. Table 16 lists some estimated values of K_1 and Δ as determined by the Boeing Company using data generated by Boeing and IBM along with some values for ϵ. These values for Δ and K_1 differ in some instances from those determined by Diamond Ordnance Fuze Laboratory.

Tables 17 through 21 are a compilation of the data available on the transient radiation effects on the conductivity of capacitors. Data that were too meager to be useful are not presented in the tables. Using the reported data, no means could be found to convert the measured effect to a common term, so the data are presented as reported. To aid in the evaluation of the data, the test circuits are presented in Figures 15 and 16.

The transient-radiation-effects data on capacitors are not of sufficient quantity and quality to make firm conclusions. The hypotheses that have been generated should aid the engineer in designing a system to operate in a radiation environment. For this reason, the following hypotheses are presented:

(1) The transient radiation effect on capacitors is of a transient nature, there being no positive indications of permanent damage.

(2) The major effect of transient radiation on capacitors is the temporary reduction in leakage resistance due to the increase in the dielectric conductivity.

(3) The ionization and increased conduction in the dielectric material apparently cause no large decrease in electric strength for the materials tested.[31]

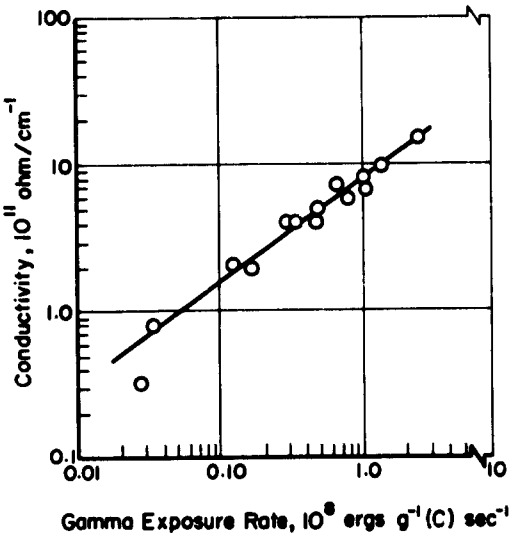

FIGURE 12. CONDUCTIVITY VERSUS RADIATION RATE FOR SPRAGUE VITAMIN Q IMPREGNATED PAPER CAPACITORS[31]

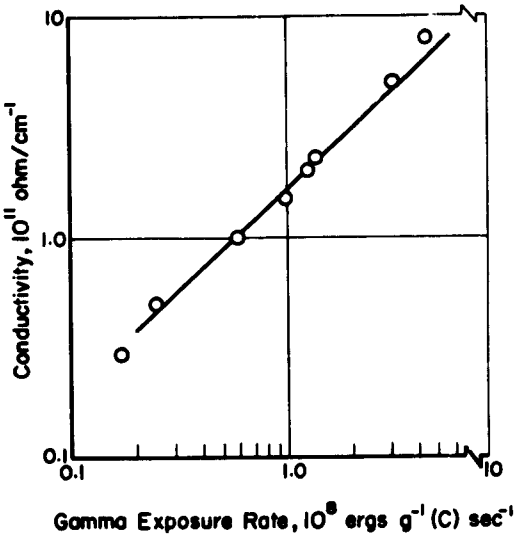

FIGURE 13. CONDUCTIVITY VERSUS RADIATION RATE FOR MYLAR CAPACITORS[31]

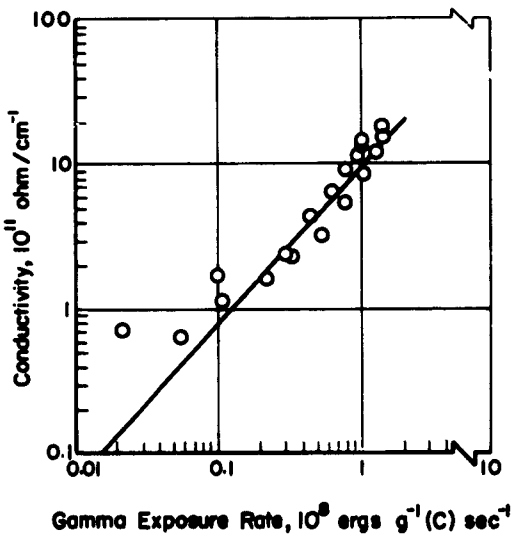

FIGURE 14. CONDUCTIVITY VERSUS RADIATION RATE FOR OIL-IMPREGNATED PAPER CAPACITORS[31]

TABLE 16. SUMMARY OF D-C CONDUCTIVITY DATA[30]

Dielectric	ϵ	K_1, $\frac{\text{sec}}{\Omega\ \text{cm}\ r}$	Δ
Mylar	3	4.2×10^{-7}	0.9
Vitamin Q impregnated paper	11	5.2×10^{-15}	0.7
Tantalum oxide[a]	25	9.5×10^{-18}	1.0
Aluminum oxide	7	3.3×10^{-18}	1.0
Glass	~6.5	2.0×10^{-17}	1.0 (estimated)
Oil-impregnated paper	~7	7.4×10^{-17}	~1.0
Teflon	2	4.2×10^{-18}	~1.0
Silastic + DC-200	--	$\sim 5.1 \times 10^{-15}$	~1.0
Mica	6.8	$\sim 1.0 \times 10^{-17}$	1.0 (estimated)
Ceramic	~20	$\sim 4.0 \times 10^{-17}$	1.0

(a) Other values for tantalum oxide: $K_2 = 2.3 \times 10^{-14}$
$r_2 = 2.18 \times 10^{-4}$

TABLE 17. SUMMARY OF TRANSIENT RADIATION EFFECTS ON TANTALUM CAPACITORS

Nominal Capacitance, μf	Working Volts, dc	Potting Compound	Test Voltage, v	Gamma Exposure, ergs g^{-1}(C) x 10^4	Maximum Gamma Exposure Rate, ergs g^{-1}(C) sec^{-1} x 10^8	Maximum Current, μa	Maximum Voltage Change, v	Manufacturer	Type	Reactor	Experiment	Date of Test	Reference
0.01			10.9		9.88	8.50				Godiva	IBM	Jul 60	14
0.01			34		9.81	44.73				Godiva	IBM	Jul 60	14
0.01			22.5		69.05[a]	119		Sprague		Godiva	IBM	Aug 58	11
0.01			22.5		53.63[a]	55		Sprague		Godiva	IBM	Aug 58	11
0.01		Paraffin	18.5		33.63[a]	26.6		Sprague	150D	Godiva	IBM	May 59	26
0.01			23.0	28.3		45.8 ± 5		Sprague	150D	Godiva	IBM	Apr 60	11
0.01			22.5	28.0	17.27	50.36 ± 8		Sprague	150L	Godiva	IBM	Apr 60	11
0.01		Paraffin	9.38		34.1	34.9				SPRF	IBM	Jun 61	22
0.01		Paraffin	34.22		32.5	129				SPRF	IBM	jun 61	22
0.01		Paraffin	23.36		10.4	25.8				SPRF	IBM	Jun 61	
0.02			23		8.10	16.39				Godiva	IBM	Jul 60	14
0.1		Paraffin	6.2	29.1	20.91	166				Godiva	IBM	Oct 60	21
0.1		Paraffin	23.2	26.6	16.36	813				Godiva	IBM	Oct 60	21
0.1		Paraffin	10	22.6	9.09	155				Godiva	IBM	Oct 60	21
0.1		Paraffin	27	33.6	18.18	707				Godiva	IBM	Oct 60	21
0.1		Paraffin	16.5	31.4	16.36	2670				Godiva	IBM	Oct 60	21
0.1			22.8	22.9	14.54	462 ± 15		Sprague	150D	Godiva	IBM	Apr 60	29
0.1		Paraffin	34.13			1130				SPRF	IBM	Jun 61	22
0.1		Paraffin	23.40		1.14	389				SPRF	IBM	Jun 61	22
0.1		Paraffin	0		3.75	48.6				SPRF	IBM	Jun 61	22
1.0	30		-20		2.28		0			Godiva	Hughes	1958	9
1.0	30	Acrylic		.02-.03[b]			0			Linac	Hughes	1957	27
1.0		Paraffin	6.2	29.1	20.91	593				Godiva	IBM	Oct 60	21
1.0		Paraffin	22.5	28.9	14.54	4470				Godiva	IBM	Oct 60	21
1.0		Paraffin	10.9	22.6	9.09	893				Godiva	IBM	Oct 60	21
1.0		Paraffin	28	33.6	18.18	670				Godiva	IBM	Oct 60	21

TABLE 17. (Continued)

Nominal Capacitance, μf	Working Volts, dc	Potting Compound	Test Voltage, v	Gamma Exposure, ergs g^{-1}(C) x 10^4	Maximum Gamma Exposure Rate, ergs g^{-1}(C) sec^{-1} x 10^8	Maximum Current, μa	Maximum Voltage Change, v	Manufacturer	Type	Reactor	Experiment	Date of Test	Reference
1.0		Paraffin	22.5	28.9	14.54	4470				Godiva	IBM	Oct 60	21
1.0		Paraffin	10.9	22.6	9.09	893				Godiva	IBM	Oct 60	21
1.0		Paraffin	28	33.6	18.18	4670				Godiva	IBM	Oct 60	21
1.0		Paraffin	17	31.4	16.36	1670				Godiva	IBM	Oct 60	21
1.0			23	23.5	13.64	2194 ± 40		Sprague	150D	Godiva	IBM	Apr 60	29
1.0			22	4.7	2.73	264 ± 5		Sprague	130C	Godiva	IBM	Apr 60	29
1.0		Paraffin	0		34.0	100 ± 13				SPRF	IBM	Jun 61	22
4.0		Paraffin	23.5		19.73[a]	>1330		Sprague	120D	Godiva	IBM	May 59	26
10		Paraffin	12		29.82[a]	453		Sprague	109D	Godiva	IBM	May 59	26
10		Paraffin	22.5		-8.18[a]	19.7		Sprague	120D	Godiva	IBM	May 59	26
10		Paraffin	23.5		17.00[a]	872		Sprague	109D	Godiva	IBM	May 59	26
10		Paraffin	18.5		7.45[d]	>160		Sprague	150D	Godiva	IBM	May 59	26
10		Paraffin	6.3	29.1	20.91	1600				Godiva	IBM	Oct 60	21
10		Paraffin	34.2	28.9	14.54	7200				Godiva	IBM	Oct 60	21
10		Paraffin	11.0	22.6	9.09	1930				Godiva	IBM	Oct 60	21
10		Paraffin	28	33.6	18.18	6400				Godiva	IBM	Oct 60	21
10		Paraffin	17.2	31.4	16.36	3330				Godiva	IBM	Oct 60	21
10			23.0	24.4	14.54	5750 ± 100		Sprague	150D	Godiva	IBM	Apr 60	29
10			22.0	4.9	2.91	4440 ± 20		Sprague	150D	Godiva	IBM	Apr 60	29
10		Paraffin	0			510				SPRF	IBM	Jun 61	22
33	15					20[c,d]		Texas Instruments	Solid	Godiva	USASRDL	Aug 59	25
60	50					150[b,d]		Sprague	Foil	Godiva	USASRDL	Aug 59	25
60	50					40		Fansteel	Slug	Godiva	USASRDL	Aug 59	24
60	50					40					USASRDL	1958	28

(a) Overestimates of actual exposure rate.
(b) Average value per pulse.
(c) Average value.
(d) Cable effects are known not to have been considered.

TABLE 18. SUMMARY OF TRANSIENT RADIATION EFFECTS ON PAPER CAPACITORS

Nominal Capacitance, μf	Working Volts, dc	Potting Compound	Test Voltage, v	Gamma Exposure, ergs g^{-1}(C) x 10^4	Maximum Gamma Exposure Rate, ergs g^{-1}(C) sec^{-1} x 10^8	Maximum Current, μa	Maximum Voltage Change, v	Manufacturer	Type	Reactor	Experiment	Date of Test	Reference
0.001	600	Acrylic	500	0.02-0.03	(a)		0.04			Linac	Hughes	1957	27
0.01			135		67.3(b)	600		Sprague	Procar	Godiva	IBM	Aug 58	11
0.01			135		17.3(b)	630		Sprague	Procar	Godiva	IBM	Aug 58	11
0.01			135		44.5(b)	50		Sprague	Vitamin Q	Godiva	IBM	Aug 58	11
0.01			135		90.9(b)	206		Sprague	Vitamin Q	Godiva	IBM	Aug 58	11
0.01		Paraffin	370	26.5	16.4	1267				Godiva	IBM	Oct 60	21
0.01		Paraffin	582	25.4	12.7	2530				Godiva	IBM	Oct 60	21
0.01		Paraffin	185	24.5	10.0	379				Godiva	IBM	Oct 60	21
0.01		Paraffin	470	32.0	17.3	1680				Godiva	IBM	Oct 60	21
0.01		Paraffin	280	29.0	14.5	693				Godiva	IBM	Oct 60	21
0.01	600		600	(c)	(c)		1.34			Godiva	Hughes	1959	16
0.01	600		600	(c)	(c)		1.35			Godiva	Hughes	1959	16
0.01	600		600	(c)	(c)		1.26			Godiva	Hughes	1959	16
0.01		Paraffin	116.8		51.4	275				SPRF	IBM	Jun 61	22
0.01		Paraffin	278.79		50.5	1350				SPRF	IBM	Jun 61	22
0.01		Paraffin	462.48		41.6	2400				SPRF	IBM	Jun 61	22
0.01		Paraffin	23.44		43.1	60.4				SPRF	IBM	Jun 61	22
0.01		Paraffin	9.34		41.9	67.3				SPRF	IBM	Jun 61	22
0.1			200		2.3		0.54(d)			Godiva	Hughes	1958	9
0.1	600	Epoxy Kish	600		2.1		<5.4	Comell Dubilier	Cub	Kukla	Boeing	Jun 60	31
0.1		Paraffin	93	24.5	17.3	1700				Godiva	IBM	Oct 60	21
0.1		Paraffin	370	26.5	16.4	14070				Godiva	IBM	Oct 60	21

TABLE 18. (CONTINUED)

Nominal Capacitance, μf	Working Volts, dc	Potting Compound	Test Voltage, v	Gamma Exposure, erg g^{-1}(C) x 10^4	Maximum Gamma Exposure Rate, erg g^{-1}(C) sec^{-1} x 10^8	Maximum Current, μa	Maximum Voltage Change, v	Manufacturer	Type	Reactor	Experiment	Date of Test	Reference
0.1		Paraffin	185	24.5	10.0	3040				Godiva	IBM	Oct 60	21
0.1		Paraffin	470	32.0	17.3	17070				Godiva	IBM	Oct 60	21
0.1		Paraffin	280	29.0	14.5	4320				Godiva	IBM	Oct 60	21
0.1			22.5	20.1	13.6	667±25			Paper	Godiva	IBM	Apr 60	29
0.1		Paraffin	117.5		[illegible]	3950			Mylar	SPRF	IBM	Jun 61	22
0.1		Paraffin	280.83		57.6	25600				SPRF	IBM	Jun 61	22
0.1		Paraffin	468.35		43.8	40700				SPRF	IBM	Jun 61	22
0.1		Paraffin	23.28		23.8	1230				SPRF	IBM	Jun 61	22
0.1		Paraffin	9.38		42.6	780				SPRF	IBM	Jun 61	22
1.0		Paraffin	93	24.5	17.3	7600				Godiva	IBM	Oct 60	21
1.0		Paraffin	138	25.4	12.7	7670				Godiva	IBM	Oct 60	21
1.0		Paraffin	185	24.5	10.0	8890				Godiva	IBM	Oct 60	21
1.0		Paraffin	46.7	32.0	17.3	3410				Godiva	IBM	Oct 60	21
1.0		Paraffin	280	29.0	14.5	14930				Godiva	IBM	Oct 60	21
6.0	600	Epoxy Kish	600		1.1		10.8	Comell Dubilier	Pup	Kukla	Boeing	Jun 60	31
6.0	600	Epoxy Kish	600		0.6		3.0	Comell Dubilier	Pup	Kukla	Boeing	Jun 60	31

(a) Overestimates of actual exposure rates.
Average value per pulse.
, Average value.
(d) Cable effects are known not to have been considered.

TABLE 19. SUMMARY OF TRANSIENT RADIATION EFFECTS ON GLASS CAPACITORS

Nominal Capacitance, μf	Potting Compound	Test Voltage, v	Gamma Exposure, ergs $g^{-1}(C) \times 10^4$	Maximum Gamma Exposure Rate, ergs $g^{-1}(C)$ $sec^{-1} \times 10^8$	Maximum Current, μa	Manufacturer	Type	Reactor	Experiment	Date of Test	Reference
0.001	Paraffin	465	26.8	13.6	277			Godiva	IBM	Oct 60	21
0.001	Paraffin	380	32.0	17.3	81			Godiva	IBM	Oct 60	21
0.001	Paraffin	185	29.1	15.5	501			Godiva	IBM	Oct 60	21
0.01		47		10.4	55.6			Godiva	IBM	Jul 60	14
0.01		93		8.7	54.41			Godiva	IBM	Jul 60	14
0.01		135		127.3[a]	316	Corning Glass		Godiva	IBM	Aug 58	11
0.01		135		90.9[a]	425	Corning Glass		Godiva	IBM	Aug 58	11
0.01	Paraffin	9.4		57.9[a]	64.0	IBM	Evap.	Godiva	IBM	May 59	26
0.01	Paraffin	9.4		31.8[a]	42.6	IBM	Evap.	Godiva	IBM	May 59	26
0.01		23.0	5.2		15.35	Corning Glass	CY	Godiva	IBM	Apr 60	29
0.01		273.0	21.1	12.7	865[b]	Corning Glass	CY	Godiva	IBM	Apr 60	29

(a) Overestimates of actual exposure rates.

(b) Estimated value.

TABLE 20. SUMMARY OF TRANSIENT RADIATION EFFECTS ON CERAMIC CAPACITORS

Nominal Capacitance, μf	Working Volts, dc	Potting Compound	Test Voltage, v	Gamma Exposure, ergs $g^{-1}(C) \times 10^4$	Maximum Gamma Exposure Rate, ergs $g^{-1}(C)$ $sec^{-1} \times 10^8$	Maximum Current, μa	Maximum Voltage Change, v	Manufacturer	Type	Reactor	Experiment	Date of Test	Reference
0.0005		Paraffin	91	24.5	17.3	320				Godiva	IBM	Oct 60	21
0.0005		Paraffin	630	32.0	17.3	107				Godiva	IBM	Oct 60	21
0.0005		Paraffin	820	28.3	14.5	333				Godiva	IBM	Oct 60	21
0.0033						2.0[b]		Erie		Godiva	USASRDL	Aug 59	25
0.0047						4				KEWS	USASRDL	1958	28
0.005		Paraffin	555	25.4	12.7	75				Godiva	IBM	Oct 60	21
0.005		Paraffin	940	23.6	9.1	867				Godiva	IBM	Oct 60	21
0.01	600	Acrylic		0.02-0.03[a]			0		Disc	Linac	Hughes	1957	27
0.01						0.1[c]		Cornell Dublier	H.K.	Godiva	USASRDL	Aug 59	25
0.01			300		2.3		0.08		Disc	Godiva	Hughes	1958	9
0.02		Paraffin	820	28.3	14.5		507			Godiva	IBM	Oct 60	21

(a) Average value per pulse.
(b) Average value.
(c) Cable effects are known not to have been considered.

TABLE 21. SUMMARY OF TRANSIENT RADIATION EFFECTS ON MISCELLANEOUS CAPACITORS

Nominal Capacitance, μf	Working Volts, dc	Potting Compound	Test Voltage, v	Gamma Exposure, ergs g^{-1}(C) x 10^4	Maximum Gamma Exposure Rate, ergs g^{-1}(C) sec^{-1} x 10^8	Maximum Current, μa	Maximum Voltage Change, v	Manufacturer	Type	Reactor	Experiment	Date of Test	Reference
Mica													
0.001			-140		2.3		0.16		Silver Mica	Godiva	Hughes	1958	9
0.001		Paraffin	380	24.5	11.8	181				Godiva	IBM	Oct 60	21
0.0025		Paraffin	185	30.5	13.6	88				Godiva	IBM	Oct 60	21
0.0025		Paraffin	283	25.5	15.5	1800				Godiva	IBM	Oct 60	21
0.1	500	Epoxy Kish	600		2.6		3.6	El Menco	Silver Mica	Kukla	Boeing	Jun 60	31
0.1	500	Epoxy Kish	600		2.1		5.4	El Menco	Silver Mica	Kukla	Boeing	Jun 60	31
Electrolytic													
1	450	Acrylic		0.2-0.03[a]			0q			Linac	Hughes	1957	27
1	450		450		2.3		0.195			Godiva	Hughes	1958	9
1	450		450		2.3		0.125			Godiva	Hughes	1958	9
10		Paraffin	230		16.2[b]	2270		Sprague	TVL	Godiva	IBM	May 59	26
40		Paraffin	225		9.3[b]	2270		Sprague	TVL	Godiva	IBM	May 59	26
100		Paraffin	90		14.5[b]	387		Sprague	TVL	Godiva	IBM	May 59	26
100		Paraffin	80		8.3[b]	569		Sprague	TVL	Godiva	IBM	May 59	26
Teflon													
0.0002			363.0	20.1	16.4	318 ± 5		Balco		Godiva	IBM	Apr 60	29
0.03			363.0	4.7	4.4	852 ± 10		Balco		Godiva	IBM	Apr 60	29

(a) Average value per pulse.

(b) Overestimates of actual exposure rates.

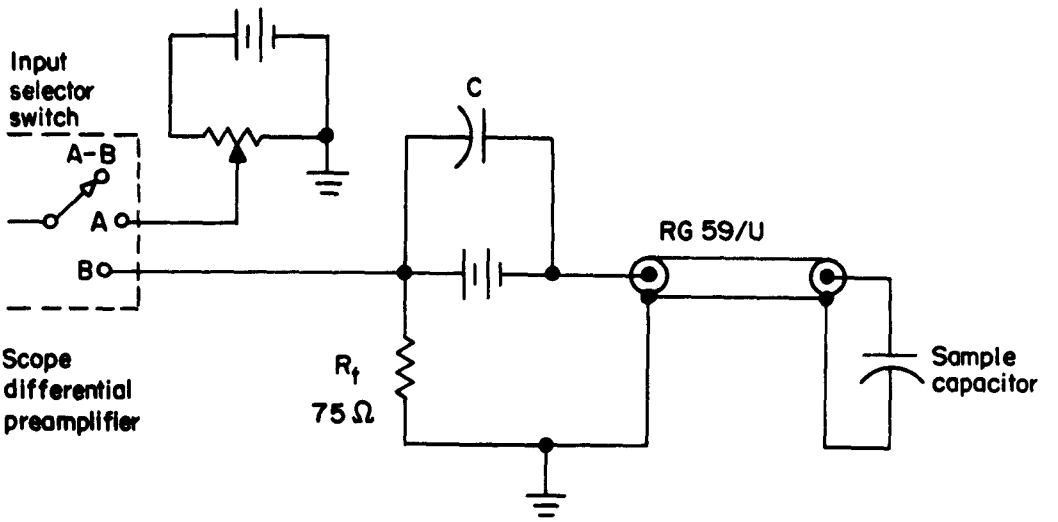

FIGURE 15. CAPACITOR TRANSIENT EFFECTS TEST CIRCUIT USED BY IBM

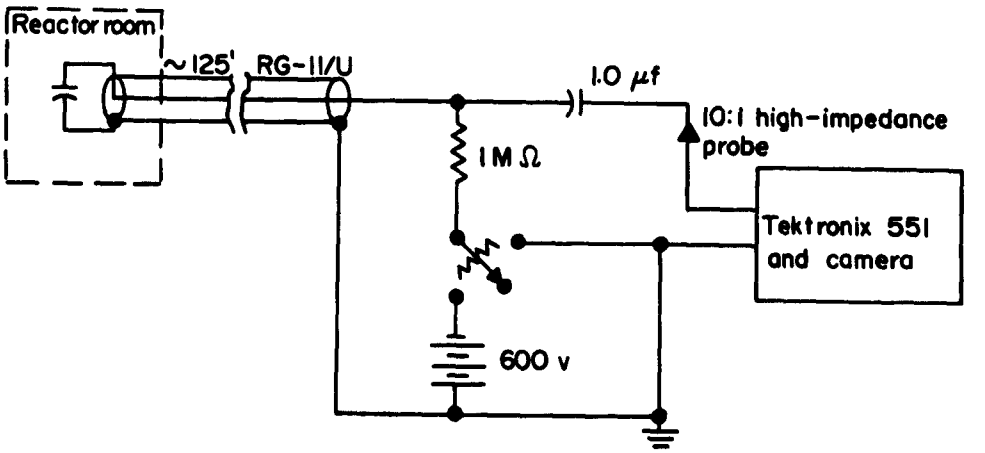

FIGURE 16. D-C EQUIPMENT AND CIRCUITRY USED BY BOEING TO TEST CAPACITORS

(4) The time it takes for a capacitor to regain its prepulse characteristics is a function of the time constant of the measuring circuit.[26,31]

(5) The conductivity of capacitor materials is a function of the gamma exposure rate.

(6) For gas capacitors, the general trend of data shows that the leakage current is an increasing function of the gamma exposure rate and the ratio of the electrical-field strength to the gas pressure.[26]

Quartz Crystals

The most popular piezoelectric crystal material used in practical application is quartz, since it is suitable for precise control of frequency in transmitting, monitoring, and receiving circuits, and in other highly selective circuits. One of the most common applications for crystals possessing piezoelectric characteristics is in transducers and accelerometers. Secondary in application are the electro-optical and piezo-optical effects caused, respectively, by the change in dielectric constant resulting from an applied electrical or mechanical stress. Due to the need for precision in control and operation of electronic circuitry controlled by crystals, their operation in a nuclear environment is an item of concern. The special methods used to maintain accurate temperature conditions and efforts in developing special techniques for cutting accurate crystal sections, in addition to precise mountings, can be fruitless if the critical functions are impaired during irradiation in a nuclear environment.

Several decades ago, the state-of-the-art knowledge that certain types of radiation reduce the elastic constants of quartz crystals was used as a convenient means for making precise adjustment to their frequency characteristics. It was believed that irradiations reduced the characteristic frequency because electrons are expelled from orbits around silicon atoms, causing lower energy binding between molecules. Such changes were of a semipermanent nature, as later evidenced by the restoration of the crystal units to their original characteristic frequency after baking. Thus, it would appear that for all practical purposes some degree of permancency with regard to radiation effects is well established. The question therefore arises as to whether radiation exposures of high intensity for short durations, such as would be experienced in critical assemblies which produce a pulse of neutrons, or nuclear-bomb detonations, cause serious temporary effects and possible permanent damage to the crystals.

The selection of a particular quartz crystal for application in an electronic circuit which might be exposed to transient radiation involves a wide variety of considerations. From the circuit designer's standpoint, such electrical parameters as (1) series resonant frequency, (2) parallel resonant frequency, (3) equivalent parallel impedance, (4) equivalent series impedance, and (5) electrostatic shunt capacitance are some of the factors which must be considered when weighing the effects of damaging radiation pulses. Some knowledge as to the magnitude of changes in the various parameter values can serve to point out areas of concern with respect to how much change can be tolerated under anticipated environmental conditions. From the component engineer's standpoint, such factors as (1) type of crystal by section, (2) mounting hardware, (3) manufacturer or source, (4) crystal make-up (synthetic or natural), and (5) manufacturing processes become important since each has some bearing as to the capabilities of the selected crystal unit to withstand damaging effects of nuclear-radiation pulses. Unfortunately, no complete

investigation encompassing the effects to various crystal parameters, singularly or collectively, has been conducted. Also, no conclusive study has been made as to how much influence the various physical factors contribute to measurable degradations noted during transient radiation experiments. The research reported to date is of a fragmentary nature, with results indicating that the various parameters show effects of transient radiation and that factors of a physical nature can contribute to differences in performance when crystals are exposed to nuclear detonations and transient radiation.

The two areas of concern associated with the effects of transient radiation on quartz crystals are related to permanent degradation and changes in electrical characteristics that are short-lived. In a sense, studies conducted to evaluate the permanent effects of transient radiations tend to simulate conditions that might be encountered under storage circumstances. Also, the evaluations tend to forewarn a possible user of the extent that such exposures may have on the prime function of the quartz crystal. Although in some instances where no permanent effects to electrical characteristics that are appreciable are indicated by postirradiation observations, no assurance is gained that the unit will function properly in a circuit at the instant of maximum levels of transient radiation. This latter effect is of major concern since quartz crystals perform a function requiring extreme precision in control of frequency and regulation in many critical circuits. To expand the knowledge in this area, a number of studies have been conducted and are in progress for the purpose of determining whether the crystal will perform its function in an operating circuit closely resembling its actual application. This type of approach is used primarily because of the insurmountable problems the researcher encounters in attempting to measure quartz-crystal electrical parameters when the units are exposed to radiation pulses that occur at extremely short intervals.

It has been mentioned that the component engineer is faced with many weighing factors prior to making a decision as to which crystal unit will be least susceptible to transient radiation effects. Knowledge of postirradiation effects can be an initial step in deriving some physical concepts as to the type of crystal cut, crystal make-up, and designation nomenclature related to the least-radiation-affected crystal unit. Toward this objective, some information has been compiled from pertinent experiments, and is presented in Table 22. To provide the data summary, results from three experiments were blended. The first experiment[37] involves nuclear-blast effects on the impedance and resonant frequency of various crystal units frequently used in military equipment. The second experiment[38] involves studies conducted at the Godiva II facility with crystals that were known for their physical make-up and crystal-cut type. The third experiment is associated with the crystal's capability for operation during a high-intensity pulse of nuclear energy.

For purposes of comparison, most of the crystal units listed in Table 22 were expected to conform with military specifications requiring frequency tolerances varying between 50 and 100 parts per million. Using these requirements as failure criteria, the Type CR-23/U crystals with the AT cut may have been the only crystal units that survived the burst of nuclear radiation. The highest radiation-burst exposure (8×10^6 ergs $g^{-1}(C)$ seems to have caused the most damage in a majority of cases and, as indicated by maximum changes pertaining to nonfailed units, showed the greatest measurable effects. There was a central tendency for the least severe radiation exposure (4.1×10^6 ergs $g^{-1}(C)$) to show the least effects of the burst, as would be expected. In general, the operation "Teapot" experiment[37] showed that quartz crystals, when exposed to the various gamma-radiation burst levels, do not change systematically, and the manufacturing processes and crystal cuts influence the results. The data show that the crystals of the type studied are susceptible to radiation damage since approximately 20 per cent

TABLE 22. CHANGES IN FREQUENCY AND IMPEDANCE PARAMETERS OF CRYSTAL UNITS DUE TO TRANSIENT RADIATION

Sample Size	Crystal Cut	Crystal Type or Make	Radiation Facility	Radiation Environment: Gamma Exposure Level, ergs g^{-1} (C)	Radiation Environment: Neutron Flux Level, n cm^{-2}	Number of Failures	Frequency Effects: Median Change, ppm	Frequency Effects: Maximum Change(a), ppm	Impedance Effects: Median Change, per cent	Impedance Effects: Maximum Change, per cent	Reference	General Comments
6	AT	CR-23/U	"Teapot" blast	4.1×10^6	--	3	3.4	-3.4	10.0	10.0	37	Failures occurred in crystal breakage form
30	AT	CR-18/U	Ditto	6.1×10^6	--	3	7.1	-33.2	21.0	430.0	37	Failures occurred in crystal mountings
18	AT	CR-23/U	"	6.1×10^6	--	0	1.4	-5.2	10.0	-20.0	37	No failures
6	AT	CR-23/U	"	8.1×10^6	--	3	1.9	2.4	19.0	19.0	37	Failures occurred in crystal breakage form
10	AT	Natural quartz	Godiva II	--	1.8×10^{12}	0	3.7	6.4	10.0	38.0	38	Units optically polished and aluminum plated; housed in HC-6 cans
10	AT	Synthetic quartz	Godiva II	--	1.8×10^{12}	0	3.3	7.4	5.0	33.0	38	Units manufactured at Clevite Research Center; mounted in HC-6 can; Y-bar seed
10	AT	Synthetic quartz	Godiva II	--	1.8×10^{12}	0	5.6	14.7	4.8	13.0	38	Units manufactured at Clevite Research Center; mounted in HC-6 cans; AT-Seed
12	AT	Synthetic quartz	Godiva II	--	1.8×10^{12}	0	2.1	5.33	6.3	21.2	38	Units manufactured at Bell Tel. Lab.; mounted in HC-6 cans
9	AT	Synthetic quartz	Godiva II	--	1.8×10^{12}	(	5.3	8.1	4.8	10.3	38	Units manufactured by General Electric of England; Z-cut seed; mounted in HC-6 cans
5	ET	CR-37/U	"Teapot" blast	4.1×10^6	--	0	-12.0	-26.0	-7.0	17.0	37	No failures
12	ET	CR-37/U	Ditto	6.1×10^6	--	1	-22.8	-118.0	80.0	245.0	37	Mounting and crystal damage
5	ET	CR-37/U	"	8.1×10^6	--	2	-30.6	-130.0	171.0	171.0	37	Mounting and crystal damage
13	DT	CR-38/U	"Teapot" blast	4.1×10^6	--	1	-5.0	536.7	2.9	42.8	37	Failure indicated by crystal breakage

TABLE 22. (Continued)

Sample Size	Crystal Cut	Crystal Type or Make	Radiation Facility	Radiation Environment: Gamma Exposure Level, ergs g^{-1} (C)	Radiation Environment: Neutron Flux Level, n cm^{-2}	Number of Failures	Frequency Effects: Median Change, ppm	Frequency Effects: Maximum Change(a), ppm	Impedance Effects: Median Change, ppm	Impedance Effects: Maximum Change, per cent	Reference	General Comments
17	DT	CR-47/U	"Teapot" blast	8.1×10^6		4	2505.0	-3829.0	8.7	35.1	37	Failure indicated by crystal breakage
9	DT	Natural quartz	Godiva II	--	1.8×10^{12}	0	12.0	21.0	8.7	35.0	38	Low frequency (328 KC), silver plated; mounted in an EC-6 can
8	NT	CR-38/U	"Teapot" blast	4.1×10^6	--	3	-25.9	-65.3	14.0	38.0	37	Failure indicated by damage to both crystal and mounting
14	NT	CR-38/U	Ditto	6.1×10^6	--	3	-35.6	-53.8	27.0	51.0	37	Failure indicated by damage to both crystal and mounting
8	NT	CR-38/U	"	8.1×10^6	--	4	-22.8	-41.7	17.0	43.0	37	Failure indicated by damage to both crystal and mounting
5	BT	Natural quartz	Godiva II	--	1.8×10^{12}	0	0.8	1.7	17.0	20.0	38	Semipolished, aluminum plated, and mounted in RC-6 cans
9	CT	Natural quartz	Godiva II	--	1.8×10^{12}	1	10.0	724.0	4.3	20.0	38	Gold-plated and mounted in HC-6 cans; 500-KC crystals
1	--	Bulova 300/GAX	Godiva II	--	1.9×10^9	0	--	--	--	50.0	24	Frequency remained stable, but amplitude decreased approximately 50 per cent

(a) Maximum changes shown for nonfailed crystals only.

were rendered inoperable. Of interest were appreciable changes in resonant impedance for the AT cut crystals. The increases in resonant impedance were attributed to the plastic bonding cement used in mounting the crystal which led to the recommendation that a more-radiation-resistant bonding material such as indium be used.

The crystals exposed to the transient radiation at the Godiva II facility were used to determine such influences as crystal cut and crystal make-up on frequency and resonant impedance characteristics after the radiation exposure. It can be seen (in Table 22) that differences between natural and synthetic quartz crystals are not brought out at the neutron-flux level (1.8×10^{12} n cm^{-2}) to which they were exposed. This should not be construed as indicating that the make-up does not influence the degree of radiation damage, but that more research is needed under more severe radiation environments than has been used in past tests. Slight differences between various crystal-cut configurations can be detected, with indications that the ET and DT crystal cuts are more prone to permanent radiation damage than the other configurations. A point of interest brought out by researchers associated with experiments conducted at the Godiva II facility emphasizes that some caution should be exercised in drawing conclusions concerning aging characteristics of quartz crystals on the basis of results obtained at the pulsed reactor. The accumulated effects shown for each crystal unit cannot be attributed to transient radiation effects alone, but include the effects from normal aging and temperature conditions. This behavior appears logical for quartz crystals that have been processed by the manufacturer through use of X-ray exposure for frequency adjustment. It has been mentioned that a convenient process for establishing the resonant frequency is to prepare the crystal seed for a frequency that is slightly higher than desired. This step in production is followed by exposure of the crystal to X-rays which tend to decrease the resonant frequency up to a saturation point. Thus, the manufacturing process may influence the extent of frequency change that might occur due to subsequent transient irradiation, depending upon the extent to which the characteristic frequency has been adjusted by X-ray treatment.

Information as to how the various electrical parameters of quartz crystals are affected at the instant of peak radiation exposure is extremely limited. Since it is desirable to ascertain the extent of malfunction that may be caused by transient radiation, most experimenters have attempted to study the effects on quartz crystals by operating them in an oscillator circuit and exposing only the crystal. In one instance[24] a Bulova 300 GAX crystal was exposed to a radiation pulse at an exposure rate of approximately 10^9 ergs $g^{-1}(C)$ sec^{-1}. By monitoring the output of the oscillator it was possible to observe a 50 per cent decrease in amplitude with no measureable change in frequency. The change in amplitude was explained as having been caused by a shunt-leakage path across the crystal terminals during the radiation pulse. Similar experiments, which produced conflicting results, were performed with quartz crystals at the Godiva II critical assembly[15] where the units were tested to determine transient radiation effects on the amplitude and frequency of resonant oscillations. For this experiment, no change of amplitude was detected during the pulse and only a slight change in frequency was observed. Other experimental efforts have resulted in further conflict of results by reporting loss of oscillator output amplitude, momentary interruption of oscillations, changes in frequency, and frequency shifts. In view of the many conflicting results, there is no question but that some major differences other than the general classification of the component may be biasing the experimental results. These differences between the quartz crystals may be those discussed, namely, crystal make-up, type of crystal cut, methods of mounting, and final processing by the manufacturers.

It is recognized that certain handicaps face the designer and component engineer in their selection of a radiation-resistant quartz crystal. However, with the limited amount of information that has been made available from steady-state and transient-radiation-effects studies, a certain amount of precaution in crystal selection is indicated. It must be realized that no one manufacturer produces crystal assemblies which are radiation resistant throughout their frequency range. Certain crystal cuts are more sensitive to radiation than others, perhaps because of certain orientation factors between the plate dimensions and the crystallographic planes. The fact that higher frequency crystals are prone to change drastically when subjected to transient radiation must be considered. Changes in impedance, which have attributed to the bonding cement frequently used, should be studied from a material standpoint. In studying these and other factors, a composite picture of a radiation-resistant quartz-crystal assembly will eventually materialize.

Magnetic Devices

Because magnetic devices have undergone considerable development during the past decade, magnetic materials are being utilized more frequently in electronic and electrical systems. The performance of magnetic devices depends upon the properties of the magnetic core; therefore, the core materials and their stability in a nuclear environment are of considerable concern. For optimum performance[39], the core material should have the following magnetic properties: (1) minimum hysteresis and eddy-current losses (high resistivity, low coercive force, and ability to be made in thin laminations or tapes), (2) high saturation-flux density, (3) magnetization curve shaped as closely as possible to a rectangular hysteresis loop, and (4) stable magnetic characteristics under changing temperature, mechanical strain, and shock conditions.

Of the various types of commercially available core materials that may be used for magnetic devices, nickel-iron alloys, particularly the grain-oriented rectangular-hysteresis-loop materials (Permenorm 5000 Z alloy, Orthonal, Deltames, etc.) have the most suitable properties. Cores of cold-rolled silicon steel tape may also be suitable in many cases, especially for higher power outputs. The saturation-flux-density values of the high-permeability materials (Permalloy C, Mumetal, 1040 alloy, etc.) as used in low-level input circuits are much lower than those of the rectangular-hysteresis-loop materials, which have proved most suitable for output-stage amplifier circuits.

The magnetic properties of core materials have been measured in many steady-state nuclear-radiation experiments to determine their reaction to prolonged exposures. These studies indicated that high-nickel-iron alloys should be avoided because the changes in permeability, coercive force, remanence, and loop rectangularity were prohibitive. On the other hand, silicon- and aluminum-iron alloys were considered highly resistant to changes in the mentioned magnetic properties. Unfortunately, none of the early research yielded information as to whether dose rate was an important factor.

The knowledge gained through steady-state radiation experiments may have been responsible, with some exceptions, for the exclusion of high-nickel-iron alloy in various applications as well as transient-radiation-effects studies. For this reason most current transient studies involve core materials containing no nickel ingredient in the alloy, or those containing a small per cent of nickel. This was indicated by one of the early studies where six Mn-Mg ferrite cores[11] with 50 turns of wire were subjected to Godiva pulse at a rate of 10^{17} n cm^{-2} sec^{-1}. The magnetic cores were in a nondriven or static state

when they were exposed to the radiation pulse with the objective of determining whether voltages would be induced in the coils at the instant of peak radiation level. It was also of interest to determine to what extent permanent damage to the magnetic properties occurred. The findings from this study indicated that no measurable output pulses were detected, and that no significant changes in the magnetic properties resulted.

Until recently, very scant information that could be useful to the designer and component engineer concerning transient radiation effects has been made available. Information of this nature is very important to the designer because of his concern as to whether the dynamic characteristics are changed sufficiently to cause an electronic system to malfunction during operation. Knowledge of pre- and postirradiation effects gained from steady-state irradiation experiments fails as a means for predicting system behavior during transient-type radiation. Of great value to the designer is knowledge concerning the instantaneous changes in threshold, remnant (B_r) or saturation flux density (B_s), or in the B_r/B_s ratio as would be indicated by changes in the amplitude or wave shape of the core output voltage during a burst of nuclear radiation. In addition to this knowledge, the extent to which transitory radiation affects an excited or driven magnetic core commonly encountered in various applications would provide considerable insight for determining which type of magnetic core material is most desirable for use in a transient nuclear environment. Research experiments which include (1) pulse tests, (2) write disturb – "zero" (wVz) output tests, (3) disturb tests, (4) "1-0" tests, and (5) static tests have been designed and conducted to provide information for application purposes. Some results of these experiments, which were conducted at the Sandia Pulsed Reactor[42] and the Godiva II critical assembly[40], have been included in this section because they represent the most recent and comprehensive coverage of the subject.

Pulse Tests. The magnetic core and tape materials used in the pulse test at the Sandia Pulsed Reactor (SPR) were Mg-Mn, Mn-Zn, and Cr-Mn-Ni-Zn ferrites, and 4-79 Mo-Permalloy tapes.[40] The general applications of the test items were for switching, memory, and logic circuits. Three of each material type were used under different conditions of "read" and "write" drive. For purpose of clarification, the drive conditions are referred to in Figure 17 as points "a", "b", "c", and "d" on a typical rectangular hysteresis loop. In the laboratory arrnagement, each magnetic core was in the shape of a toroid with three coils. The first coil in each of the cores was connected in series and energized with current pulses sufficient to drive the write current winding of the first core to point "a", the second core to point "b" and the third core to point "c". The second coil on each core was used to switch the core to negative saturation, or point "d" of the hysteresis loop. The third coil on each core was used to monitor the output voltage produced by the read and write current pulses in addition to any transient-radiation-induced voltages that might occur during the radiation burst. The monitored output voltage was also useful for determining whether the cores were affected permanently. With this arrangement, a major portion of the magnetic properties can be evaluated for transient radiation effects. Changes in threshold, remnant (B_r), or saturation flux density (B_s) would be indicated by changes in the amplitude or wave shape of the core output voltage during the burst.

The results of the SPR experiment[43] are presented in Table 23 which lists the details of pulse current drive, output voltages, and radiation environment for each core tested. A review of the results shown in Table 23 indicated to the researchers that the magnetic materials tested did not exhibit any major degradations. No permanent changes were anticipated at the integrated flux (2×10^{12} n cm^{-2}) to which the ferrites were exposed.

TABLE 23. TRANSIENT RADIATION EFFECTS ON VARIOUS MAGNETIC CORES AND TAPES WHEN SUBJECTED TO PULSE TEST (CURRENT) CONDITIONS

Magnetic Core Material	Application	Write Drive, ma-turns	Read Drive, ma-turns	Read Output Voltages, mv			Write Output Voltages, mv			Transient Radiation Environment		
				Pretest	During Radiation Pulse	Posttest	Pretest	During Radiation Pulse	Posttest	Gamma Exposure Rate 10^9 ergs $g^{-1}(C)$ sec^{-1}	Gamma Exposure, 10^8 ergs $g^{-1}(C)$	Integrated Neutron Flux, 10^{12} n cm^{-2}
Mg-Mn ferrite (wide temp range)	Memory	300	600	+15.6	+15.6	+15.0	-9.0	-9.0	-9.0	3.42	3.33	1.674
Ditto	Ditto	450	600	+15.6	+15.6	+15.8	-3.0	-3.0	-3.0	3.42	3.33	1.674
"	"	600	600	+48.5	+48.5	+48.5	-48.5	-48.5	-49.0	3.42	3.33	1.674
Mn-Zn ferrite	"	180	554	+790	+790	+790	-255	-255	-255	4.83	3.84	1.790
Ditto	"	360	554	+825	+825 / +520 (a)	+815	-960	-900 / -960 (a)	-960	4.83	3.84	1.790
"	"	540	554	+440	+360 / +440 (a)	+440	-1900	-1530 / -1900 (a)	-1900	4.83	3.84	1.790
Cr-Mn-Ni-Zn ferrite	Switch core	160	560	+95	+95	+95	-20.5	-20.5	-20.5	4.31	3.80	1.732
Ditto	Ditto	320	560	+540	+540	+540	-110	-110	-110	4.31	3.80	1.732
"	"	480	560	+650	+650	+650	-425	-425	-425	4.31	3.80	1.732
4-79 Mo-Permalloy tape	Logic	120	383	+17	+16	+16	-5	-5	-5	5.42	4.09	1.796
Ditto	Ditto	240	383	+46	+44	+30	-13	-12	-10	5.42	4.09	1.796
"	"	360	383	+38	+38	+27	-32	-32	-23	5.42	4.09	1.796
4-79 Mo-Permalloy tape	Switch core	146	624	+240	+240	+240	-60	-60	-60	6.38	4.81	2.200
Ditto	Ditto	292	624	+400	+400	+400	-80	-80	-80	6.38	4.81	2.200
"	"	438	624	+950	+950	+950	-450	-450	-450	6.38	4.81	2.200

(a) These voltages represent the range at which they fluctuated during the radiation pulse.

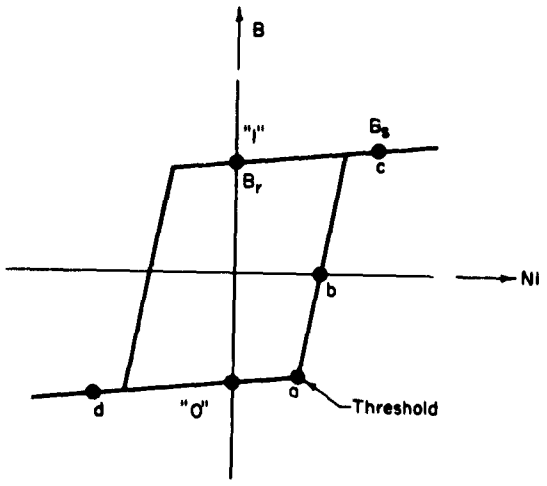

FIGURE 17. TYPICAL RECTANGULAR HYSTERESIS LOOP

Of primary interest was whether the output voltages of each core would be disturbed during the pulse. In most cases no changes in the output-voltage pulses were detected. In cases where the pulse voltages exhibited changes, some inconsistencies were noted. Two of the Mn-Zn cores exhibited sporadic changes in output voltage during both read and write pulses. The inconsistency arises in that the core with a write drive at the threshold (point "a") shows no change in output pulse, whereas the core excited by current pulses to saturation (point "c") does exhibit the output voltage fluctuations. It is conceivable that the core which was excited to point "b" on the hysteresis loop could be in a critical state in which an induced current could be reflected in pronounced output voltages. Regardless of the inconsistencies, it is possible to envision that in the cases where output voltages were disturbed by the nuclear pulse, the write current pulses may have driven the first core to negative saturation (below point "a") and thus were not reflected in the output voltage measured at the instant of the radiation pulse. From an earlier reference[39], it was mentioned that the high-nickel alloys were susceptible to radiation damage. The 4-70 Mo-Permalloy tapes used in this study fall in the class of those magnetic materials with high-nickel content. The difference between the two core types was in the thickness, width, and the number of wraps. The cores with the smallest dimensions and the lesser number of wraps exhibited the greatest changes in output-voltage pulses for both transient and posttest observations. Again, the second core with write drive current conditions (point "b") and the third core with drive current conditions (point "c") at saturation showed the greatest effects. No explanation for differences between the performance of large and small 4-79 Mo-Permalloy tapes can be given at this time.

The research experiment that was conducted at the Godiva II critical assembly[41] concerned Mg-Mn and Cu-Mn ferrites. The instrumentation and experimental design used were identical to those used in the SPR series. One difference in the experiment was the use of two air coils to gain assurance that any indication of voltage output observed during the radiation pulse could be attributed to transient radiation effects on the magnetic core. The results of the Godiva II series are presented in Table 24. The findings observed from the experiment were somewhat similar to those noted for the SPR series in that the cores that were driven ot point "b" (see Figure 17) on the

TABLE 24. TRANSIENT EFFECTS ON VARIOUS MAGNETIC CORES WHEN SUBJECTED TO PULSE TEST (CURRENT) CONDITIONS

Magnetic Core Material	Application	Write Drive (NI_w), ma-turns	Read Drive (NI_r), ma-turns	Read Output Voltages, mv			Write Output Voltages, mv		
				Pretest	During Radiation Pulse	Posttest	Pretest	During Radiation Pulse	Posttest
Mg-Mn ferrite (2 μsec)	Memory	140	300	+11.5	--		-3.0	--	--
Ditto	Ditto	210	300	+27.0	--	+27.0	-23.0	--	-22.0
"	"								
"	"	280	300	+10.0	+10.0	+10.0	-2.0	-2.0	-2.0
Mg-Mn ferrite (1μ sec)	Memory	200	500	+11.0	+11.0	+11.0	-1.5	-1.5	-1.5
Ditto	Ditto	300	500	+28.0	+29.0	+29.0	-5.5	-5.5	-5.5
"									
"	"	400	500	+56.0	+56.0	+55.0	-27.0	-28.0	-28.0
Cu-Mn ferrite (1μ sec)	Memory	280	600	+15.5	+15.0	+15.0	-2.5	-2.0	-2.0
Ditto	Ditto	420	600	+37.0	+33.0	+33.0	-10.0	-9.0	-9.0
"	"	560	600	+53.0	+53.0	+53.0	-45.0	-45.0	-45.0
None	--	210	300	+2.0	--	+2.0	+0.3	--	+0.3
None	--	210	300	+2.0	+2.0	+2.0	+0.5	+0.5	+0.5

Note: Radiation environment at Godiva II critical assembly; gamma radiation maximum rate, 1.04×10^3 ergs g^{-1} (C) sec^{-1}, total exposure, 2.73×10^5 ergs g^{-1} (C), neutron radiation; 12.2×10^{11} n cm^{-2} En >2.5 mev and 8.52×10^{12} n cm^{-2} En >0.75 mev.

hysteresis loop exhibited some tendency to change at the instant of peak radiation exposure level. The greatest change, both transient and permanent, was indicated for the Cu-Mn ferrite. It would be expected that some change could be expected since the cores most affected were those that were excited to a critical point on the hysteresis loop. The Mg-Mn ferrite (2 μ-sec) was only slightly affected, which might indicate that the Cu-Mn ferrite core material may be susceptible to transient radiation damage. The switching time for the ferrites was measured. The results of these measurements, taken under different write drive current conditions, are shown in Table 25. It was concluded that no problems would be encountered with respect to changes in switching time because of the exposures to transient radiation.

Write Disturb Zero Test. The "write disturb zero" or wVz test was concieved for the purpose of dynamically checking transient radiation effects on a write disturb zero signal. This signal was the output voltage generated by a full read current pulse after four half-select write current pulses were applied to the memory cores that were initially in the zero saturation state (see Figure 17). Changes in remnant and saturation flux ratio (B_r/B_s) or a change in the core threshold would be indicated by changes in the amplitude or wave shape of the wVx signal. In this phase of the experiment, the write current was adjusted to excite the core to point "a" (half-select write) and the read current was set to drive the core to point "d" (full-select read) on the hysteresis loop. The signal voltage values measured prior to the radiation pulse, during the pulse, and again after the pulse are shown in Table 26. In general, the observations noted during the SPR series indicated that the radiation pulses at the specified rate and exposure level did not affect the B_r/B_s ratio of the memory cores, nor were there any indications of changes in threshold. In some instances, the data were lost due to instrumentation or other difficulties; however, it was concluded that sufficient information was obtained to indicate that the core magnetic states were not affected. The experimental results from the Godiva II series[41] which involved Mg-Mn and Cu-Mn ferrites under similar instrument and circuit conditions are shown in Table 27. These results confirm the fact that the radiation pulse in the exposure rate and level listed cannot be expected to alter the core magnetic properties.

Disturb Tests. Disturb tests are designed to check the disturb "one" (rV_1) and "zero" (wVz) voltages of the memory cores. This is accomplished by applying half-select read and write current pulses to the memory cores, some of which are in the "one" state and others in the "zero" saturation states. The current-pulse arrangement included a 20-μ sec write current (I_w) which was used to assure full write with a half-select pulse occurring at some period during the write pulse. The write current was connected to switch half of the test samples to the "one" state and the remaining cores to the "zero" state. The half-select current (I_{hs}) was connected to "read-disturb" the cores in the "one" state by driving the cores to point "b" and "write-disturb" the cores containing "zeros" by driving them to point "a" (Figure 18). The read current (I_r) switched all cores to point "c". The current-pulse program[42] consisted of a write pulse occurring at between 1.5 and 2 μsec before the SPR pulse, continuous half-select pulses before, during, and after the pulse, and a read pulse approximately 60 μsec after the pulse. The results from the SPR series disturb test are given in Table 28.

TABLE 25. TRANSIENT AND POSTTEST RADIATION EFFECTS ON SWITCHING TIME OF 1-μSEC MEMORY CORES FOR VARIOUS DRIVE CONDITIONS

Magnetic Core Material	Drive Conditions, ma-turns		Voltage Amplitudes, μ			Posttest Switching Time, μsec
	Write(NI_w)	Read(NI_r)	Pretest	During Pulse	Posttest	
Mg-Mn ferrite	510	1000	53.5	53.5	53.5	1.3
Ditto	680	1000	83.5	86.0	86.0	0.76
"	850	1000	--	108.5	110.0	0.49
Cu-Mn ferrite	570	1000	30.8	30.8	30.8	1.76
Ditto	760	1000	69.5	69.5	71.0	0.615
"	950	1000	103.5	103.5	103.5	0.43

Note: Radiation environment at Godiva II critical assembly; gamma radiation maximum rate, 1.496×10^3 ergs $g^{-1}(C)sec^{-1}$, total dose, 2.51×10^5 ergs $g^{-1}(C)$, neutron radiation, 1.79×10^{12} n cm^{-2} En>2.5 mev, and 8.35×10^{12} n cm^{-2} En>0.75 mev.

TABLE 26. TRANSIENT RADIATION EFFECTS ON VARIOUS MAGNETIC CORES AND TAPES WHEN SUBJECTED TO wVz TEST CONDITIONS ("WRITE DISTURB ZERO" OUTPUT VOLTAGE)

Magnetic Core Material	Application	Write Drive, ma-turns	Read Drive, ma-turns	Read Output Voltages, mv			Write Output Voltages, mv			Transient Radiation Environment		
				Pretest	During Radiation Pulse	Posttest	Pretest	During Radiation Pulse	Posttest	Gamma Exposure Rate, 10^9 ergs g^{-1}(C) sec^{-1}	Gamma Exposure, 10^5 ergs g^{-1}(C)	Integrated Neutron Flux, 10^{12} n cm^{-2}
Mg-Mn ferrite (wide temp range)	Memory	390	650	+40.0	--	--	-20.0	-20.0	-20.0	3.78	3.68	1.79
Mg-Mn ferrite (wide temp range)	Memory	390	650	--	--	+40.0	-23.0	-23.0	-23.4	3.78	3.68	1.79
Mn-Zn ferrite	Memory	150	475	+1075	+1075	+1075	-175	-175	-175	4.70	3.74	1.80
Mn-Zn ferrite	Memory	150	475	+1150	+1150	+1150	-175	-175	-175	4.70	3.74	1.80
Cr-Mn-Ni-Zn ferrite	Switch core	200	475	+200	+200	-35	-35	-35	-35	4.92	4.34	1.83
Cr-Mn-Ni-Zn ferrite	Switch core	200	475	+260	+260	+260	-40	-40	-40	4.92	4.34	1.83
4-79 Mo-Permalloy tape	Logic	120	300	+48	+48	+48	-10	-10	-10	6.13	4.62	1.94
4-79 Mo-Permalloy tape	Logic	120	300	--	--	+70	-12	--	-12	6.13	4.62	1.94
4-79 Mo-Permalloy tape	Switch core	200	606	+335	+340	+340	-90	-90	-90	6.38	4.81	2.20
4-79 Mo-Permalloy tape	Switch core	200	606	--	--	--	-95	-100	-100	6.38	4.81	2.20

TABLE 27. TRANSIENT AND POSTTEST RADIATION EFFECTS ON MEMORY CORES WHEN SUBJECTED TO wVz ("WRITE DISTURB ZERO" OUTPUT VOLTAGE) TEST CONDITIONS

Magnetic Core Material	Drive Conditions, ma-turns[a]		Read Output Voltages, mv			Write Output Voltages, mv			Godiva II Radiation Environment			
	Pretest	Posttest	Pretest	During Radiation Pulse	Posttest	Pretest	During Radiation Pulse	Posttest	Gamma Exposure Rate, 10^3 ergs g^{-1} (C) sec^{-1}	Gamma Exposure, 10^5 ergs g^{-1} (C)	Neutron Flux (En > 2.6 mev), 10^{12} n cm^{-2}	Neutron Flux (En > 0.75 mev), 10^{12} n cm^{-2}
Mg-Mn ferrite (2 μsec)	158	260	+10.5	--	+10.5	-1.7	--	-1.7	0.62	1.18	0.70	3.22
Ditto	158	260	+10.0	+10.0	+10.0	-1.5	-1.5	-1.5	0.62	1.18	0.70	3.22
Mg-Mn ferrite (1 μsec)	245	400	+12.5	+12.5	+12.5	-2.8	-2.8	-2.8	0.89	2.34	1.07	7.38
Ditto	245	400	--	+20.0	+20.0	--	-3.6	-3.6	0.89	2.34	1.07	7.38
Cu-Mn ferrite (1 μsec)	275	450	+23.0	+23.0	+23.0	-2.0	-2.0	-2.0	1.07	1.74	--	18.50
Ditto	275	450	+23.0	+23.0	--	-3.6	-3.6	-3.6	1.07	1.74	--	18.50

(a) Half-select currents were approximately 60 per cent of full-select currents.

TABLE 28. TRANSIENT RADIATION EFFECTS ON MEMORY CORES AS INDICATED BY DISTURB TEST VOLTAGE OBSERVATIONS

Magnetic Core Material	Write Drive (NI_w), ma-turns	Half Select Drive (NI_{hs}), ma-turns	Read Drive (NI_r), ma-turns	Output Test Voltages, mv: Pretest	Output Test Voltages, mv: During Radiation Pulse	Output Test Voltages, mv: Posttest	Gamma Exposure Rate, 10^9 ergs g^{-1} (C) sec^{-1}	Total Gamma Exposure, 10^5 ergs g^{-1} (C)	Integrated Neutron Flux, 10^{12} n cm^{-2}
Mg-Mn ferrite (wide temp range)	650	390	650	81[a]	32	70	5.66	4.35	2.132
	650	420	650	82[b]	85	82	5.44	4.42	1.688
Ditto	650	390	650	77	32.5	69	5.66	4.35	2.132
	650	420	650	78	80	78	5.44	4.42	1.688
"	650	390	650	76	31	68	5.66	4.35	2.132
	650	420	650	78	80	78	5.44	4.42	1.688
"	650	390	650	20.5	81.5	30	5.66	4.35	2.132
	650	420	650	20.5	20	20	5.44	4.42	1.688
"	650	390	650	17.5	75	26	5.66	4.35	2.132
	650	420	650	18	18	18	5.44	4.42	1.688
"	650	390	650	140	150	150	5.66	4.35	2.132
	650	420	650	88	88	85.5	5.44	4.42	1.688
Mg-Mn ferrite ($2\mu s$)	260	158	260	41	43	43	5.96	4.24	2.227
Ditto	260	158	260	41.5	43	43	5.96	4.24	2.227
"	260	158	260	13	11.5	11.5	5.96	4.24	2.227
"	260	158	260	12	10.5	11.0	5.96	4.24	2.227
"	260	158	260	45	47	46.5	5.96	4.24	2.227
Mg-Mn ferrite ($2\mu s$)	400	245	400	87	32.5	10	5.88	3.96	2.217
Ditto	400	245	400	82	34	13.5	5.88	3.96	2.217
"	400	245	400	17	64	94	5.88	3.96	2.217
"	400	245	400	14	58	88	5.88	3.96	2.217
"	400	245	400	61.5	68	60	5.88	3.96	2.217
Cu-Mn ferrite ($2\mu s$)	478	287	478	65	72	69	2.82	2.92	0.159
Ditto	478	287	478	68	77	75	2.82	2.92	0.159
"	478	287	478	20	18	18	2.82	2.92	0.159
"	478	287	478	20	19.5	20	2.82	2.92	0.159
"	478	287	478	101	108	109	2.82	2.92	0.159

(a) Shot one.
(b) Shot two.

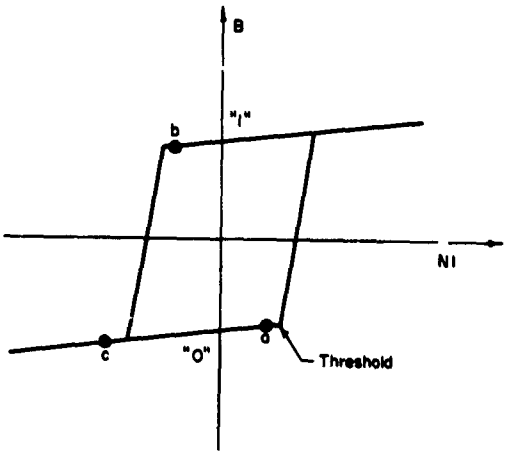

FIGURE 18. TYPICAL RECTANGULAR HYSTERESIS LOOP FOR DISTURB TESTS

The results and conclusions from the disturb test studies indicated that the memory cores consisting of Mg-Mn ferrites (2 μsec) and the Cu-Mn ferrites (1 μsec) were not affected so far as their magnetic properties and dynamic states were concerned. The Mg-Mn ferrite cores (wide-temperature-range cores) appeared to show some effects in that the "one" and "zero" flux states were approximately half-switched. A second radiation pulse on the same memory cores (results also shown in Table 28) under an increased half-select drive current (I_{hs}) and no radiation-induced effects was observed. It was suspected that the difference in results between the two shots could not be attributed to the radiation environment entirely, but that some change in circuit conditions or even perhaps the minor increase in half-select drive current may be responsible. The Mg-Mn ferrite cores (1 μsec) were also found approximately half-switched, and it was concluded that these cores were operated at a very critical point and could be expected to change to the extent observed. The effects as shown by posttest output voltages could not be explained by subsequent investigations, and it was concluded that more testing would be needed to arrive at some explanation for the effects listed. The results from the Godiva II investigations[41] on the disturb conditions of the ferrites confirmed most of the results obtained from the SPR experiments, and the main agreement between the two series was that the disturb test samples indicated variations of 10 to 15 per cent in output signal voltages.

"One-Zero" Test. The "one-zero" test was included in the SPR series for transient radiation effects on memory cores. This test was specifically designed to determine whether there would be any changes in the "one" and "zero" flux states of two-aperture Mg-Mn ferrite memory cores when subjected to a transient radiation environment. This phase of the experimental work serves adequately to point out the complexities encountered in two-aperture memory cores because of the different flux patterns that can be established. A better understanding of these complexities can be gained through discussion of drive currents and flux patterns displayed in a typical memory core application shown in the diagrams of Figure 19. In Figure 19 and the

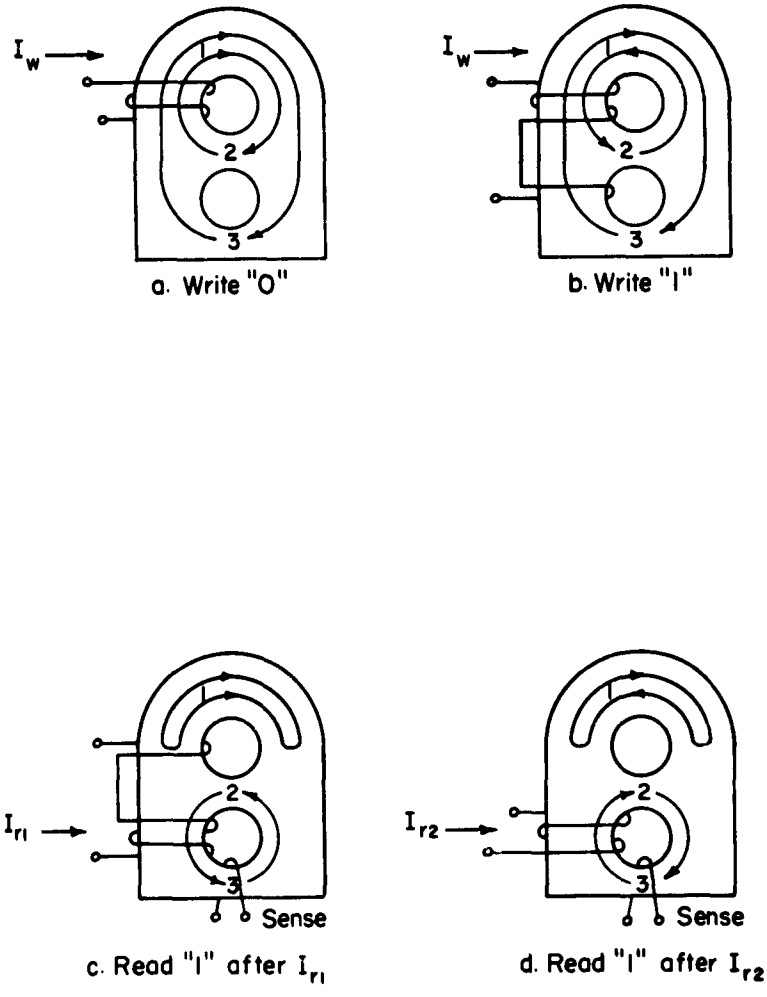

FIGURE 19. FLUX PATTERNS IN TWO-APERTURE MEMORY CORES

experimental setup, the drive current was connected to switch the first core to the "one" state and the second core to a "zero" state. The drive current (I_w) applied to the upper hole through two turns of wire, switches the flux in legs 1, 2, and 3 to a clockwise direction or "zero" state. The write "one" drive, shown as Figure 19b, consists of two turns in the upper hole which cause the flux to move counterclockwise, and the one turn in the lower hole causes the flux in Leg 3 to remain in the clockwise direction. In essence, the drive current switches the flux in Leg 2, and one-half the flux in Leg 1, counterclockwise. The flux in Leg 3, and one-half the flux in Leg 1, remain in the clockwise direction. Interrogation of the memory core is accomplished by means of a pair of read pulses. The first read pulse (I_{r1}) is connected to switch the flux in Leg 3 in a counterclockwise direction. In order that the flux in Leg 3 can switch, an equal amount of flux in Leg 2 must switch when the core is in the "one" flux state. Also, an equal amount of flux in Leg 1 must switch when the core is in the "zero" state. The ampere-turns required to switch flux in a magnetic core is proportional to the path length about which the flux is switched. Consequently, the relative hysteresis loops which are related to the "one" and "zero" flux patterns are similar to those shown in Figure 18 for the lower aperature where the read ampere-turns (NI_r) were adjusted to point "a". The drive ampere-turns switched flux in Legs 2 and 3 of a "one" flux state core, Figure 19c, but were below the threshold for switching flux in a "zero" flux state core. The one-turn winding through the upper hole acts as a bias to prevent the flux from switching in Leg 1. The flux pattern for a core in the "zero" state, after I_{r1}, remains in the "zero" state, as shown in Figure 19a. The read drive pulse (I_{r2}) was connected to drive the flux in Legs 2 and 3 in the clockwise direction. The read drive pulse (I_{r2}) switches a "one" flux state core from the flux pattern shown in Figure 19c to the pattern shown in Figure 19d. In this arrangement, no flux is switched in a "zero" flux state core. Because the read cycle and the write operation are independent, any number of read pulse pairs can be applied between write pulses. In this respect, it is a form of nondestructive read.

The results from the "one" and "zero" test experiment are shown in Table 29. Some output peak voltages are not shown because of instrumentation and photographic difficulties; however, sufficient wave-form data were available to indicate that none of the radiation pulses affected the "one" and "zero" signals at the sensing terminals.

Static Test. The knowledge that steady-state radiation and transient radiation cause a certain amount of change in the various magnetic properties of memory cores does not definitely indicate to the designer and component engineer that the device will malfunction. To gain assurance that the device can withstand nuclear bombardment, flux conditions must be prearranged to coincide closely to the application. The static test was designed to determine whether the memory cores could retain preset flux patterns after exposure to a radiation pulse. To accomplish this investigation[42], a memory plane was constructed which consisted of 16 two-aperture Mg-Mn ferrite memory cores arranged in a 4 x 4 configuration. A random pattern of "ones" and "zeros" was written into the memory plane. This was followed by exposing the memory plane to ten radiation pulses at the Sandia Pulsed Reactor. No read or write drive currents were applied during irradiations. Each core was nondestructively read after the exposure, and the results are given in Table 30. It was concluded from this investigation that variation between pretest and posttest results was within 2 millivolts for all cores with the exception of one unit. This memory core exhibited a change of 2.5 millivolts. In general, it was believed that the changes listed for this test were not excessive and that

TABLE 29. TRANSIENT RADIATION EFFECTS ON "ONE" AND "ZERO" FLUX STATES OF FERRITE (Mg-Mn) TWO-APERTURE CORES

Write Drive (I_w), ma	Read Drive (I_{r1}), ma	Read Drive (I_{r2}), ma	Read Output Voltages, mv			Write Output Voltages, mv			Transient Radiation Environment		
			Pretest	During Radiation Pulse	Posttest	Pretest	During Radiation Pulse	Posttest	Gamma Exposure Rate, 10^9 ergs g^{-1} (C) sec^{-1}	Max Gamma Exposure, 10^5 ergs g^{-1} (C)	Integrated Neutron Flux, 10^{12} n cm^{-2}
158	158	158	+19	+19	+19	Off scale	Off scale	Off scale	7.16	5.09	--
158	190	158	+30	+28	+28	-20	-19	-19	7.81	5.26	2.586
158	158	158	+17.5	+17.5	+17.5	-18.5	-18.5	-18	3.05	3.16	1.760
158	158	158	+1.75	+1.75	+1.75	-2.7	-2.7	--	7.16	5.09	--
158	190	158	+2.75	+2.60	+2.70	-3.4	--	-3.4	7.81	5.26	2.586
158	158	158	+1.85	+1.85	+2.00	-3.25	-3.00	-3.00	3.05	3.16	1.760

TABLE 30. TRANSIENT RADIATION EFFECTS[a] ON FERRITE(Mg-Mn) TWO-APERTURE CORES OF A (4 x 4) MEMORY PLANE IN A NONPULSED CURRENT STATE

Core Location		Read Voltages (I_{r1}), μ		Read Voltages (I_{r2}), μ	
X-Plane	Y-Plane	Pretest	Posttest	Pretest	Posttest
1	1	+19	+21	-19	-21
1	2	+20	+22	-20	-22
1	3	-19	-21	+19	+20
1	4	-1.5	-2	+1.5	+3
2	1	-1.5	-2.0	+2.0	+1.0
2	2	-1.5	-2.0	+5.0	+6.0
2	3	+20	+21	-20	-21
2	4	+3.5	+4.5	-5.0	-5.5
3	1	-19	-20	+19	+20
3	2	-2	-3	+6	+8.5
3	3	+2	+3	-2.5	-3.5
3	4	+20	+21	-20	-22
4	1	+4	+4.5	-7	-9
4	2	+20	+22	-20	-21
4	3	-20	-22	+20	+21
4	4	-1.5	-2.5	+2	+2.5

(a) Neutron and gamma exposures dose for 10 shots; 1.719×10^{13} n cm^{-2} and 3.68×10^{6} ergs g^{-1}(C).

for all practical purposes the irradiation had no effect on the flux states of the inactive two-aperture ferrite memory cores.

Conclusions. The tests conducted have pointed out certain areas where no concern need be shown for specific applications and to a limited extent where some caution must be exercised. It can be stated that no transient radiation effects can be expected for memory cores under application conditions described in (1) "write disturb – zero" (wVz) output, (2) "one" – "zero", and (3) static tests. The changes observed in the pulse and disturb investigations indicate that some effect from the pulse radiation may be expected; however, they also indicate that additional research is necessary before these changes can be explained thoroughly. Because no measurable permanent damage to any of the memory cores exposed to radiation pulses at both Godiva II and the Sandia reactor facilities was observed, some possibilities exist for which some of the effects observed during the radiation pulse were contributed by air ionizations and cable effects. This contribution of effects cannot be considered large since elaborate preparations, such as the potting of test units and cable termination in paraffin, were made. Also, in some phases of the studies, various control checks were made to determine whether cable influences were present.

Printed-Circuit Boards

The use of copper-foil-clad laminates for printed-circuit boards in electronic equipment has made it possible to reduce production costs as well as physical sizes of complex electronic assemblies. However, the effects of various environmental conditions, not considered important for the open-wire-type circuitry, may tend to offset some of the advantages gained. Uncoated printed-circuit boards exposed to nuclear radiation are affected in a number of ways. Of major interest seems to be degradation of insulation properties as indicated by various studies based on changes in dissipation factor, insulation resistance, and capacitance caused by nuclear radiation. Degradations in the form of metal oxides deposited on the surface of the copper-foil strips as well as discontinuities in the foil are other ways in which nuclear radiation has been found to affect printed-circuit boards. In some instances materials such as fluorocarbons have been found to melt completely.

Some difficulties encountered in the past in evaluating steady-state radiation effects on printed-circuit boards involve secondary effects caused by in-pile temperature conditions and ionization currents. An exposure to ambient temperatures of 150 C alone, without the added effects of nuclear radiation, has been known to cause certain types of laminates to crack and become distorted. Foil-clad laminates under such temperature conditions have been known to form blisters and on rare occasions have burst. Ionization currents caused by intense nuclear-radiation fields present difficulties by confusing measurements of leakage currents as well as other parameters.

Most of the basic knowledge associated with transient radiation effects on printed-circuit-board materials was derived from many of the various steady-state nuclear-radiation-effects studies. Although major differences exist between types of nuclear radiation encountered in material-test and pulsed-type reactors with respect to type of neutron radiation and energy levels, much has been achieved in providing information useful for prediction of performance in a transient radiation environment. One of the

early radiation-effects studies[44] involved experiments using the CP-5 materials test reactor, with results indicating that drastic changes in critical parameters occurred at the instant peak radiation levels were reached. In essence, this introduced the understanding that materials used for printed-circuit boards were extremely sensitive to exposure rate. Some of these results are given in Table 31 for the various materials that withstood prolonged radiation exposure and were in a physical state that would permit measurements of evaluating parameters. The conclusion from this study emphasized the existence of manufacturing-process differences and the fact that this influence was so great that the results could not be used for determining which printed-circuit-board material was most resistant to nuclear-radiation damage. It also pointed out that printed-circuit boards coated with Krylon appeared more radiation resistant than uncoated boards; however, the extent of improvement was not of a magnitude where its use could be recommended. The main point of interest from the study was that insulative coatings influenced the electrical properties of printed-circuit boards where exposure to radiation fields became a certainty.

Since it has been established that printed-circuit boards require coatings to minimize conditions of transient-radiation-induced ionization currents, a problem then exists in determining the type of coating that will reduce transient effects of nuclear radiation. Among various studies conducted to determine which coating was most appropriate, an experiment[45] was designed to explore the difference in exposure-rate sensitivity between coated and uncoated copper-clad Fiberglas-melamine boards. In this experiment, five printed-circuit boards, one uncoated and four with different insulative coatings, were evaluated. The coatings were silicone varnish, epoxy-polyamid, nitrocellulose lacquer, and polyester coatings. The leakage current between copper-foil conductors and the interelectrode capacitance was measured while the specimens were out of the radiation field and again while they were exposed to a gamma exposure rate of approximately 7×10^3 ergs $g^{-1}(C)\ sec^{-1}$. Some of the results are given in Table 32 where it can be seen that the insulative coatings caused a decrease in the ionization effects. All of the coated printed-circuit boards exhibited improvement in the various electrical characteristics as compared with the uncoated boards. The polyster coating appears to be superior to the other coatings; however, all coatings used seemed sensitive to radiation exposure rate and temperature.

Most studies conducted with radiation exposures to dielectric materials have produced results indicating that the major problems confronting the electronic designer are those involving ionization effects. Since ionization currents are to a great extent involved and designated as highly contributory to exposure-rate sensitivity, they can be classified as equivalent power sources in a circuit configuration. In this respect, it would then be logical that circuit potentials and currents would be in some way be affected by radiation-induced currents and voltages. To explore the nature of these added difficulties that may influence design considerations, experiments were conducted to provide some insight to the transient-radiation problem to determine how circuit impedance, protective coatings, and applied potential would change the characteristic appearance of the radiation-induced current pulses. In the experiment[27], the printed-circuit boards tested were phenolic and epoxy, 1/16 inch thick, with a printed-circuit grid consisting of two comblike configurations intermeshed, but not making contact. The space between the adjacent conductors was 3/64 inch, and each comb consisted of 5 teeth, 1-1/4 inches long. The radiation pulse used in this study was produced by a traveling-wave linear accelerator which generated a pulsed narrow beam of high-energy electrons for a period of approximately 10 microseconds. The radiation pulses averaged 2.38×10^8 ergs $g^{-1}(C)\ sec^{-1}$.

TABLE 31. SUMMARY OF IN-PILE MEASUREMENTS OF CRITICAL PARAMETERS OF PRINTED-CIRCUIT BOARDS[a]

Evaluation Parameters Measured	Average of Preirradiation Measurements, range of values	Range or Change of Parameters Measured Upon Exposure
	Glass-Epoxy	
Insulation Resistance, ohms	340 x 3,100 x 10^9	0.01 to 1,160 x 10^9 ohms
Capacitance, μμf	11.4 to 15.5	24 to 180 %
Dissipation Factor	0.03 to 0.08	0.45 to 0.98
	Glass-Melamine	
Insulation Resistance, ohms	2.9 to 2800 x 10^9	0.10 to 1116 x 10^9 ohms
Capacitance, μμf	13 to 33.5	0 to 60 %
Dissipation Factor	0.05 to 0.74	0.06 to 0.65
	Paper-Phenolic	
Insulation Resistance, ohms	580 to 1370 x 10^9	0.10 to 4233 x 10^9 ohms
Capacitance, μμf	10.9 to 13.9	3.0 to 30 %
Dissipation Factor	0.01 to 0.06	0.22 to 0.37
	Steatite	
Insulation Resistance, ohms	14.7 x 10^9	1.0 to 10,000 x 10^9 ohms
Capacitance, μμf	14.5	2.0 to 3.3 %
Dissipation Factor	0.038	0.12 to 0.17
	Nylon-Phenolic	
Insulation Resistance, ohms	625 to 1600 x 10^9	0.17 to 4600 x 10^9
Capacitance, μμf	10.7 to 14.1	5 to 21.0 %
Dissipation Factor	0.02 to 0.06	0.062 to 0.30

(a) Typical nuclear environment for printed-circuit boards in-pile: Neutron fluxes = 2.1 x 10^{12} (Nv_o) and 3.6 x 10^9 n cm^{-2} (epicadmium); and gamma exposure rate = 5.3 x 10^4 ergs g^{-1} (C) sec^{-1}.

TABLE 32. RADIATION EXPOSURE-RATE-AFFECTED CHANGES OF ELECTRICAL PARAMETERS FOR VARIOUS PRINTED-CIRCUIT BOARDS WITH VARIOUS INSULATIVE COATINGS

Evaluation Parameter Measured	Preirradiation Measurement	In-Pile Parameter Measurement
	Nitrocellulose Lacquer	
Leakage Current, amp	$>10^{-12}$	9.2×10^{-8}
Capacitance, $\mu\mu$f	17.1	10.2
Breakdown Voltage, kv	4.2	2.6
	Silicone Varnish	
Leakage Current, amp	$>10^{-12}$	5.6×10^{-10}
Capacitance, $\mu\mu$f	15.0	8.5
Breakdown Voltage, kv	3.7	3.2
	Epoxy-Polyamid	
Leakage Current, amp	$>10^{-12}$	9.1×10^{-9}
Capacitance, $\mu\mu$f	16.4	10.1
Breakdown Voltage, kv	4.3	3.7
	Polyester	
Leakage Current, amp	$>10^{-12}$	8.3×10^{-10}
Capacitance, $\mu\mu$f	21.3	11.0
Breakdown Voltage, kv	3.9	3.3
	Uncoated Circuit Board	
Leakage Current, amp	$>10^{-12}$	1.09×10^{-7}
Capacitance, $\mu\mu$f	14.2	10.3
Breakdown Voltage, kv	2.7	2.8

Note: Typical radiation dose rate = 7×10^3 ergs $g^{-1}(C)$ sec^{-1}.

The circuit mentioned above consisted of one comb that was connected to a regulated power supply of a variable d-c voltage up to 500 volts. The other comb was connected to ground through a series resistor located out of the radiation field. The pulses developed across this resistor by currents flowing during radiation were detected through a cathode follower whose output was connected to an oscilloscope. Two samples of each board were used (phenolic and epoxy); one sprayed with acrylic resin and the other uncoated.

Wave forms were observed on the oscilloscope for various applied voltages from 0 to 500 volts. The shape and magnitude of these pulses under conditions of voltage application and coating are shown in Figures 20 and 21. It was noted that the differences between effects on phenolic and epoxy circuit boards were insignificant. In examining the various pulses shown in Figures 20 and 21, the presence of the large negative pulse for zero applied voltage on the coated board was surprising because the uncoated board displayed a slight positive pulse. It was also noted that the large negative pulses tend to build up for a time after the radiation pulse. It was hypothesized that the thin coating of acrylic resin is a source of negative charge that continues to build up with each successive pulse due to a very high insulation resistance to ground. The opposite reaction for the uncoated boards was explained as being caused by a positive charge resulting from electron ejection and a decrease in leakage resistance through the air and across the surface of the board from one conductor to the other.

It cannot be concluded that an insulating coating is a positive solution to the reduction of radiation-induced ionization in circuit-board materials, but it does indicate that some degree of control can be achieved. Other types of coating, probably of the silicone or polyester varieties, might produce more satisfactory protection from transient radiation.

Subsystems

Past research related to transient radiation effects on electronic component parts and materials has been conducted with the objective of determining which type of component part is least susceptible to high-intensity radiation pulses and again for the purpose of predicting the functional performance of these parts in electronic circuits. For the greater part, these studies have indicated that certain component parts should not be used in radiation environments. The important outcome of the research is the insight gained with respect to additional parameters that must be considered when electronic circuits are designed for use in radiation environments. These additional parameters have been recently designated as radiation-induced parameters which consist of (1) radiation-induced currents and voltage pulses, (2) increases in surface and bulk leakage currents attributed to charge injection and scattering phenomena, and (3) permanent changes in the basic structural materials.

Two methods, both predicated by results of many theoretical and experimental programs, are currently being considered and employed in approaching the problem of hardening the circuit against radiation. The first method utilizes an approach whereby known radiation effects on electronic parts are employed in programming circuit-analysis problems on an anolog computer. In essence, the first approach is of a theoretical nature since it consists of calculating or simulating the circuit or system response

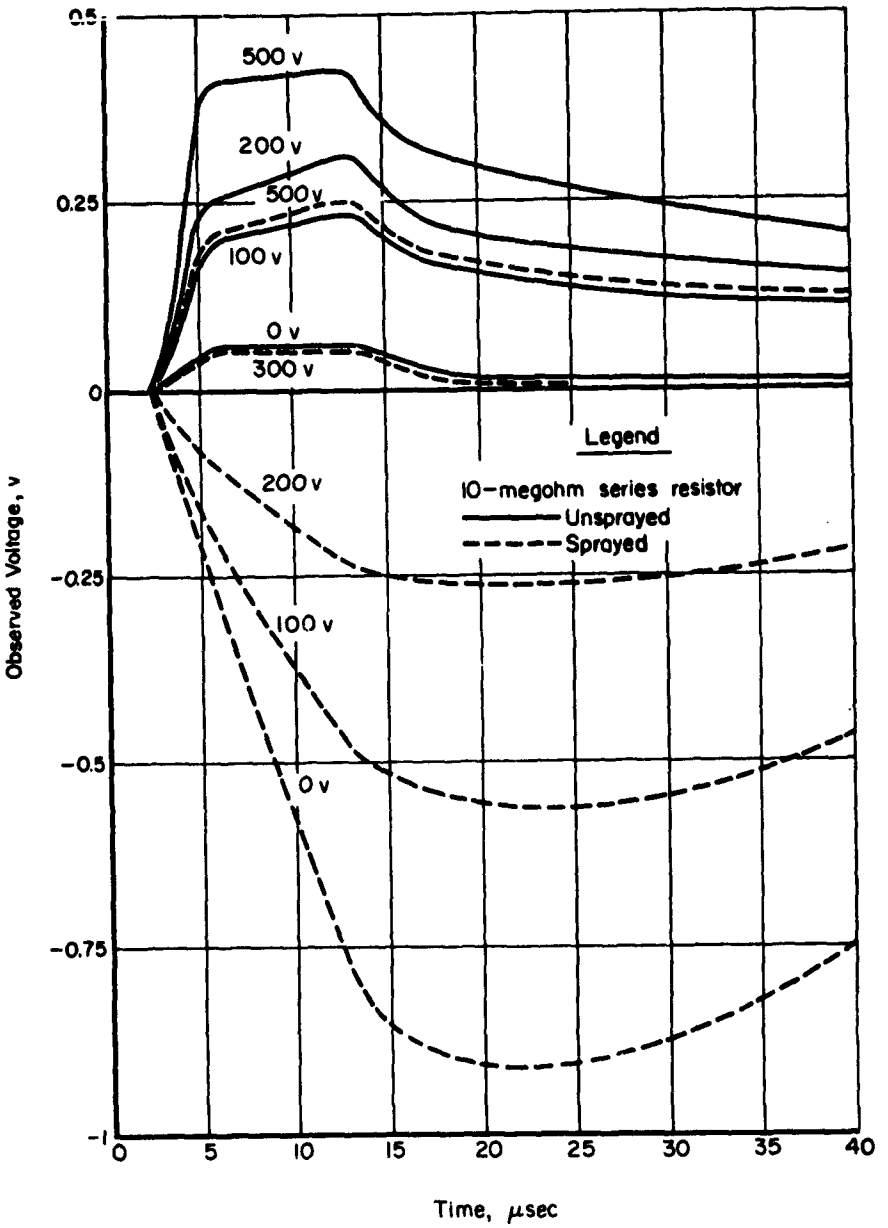

FIGURE 20. EFFECTS OF TRANSIENT RADIATION ON PRINTED-CIRCUIT BOARDS(40)

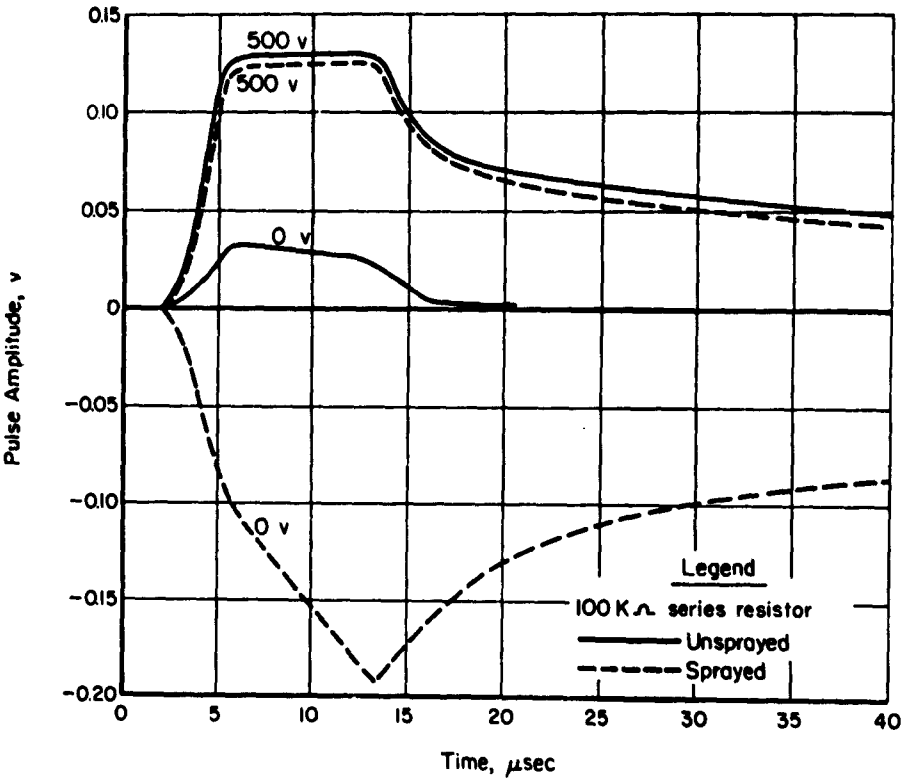

FIGURE 21. EFFECTS OF TRANSIENT RADIATION ON PRINTED-CIRCUIT BOARDS(40)

with respect to radiation-induced disturbances. The disturbances which are introduced into the calculation are based on experimental data for component parts and materials which have been investigated in various radiation-effects research programs. The second method consists of actual circuit or system testing in a pulsed-radiation-facility environment.

Recently reported studies[54] indicate that the theoretical approach for determining circuit responses to disturbances produced by radiation pulses is feasible for vacuum-tube and transistor amplifiers, multivibrators, and semiconductor detector circuits. The determination of responses was accomplished by using an analytical process for each of the circuits. This process included preparation of circuit nodal equations for both the normal circuit and the irradiated circuit. Leakage and charge-injection parameters, made available from literature surveys, were used to reconstruct the equivalent circuit. Since in some cases it is necessary to separate the leakage parameters from the charge parameters, their values were kept independent in an analog loop. The circuit nodal equations are used by the programmer to prepare a preliminary block diagram which shows the number of operations required for a solution to circuit responses. The conclusions from these studies were that an analog-computer technique can be used quite successfully for the theoretical investigation of radiation effects on electronic circuits. Results obtained from the study of the amplifier circuits were fruitful in determining nonlinear circuit response caused by radiation. Other observations noted from the data indicated that:

(1) High-impedance circuits are particularly sensitive to leakage effects.

(2) High-gain circuits are sensitive to charge-distribution phenomena such as injected currents and leakage.

(3) Transistor circuits are sensitive to leakage effects between control and output points and to injected currents that contribute to increases in base currents.

(4) The diode detector effects stem from leakage across the output.

(5) The multivibrators are affected by both leakage and charge injection in the input portion of the circuit with the change of conduction state occurring only for the large current injection and/or charge distribution.

The direct approach for determining whether a circuit will function properly during a pulse of nuclear radiation is associated with the second method involving aspects of actual testing. The principal advantages of this second approach lie in the fact that the environment provided is ideal rather than simulated and the circuit package usually is the item of concern. The main disadvantage of the second method is that the information obtained applies only to the circuit assembly used and cannot be treated under general definitions of the circuit type. Because circuit designs vary considerably from application to application, differences in component parts and their arrangements in circuits make it impossible to derive a precise pattern for transient radiation effects. Regardless of this, some insight can be gained by examining results obtained from reports on the subject. In this respect, Table 33 summarizes the results from research experiments conducted for such circuits as (1) multivibrators, (2) oscillators, (3) power supplies, and (4) amplifiers.

Multivibrators

The main factors affecting operation of a multivibrator in a radiation environment involve effects such as change in conducting state, triggering, and pulse amplitude. Most of the multivibrator circuits listed in Table 33 use transistors as the main functional component. With few exceptions, most of these circuits triggered or changed their state during the radiation pulse. In the few cases listed for vacuum-tube-type circuits, some exhibited no effects, whereas others were found to have changed their state. In one instance[50] where six transistorized units were subjected to test at the Godiva II facility, three units were classed as complete failures with the remaining three units exhibiting a decrease in output of between 70 and 80 per cent. In other cases[6], the magnitude of the amplitude was not greatly affected. However, the pulse shape changed considerably, with some ringing occurring at high repetition rate for a short time after the pulse had reached its peak flux intensity. What may prove to be interesting were results from the experiment with the transistorized Eccles-Jordan bistable flip-flop circuit. In this study, no triggering failure or erratic triggering occurred during the exposure and only a 5 per cent increase in voltage amplitude was observed during the pulse.

Oscillators

The main interest surrounding operation of an oscillator in a transient radiation environment involves effects such as frequency and amplitudy shifts as well as whether the oscillator exhibits indications of complete failure. Of the 13 oscillators subjected to transient radiation in recent studies (results shown in Table 33), 4 of the 6 of one particular type[50] of transistorized oscillator failed completely. None of the electron-tube-type oscillators failed completely during the radiation pulse, and none exhibited permanent damage. The majority of electron-tube oscillators exhibited transient effects consisting of loss of amplitude by as much as 90 per cent: however, recovery was noted as the flux intensity subsided. Frequency shifts were not excessive, as indicated by the voltage-controlled oscillator exhibiting a maximum[51] of 3.1 per cent for full band width. In this instance it was concluded that the oscillator unit should have deviated less than 1.5 per cent of center frequency and would have been less than 1.0 per cent after proper design of the filament compensation circuit.

It would then appear that transient radiation effects on operating oscillator circuits of major concern should be associated with changes in output amplitude at the instant of peak radiation intensity and that lesser concern need be shown for aftereffects.

Power Supplies

Failures or erratic operation of power supplies subjected to transient radiation conditions is of major concern because of the importance associated with their function in systems. The failure of a power supply obviously subjects all circuits associated with it to various degrees of malfunctioning. In some critical applications, the momentary fluctuation of output voltage or an excess of ripple voltage can drastically affect the operation of other radiation-hardened circuits.

TABLE 33. SUMMARY OF TRANSIENT RADIATION EFFECTS ON THE OPERATION OF VARIOUS ELECTRONIC CIRCUITS

Type of Circuit or Application	Functional Component Part	Transient Radiation Environment: Number of Radiation Pulses	Pulsed Radiation Facility	Gamma Exposure Rate, ergs g^{-1}(C) sec^{-1}	Total Gamma Exposure, ergs g^{-1}(C)	Fast-Neutron Flux Rate, n cm^{-2} sec^{-1}	Total Fast-Neutron Flux, n cm^{-2}	Pulse-Effects Evaluation Parameter	Change in Evaluation Parameter: During Radiation Pulse	Change in Evaluation Parameter: Posttest Effects	Change in Evaluation Parameter: Radiation-Induced Current or Voltage Reported	Reference or Source
Eccles-Jordon multivibrator	4 Type 2N705 transistors	6	Godiva II	--	2727	7×10^{16}	1.1×10^{13}	Output waveform	+5.0%	None	--	46
Flip-flop circuit	2 Type 2N395 transistors	1	Godiva II	--	2727	1×10^{16}	1×10^{12}	Triggering	Triggered	None	--	46
150-v d-c power supply	2N338, 2N539, and 2N575 transistors	4	Godiva II	--	2727	1.4×10^{16}	4.9×10^{12}	Output voltage	-1.4%	Poor regulation	Ripple voltage 1 v	47
250-v d-c power supply	Transistorized	4	Godiva II	--	--	10^{16}	6×10^{12}	Output voltage	0.05 v	0.08 v	Ripple voltage 0.3 mv	48
250-v d-c power supply	Transistorized	1	Godiva II	--	--	10^{16}	5×10^{12}	Output voltage	0.08 v	Unit failed	--	48
70-kc oscillator, TDI Model 1202A	Electron tubes 4 Type 611	--	Linac	1.14×10^{8}	570 per pulse	--	--	Frequency shift	+3%	None	--	48
40-kc oscillator, EMR Model 75B	Electron tubes 2 Type 5840	--	Linac	1.14×10^{5}	570 per pulse	--	--	Frequency shift	<1%	None	--	49
22-kc oscillator, TDI Model 1250A	Transistors 3 Type 2N1139 2 Type 2N495	--	Linac	1.14×10^{8}	570 per pulse	--	--	Frequency shift	-20%	+5%	--	49

TABLE 33. (Continued)

Type of Circuit or Application	Functional Component Part	Number of Radiation Pulses	Transient Radiation Environment: Pulsed Radiation Facility	Transient Radiation Environment: Gamma Exposure Rate, ergs g^{-1}(C) sec^{-1}	Transient Radiation Environment: Total Gamma Exposure, ergs g^{-1}(C)	Transient Radiation Environment: Fast-Neutron Flux Rate, n cm^{-2} sec^{-1}	Transient Radiation Environment: Total Fast-Neutron Flux, n cm^{-2}	Pulse-Effects Evaluation Parameter	Change in Evaluation Parameter: During Radiation Pulse	Change in Evaluation Parameter: Posttest Effects	Radiation-Induced Current or Voltage Reported	Reference or Source
70-kc oscillator, TDI Model 1202A	Electron tubes 4 Type 611	3	Godiva II	3.53×10^{8}	--	5.0×10^{15}	--	Frequency shift	+20%	--	--	49
40-kc oscillator, EMR Model 75B	Electron tubes 2 Type 5840	2	Godiva II	3.80×10^{8}	--	4.97×10^{15}	--	Frequency shift	-4%	--	--	49
22-kc oscillator, TDI Model 1250A	Transistors 3 Type 2N1139 2 Type 2N495	3	Godiva II	3.80×10^{8}	--	5.59×10^{15}	--	Frequency shift	+26%	--	--	49
70-kc oscillator, TDI Model 1202A	Electron tubes 4 Type 611	3	Godiva II	3.53×10^{8}	--	5.0×10^{15}	--	Amplitude shift	-60%	--	--	49
40-kc oscillator, EMR Model 75B	Electron tubes 2 Type 5840	2	Godiva II	3.80×10^{8}	--	4.97×10^{15}	--	Amplitude shift	-40%	--	--	49
22-kc oscillator, TDI Model 1250A	Transistors 3 Type 2N1139 2 Type 2N495	3	Godiva II	3.80×10^{8}	--	5.59×10^{15}	--	Amplitude shift	-90%	--	--	49
70-kc oscillator, TDI Model 1202A	Electron tubes 4 Type 611	--	Linac	1.14×10^{8}	570 per pulse	--	--	Amplitude shift	-10%	--	--	49
40-kc oscillator, EMR Model 75B	Electron tubes 2 Type 5840	--	Linac	1.14×10^{8}	570 per pulse	--	--	Amplitude shift	-7%	--	--	49

TABLE 33. (Continued)

Type of Circuit or Application	Functional Component Part	Number of Radiation Pulses	Transient Radiation Environment: Pulsed Radiation Facility	Transient Radiation Environment: Gamma Exposure Rate, ergs g^{-1}(C) sec^{-1}	Transient Radiation Environment: Total Gamma Exposure, ergs g^{-1}(C)	Transient Radiation Environment: Fast-Neutron Flux Rate, n cm^{-2} sec^{-1}	Transient Radiation Environment: Total Fast-Neutron Flux, n cm^{-2}	Pulse-Effects Evaluation Parameter	Change in Evaluation Parameter: During Radiation Pulse	Change in Evaluation Parameter: Posttest Effects	Change in Evaluation Parameter: Radiation-Induced Current or Voltage Reported	Reference or Source
22-kc oscillator, TDI Model 1250A	Transistors 3 Type 2M1139 2 Type 2N495	--	Linac	1.14×10^8	570 per pulse	--	--	Amplitude shift	-30%	--	--	49
Blocking (6 units) oscillator (multivibrator)	Diodes and transistors 1N137A and 2N904	2	Godiva II	--	--	10^{16}	10^{13} to 10^{12}	Output amplitude	--	-70 to -80%	3 failed at 10^{12} nvt	50
Two-stage instrument amplifier	Transistor 2N43A and 2N952	1	Godiva II	--	--	10^{16}	10^{13}	Amplifier gain	--	-8%	--	50
Low-level servo amplifier	Transistor 3 Type 2N43	1	Godiva II	--	--	10^{16}	10^{13}	Amplifier gain	--	-15%	--	50
Mixer or buffer magnetic amplifier	Diodes 4 Types HD6006	1	Godiva II	--	--	10^{16}	10^{13}	Amplifier gain	--	None	--	50
900 CPS oscillators, 6 units	Transistors 3 Type 2N903	1	Godiva II	--	--	10^{16}	10^{11} and 10^{12}	Operation	--	4 units failed	--	50
Flip-flop circuit	Transistors Type 2N167	1	Godiva II	3×10^3	--	10^{16}	10^{12}	Trigger	Fast trigger	Failed	--	6

TABLE 33. (Continued)

Type of Circuit or Application	Functional Component Part	Number of Radiation Pulses	Transient Radiation Environment						Change in Evaluation Parameter			Reference or Source
			Pulsed Radiation Facility	Gamma Exposure Rate, ergs g^{-1}(C) sec^{-1}	Total Gamma Exposure, ergs g^{-1}(C)	Fast-Neutron Flux Rate, n cm^{-2} sec^{-1}	Total Fast-Neutron Flux, n cm^{-2}	Pulse-Effects Evaluation Parameter	During Radiation Pulse	Posttest Effects	Radiation-Induced Current or Voltage Reported	
EMR voltage controlled oscillator Model 75B, 2 units	Electron tubes Types 5840, 5718, 5719 (40KC)	3	Triga	8.7×10^8	--	10^{15}	3.5×10^{12}	Center frequency shift	+0.93 to -0.6%, +3.1 to -2.1 FBW	--	--	51
Ditto	Ditto (70KC)	--	Triga	8.7×10^8	--	10^{15}	3.5×10^{12}	Center frequency shift	+0.4 to -0.45%, +1.6 to -1.5 FBW	--	--	51
150-volt power supply	Transistors 1 Type 2N498 3 Type 2N575A	4	Godiva II	--	--	10^{16}	0.8 to 5 x 10^{12}	Output voltage	-0.05 to 2.0 v	--	560-mv ripple at 110 v ac	52

Power supplies can be affected in several ways depending on whether their main functional components are transistors or electron tubes. Most concern is indicated for malfunctions such as increased ripple voltage, poor voltage regulation, increase or decrease in voltages during the pulse of radiation, and subsequent permanent damage. The most common effects are the increases in ripple voltage which have been measured[47] and found to exceed 1 volt. These conditions are often accompanied with indications of poor regulation for irradiated power supplies that have been tested in the postradiation state throughout their load range. In some instances the irradiated power supply tends to display considerable ripple, with reduction in line voltage within the unit's specified limits. Increases in line voltage to these irradiated units seem to correct the condition of excessive ripple, and for this reason it is believed that the regulation portion of the circuit may be susceptible to radiation damage. In regard to circuit component parts, Table 33 summarizes transistorized power supplies only because results for electron-tube-type power supplies are not available.

Amplifiers

Of major interest in transient radiation effects on amplifiers is whether radiation-induced currents or voltages at the amplifier input will cause an amplified effect at the output portion of the circuit. To investigate this mechanism of damage, researchers have exposed single-stage amplifiers[27] to radiation pulses from a linear accelerator while observing the effects on the output portion of the circuit. In this particular program, the effects of coatings were explored to determine whether such applications would effect appreciable improvement in operation of the amplifiers in a radiation environment. The single-stage amplifiers employing electron tubes showed some improvement (shown in Table 33), whereas the transistorized amplifier seemed to increase in amplified signals for the sprayed unit. Posttest measurements indicate that radiation pulses in intensities encountered at the Godiva II critical assembly caused some transistorized amplifiers to decrease in gain. It was believed that the main cause for this occurrence is degradation of the transistors.

Conclusions

Both theoretical and experimental studies of radiation effects on circuits have indicated that the designer must consider two types of transient radiation effects when designing circuits that will be required to function in a pulse radiation environment. The first type can be designated as a noise transient which may appear as a voltage or current pulse induced in the circuit by ionization and/or displacements. This effect tends to affect operating characteristics by changing leakage conditions of insulating materials and ultimately changing circuit impedances. The second effect is related to changes in component-part characteristics which cause a transient distortion of the normal circuit signals. The initial approach to selecting and designing a circuit for application in a nuclear environment must include the study of component-part radiation-damage susceptibility. This is necessary because, in the mathematical analysis of a circuit, transient radiation effects are introduced as radiation-induced parameters into network equations in accordance with the mechanisms involved.

Changes in properties of circuit components influence time-dependency characteristics in the circuit parameters. External leakages associated with ionization effects

become parallel components in the equivalent-circuit configuration during the circuit analysis. Charge injection and scattering have been treated as current and voltage generators, thus influencing the circuit-analysis equations as though the effects were additional driving-force terms. Obviously, these transient effects are important only during the finite time interval covering a period slightly longer than the radiation burst.

Some general concepts and insight have evolved from theoretical analysis and experimental results. For example, circuits involving high impedances are generally more susceptible to transient effects than low-impedance circuits. This has been substantiated in experiments where circuits identical in all respects with the exception of impedance were tested and it was found that the low-impedance circuits were least affected. The use of high-gain circuits in preference to multiple low-gain circuits, frequently considered for miniaturization reasons, should be avoided where possible. This is suggested because high-gain circuits and high impedance go hand-in-hand. Conditions conducive to ionization should be recognized and attempts made to either avoid the condition or reduce it by application of coatings.

REFERENCES

(1) van Lint, V.A.J., "Mechanisms of Transient Radiation Effects State of the Art", General Atomic Report GA-2886, January, 1962.

(2) Easley, J. W., and Blair, R. R., "Transient Phenomena in Semiconductor Devices", Appendix E to Nuclear Electronic Effects Program, Third Triannual Technical Note, WADC TN 60-160, March 15, 1960.

(3) Brown, W. L., and Easley, J. W., "The Transient Ionization Pulse in a Semiconductor Junction", paper presented at the Conference on Pulse Radiation Testing, Kirtland Air Force Base, New Mexico, September, 1960.

(4) van Lint, V.A.J., "Transient Radiation Effects-Physics and Tests", General Atomic Report GA-1827, November 1960.

(5) van Lint, V.A.J., "Transient Radiation Effects in Semiconductors", Proceedings of the Second AGET Conference on Nuclear Radiation Effects on Semiconductors, September, 1959.

(6) IBM Radiation Research Group, "Some Effects of Pulsed Neutron Radiation on Electrical Components-I", October 9, 1958.

(7) IBM Radiation Research Group, "Burst Radiation Effects on Semiconductor Components", March 12, 1958.

(8) Bohan, W. A., Maxey, J. D., and Pecoraro, R. P., "Semiconductor Device Operation in a Pulsed Nuclear Environment", presented at the National Telemetering Conference, May, 1959.

(9) Sauer, S., "A Study of Radiation Effects on Electronic Devices", Edgerton, Germeshausen, & Grier, Boston, Massachusetts (December 14, 1959), Second Interim Report, Part I, September 1, 1959, to November 30, 1959.

(10) Denny, J. M., "Pulsed Neutron Irradiation of Electronic Components", Hughes Aircraft Company Technical Memorandum No. 522, July 16, 1958.

(11) "Some Effects of Pulsed Neutron Radiation on Electronic Components. 2. Result of August 1958 Godiva Test Series", International Business Machines Corporation, Military Products Division, Owego, New York (no date given).

(12) Bohan, W. A., "Effects of Pulsed X-ray Radiation on Semiconductor Devices", IBM Radiation Research Group (no date given).

(13) Steele, H. L., "Effects of Continuous Gamma Ray or Pulsed Neutron Radiation on Semiconductor Diodes", Boeing Airplane Company Document No. D2-2123, December 2, 1958.

(14) IBM Radiation Research Group, "Pulsed Effects on Electronic Components", Second Triannual Report under Contract AF 33(600)-40462, October 31, 1960.

(15) Perkins, C. W., Denny, J. M., and Downing, R. G., "Second Experiment on Pulsed Neutron Radiation Effects", Hughes Aircraft Company Technical Memorandum No. 622, September, 1959.

(16) Perkins, C. W., Denny, J..M., and Downing, R. G., "Third Experiment on Pulsed Neutron Radiation Effects", Hughes Aircraft Company Technical Memorandum No. 623, October, 1959.

(17) Berger, A. G., "Transient Radiation Effects on Electronics-Part 1", Boeing Report D2-7899, January, 1961.

(18) Caldwell, R. S., "Transient Radiation Effects to Electronic Parts and Materials" Vol. 2, Sec. 3, Boeing Report D2-6594, February, 1961.

(19) Degenhart, H. J., and Long, A. L., "Transient Effects of Pulse Radiation on Electronic Parts", U.S. Army Signal Research and Development Laboratory, Fort Monmouth, New Jersey, October 6, 1958.

(20) Long, A. L., "Nuclear Radiation Induced Voltages in Coaxial Cables", U.S. Army Signal Research and Development Laboratory, Fort Monmouth, New Jersey, Technical Memorandum, August 12, 1960.

(21) "Pulsed Radiation Effects on Electronic Components", Third Triannual Report under Contract AF 33(600)-40462, International Business Machines Corporation, Federal Systems Division, Space Guidance Center, Owego, New York, February 28, 1961.

(22) "Pulsed Radiation Effects on Electronic Components", Fourth Triannual Report under Contract AF 33(600)-40462, International Business Machines Corporation, Federal Systems Division, Space Guidance Center, Owego, New York, 31 October, 1961.

(23) Conrad, E., Personal Communication, Diamond Ordnance Fuze Laboratory, Washington, D. C.

(24) "Some Effects of Pulsed Radiation on Electronic Components III, Results of January, 1959, Godiva Test Series", International Business Machines Corporation Federal Systems Division, Owego, New York.

(25) Schlosser, W., "Report on Radiation Effects Studies, Godiva Exposure IV, 27 and 28 August 1959, U.S. Army Signal Research and Development Laboratory, Fort Monmouth, New Jersey, October 27, 1959.

(26) "Some Effects of Pulsed Neutron Radiation on Electronic Components", Final Report, International Business Machines Corporation, Federal Systems Division, Owego, New York, January, 1960.

(27) Perkins, C. W., et al., "First Experiments on the Effects of Radiation Pulses on Electronic Circuits and Components", Hughes Aircraft Company, Research Laboratories, February 3, 1958.

(28) Markow, D., Degenhart, H. J., and Murphy, H. M., Jr., "Effects of Mixed Neutron-Gamma Pulses on Electronic Components", U.S. Army Signal Research and Development Laboratory, Fort Monmouth, New Jersey, September 30, 1959.

(29) "Pulsed Radiation Effects on Electronic Components, First Triannual Report", International Business Machines Corporation, Federal System Division, Owego, New York, July 20, 1960.

(30) Wicklein, H. W., and Dickhaut, R. H., "Transient Radiation Effects in Capacitors and Dielectric Materials", The Boeing Company, Seattle, Washington.

(31) Wicklein, H. W., Spencer, W. E., Sandifer, C. W., "Transient Radiation Effects on Electronics, Part 1", Kukla Transient Radiation Test, Appendix III, The Boeing Company, Seattle, Washington, January, 1961.

(32) Wicklein, H. W., Personal Communication, The Boeing Company, Seattle, Washington.

(33) Schaefer, D. L., "The Effects of Nuclear Radiation on the Performance of the Image Orthicon Television Camera Tube", General Electric Company, January 29, 1961.

(34) Chandler, H. G., "Effects of Pulsed Nuclear Radiation on Nonoperating Tubes and Transistors", Diamond Ordnance Fuze Laboratories, Department of the Army, Washington, D. C., November 20, 1959.

(35) Saelens, R. G., "Radiation Effects on Ceramic Electron Tube Types at Godiva II Facility", U.S. Army Signal Research and Development Laboratory, Fort Monmouth, New Jersey, March 17, 1959.

(36) Kothstein, T. F., "Nuclear Pulse Testing of Viokon and Image Orthicon Camera Heads", Frankford Arsenal, U.S. Army Ordnance, Philadelphia 37, Pennsylvania, October, 1961.

(37) Hammond, D. L., "Effects of Radiation on Quartz Crystal Units", Signal Corps Engineering Laboratories, Fort Monmouth, New Jersey, Technical Memorandum No. M-1785, June 25, 1956.

(38) Stanley, J. M., "Effects of Nuclear Radiation on Quartz Crystals", U.S. Army Signal Research and Development Laboratory, Fort Monmouth, New Jersey, Memorandum Report No. FCD-M-33-58, November 17, 1958.

(39) Reid, F. J., and Moody, J. W., "The Effect of Nuclear Radiation on Magnetic Materials", Battelle Memorial Institute, Columbus, Ohio, REIC Technical Memorandum No. 12, December 31, 1958.

(40) "Study of Effect of High-Intensity Pulsed Nuclear Radiation on Electronic Parts and Materials (SCORRE)", Report No. 1, Signal Corps Contract Number AD-36-039-SC-85395, Department of the Army Project No. DA-3G-93-01-001-01, First Quarterly Report, 1 July 1960 to 30 September 1960, for the U.S. Army Signal Research and Development Laboratory, Fort Monmouth, New Jersey, International Business Machines Corporation, Federal Systems Division, Owego, New York.

(41) "Study of Effect of High-Intensity Pulsed Nuclear Radiation on Electronic Parts and Materials (SCORRE)", Report No. 2, Signal Corps Contract Number AD-36-039-SC-85395, Department of the Army Project No. DA-3G-93-01-001-01, Second Quarterly Report, 1 January 1961 to 31 March 1961, for the U.S. Army Signal Research and Development Laboratory, Fort Monmouth, New Jersey, International Business Machines Corporation, Federal Systems Division, Owego, New York.

(42) "Study of Effect of High-Intensity Pulsed Nuclear Radiation on Electronic Parts and Materials (SCORRE)", Report No. 3, Signal Corps Contract Number AD-36-039-SC-85395, Department of the Army Project No. DA-3G-93-01-001-01, Third Quarterly Report, 1 January 1961 to 31 March 1961, for the U.S. Army Signal Research and Development Laboratory, Fort Monmouth, New Jersey, International Business Machines Corporation, Federal Systems Division, Owego, New York.

(43) "Study of Effect of High-Intensity Pulsed Nuclear Radiation on Electronic Parts and Materials (SCORRE)", Report No. 4, Signal Corps Contract Number AD-36-039-SC-85395, Department of the Army Project No. DA-3G-93-01-001-01, Fourth Quarterly Progress Report, 1 April 1961 to 30 June 1961, for the U.S. Army Signal Research and Development Laboratory, Fort Monmouth, New Jersey, International Business Machines Corporation, Federal Systems Division, Owego, New York.

(44) Pfaff, E. R., and Shelton, R. D., "Effects of Nuclear Radiation on Electronic Components", Admiral Corporation, WADC TR-57-361, Part 2, AF 33(616)-3091, ASTIA, AD 155790, August, 1958.

(45) Hansen, J. F., and Cary, H., "Final Report on the Effects of Gamma-Induced Ionization on the Electrical Properties of Printed Circuits and Connectors", to Chance Vought Aircraft from Battelle Memorial Institute, March 5, 1959.

(46) Almond, H. B., and Spencer, W. E., "Nuclear Radiation Tests of Minuteman Flip-Flop Circuit at the Godiva II Facility", Los Alamos, New Mexico, Technical Memorandum No. 5-7870-7839 (BRC 11770) 9 September 1959.

(47) Almond, H. B., and Spencer, W. E., "Preliminary Data from Nuclear Radiation Tests of the PS-210 Power Supply", Technical Memorandum No. 5-7870-7739 (BRC 11769), 30 July 1959.

(48) Almond, H. B., and Perkins, L. C., "Radiation Damage Tests on P.S. 223 Transistorized 250 Volt Regulated Power Supply", Technical Memorandum No. PAS-APS-5/0146 (BRC 11771), 23 January 1959.

(49) Perkins, C. W., "Effect of Radiation on Ordnance Missile Components", for Diamond Fuze Ordnance Laboratories, Hughes Aircraft Company (BRC 13497), December 1960.

(50) Behrens, R. G., "Effects of Fast Neutrons on Circuitry Employing Semiconductor Devices", for Boeing Airplane Company, Seattle, Washington, Document No. D5-2245 (BRC 11892), 5 November 1957.

(51) Oertel, M. F., and Ashwood, C. R., "Performance of EMR Voltage-Controlled Oscillator Units in a Nuclear Environment", Technical Report No. 849, Diamond Ordnance Fuze Laboratories (BRC 12668) , 29 July 1960.

(52) Vassilakos, D., "Radiation Test on the PS 210 Transistorized 150 Volt Regulated Power Supply", Document No. D5-5851, Boeing Airplane Company, Seattle, Washington, Contract No. AF 33(600)-35030 (BRC 11746), 14 October 1959.

(53) Stralser, B. J., "First Experiment on Transient Effects of Nuclear Radiation of Electronic Parts and Circuits", U.S. Navy Electronics Laboratory, San Diego, California, Technical Memorandum No. TM-301 (BRC 12851), 9 September 1958.

(54) Bell, J. E., and Walker, K. R., "Theoretical Study of Burst Introduced Transient Radiation Effects in Basic Electronic Circuits", for the Air Force Special Weapons Center, Air Research and Development Command, Kirkland Air Force Base, New Mexico, Final Report, Hughes Aircraft Company (BRC 14963), 15 May 1961.

DCJ/FJR/WEC/DJH/ENW:mjd

LIST OF AVAILABLE REIC PUBLICATIONS

Radiation Effects Information Center
Battelle Memorial Institute
Columbus 1, Ohio

Requests for unclassified information or unclassified REIC published reports and memoranda should be sent:	Requests for classified REIC published reports and memoranda should be sent, via your contracting officer for endorsement, to the following address:
Radiation Effects Information Center Battelle Memorial Institute 505 King Avenue Columbus 1, Ohio Attention E. N. Wyler	ASD (ASTEVC, Mr. Robert G. Merkle) Wright-Patterson AFB, Ohio

Unclassified Reports

Report Number	Title
1	The Effect of Nuclear Radiation on Semiconductor Materials (December 20, 1957), AD 147399
1 (First Addendum)	The Effect of Nuclear Radiation on Semiconductor Materials (March 31, 1959), AD 210758
*6	A Survey of Current Research and Developments in the Field of Dosimetry (May 31, 1958), AD 157172
6 (First Addendum)	A Survey of Current Research and Developments in the Field of Dosimetry (March 31, 1959), AD 210766
10	The Effect of Nuclear Radiation on Semiconductor Devices (April 30, 1960), AD 240433 (Supersedes Memos Nos. 4, 5, 6)
10 (First Addendum	The Effect of Nuclear Radiation on Semiconductor Devices (July 15, 1961), AD 262081
16	Survey of Irradiation Facilities (February 28, 1961), AD 256953
17	The Effect of Nuclear Radiation on Structural Adhesives (March 1, 1961), AD 256954 (Supersedes Reports Nos. 7 and 11)
18	The Effect of Nuclear Radiation on Electronic Components (June 1, 1961), AD 260303 (Supersedes Reports Nos. 2, 8, 12, 14, and 15 and Memos Nos. 2, 7, 12, 14, and 20)
19	The Effect of Nuclear Radiation on Lubricants and Hydraulic Fluids (May 31, 1961), AD 261278 (Supersedes Report No. 4)
20	The Effect of Nuclear Radiation on Structural Metals (September 15, 1961), AD 265839 (Supersedes Report No. 5)
21	The Effect of Nuclear Radiation on Elastomeric and Plastic Components and Materials (September 1, 1961) AD 267890 (Supersedes Reports Nos. 3, 9, and 13 and Memos Nos. 1, 3, 8, 13, and 17)
23	Proton and Electron Damage to Solar Cells (April 1, 1962)
24	Radiation Effects State of the Art 1961-1962 (June 30, 1962), NASA N62-16454

*Out of Print in REIC; Available only from ASTIA, Armed Services Technical Information Agency, Document Service Center, Arlington Hall Station, Arlington, Virginia.

Classified Reports

Report Number	Title
1-C	The Effect of Nuclear Radiation on Hydraulic, Pneumatic, and Mechanical Systems for Subsonic, Transonic, and Low-Supersonic Speed Aircraft (Title Unclassified) (Secret, Restricted Data) (May 31, 1958)
1-C (First Addendum)	The Effect of Nuclear Radiation on Hydraulic, Pneumatic, and Mechanical Systems for Subsonic, Transonic, and Low-Supersonic Speed Aircraft (Title Unclassified) (Secret, Restricted Data) (March 31, 1959)
1-C (Second Addendum)	The Effect of Nuclear Radiation on Hydraulic, Pneumatic, and Mechanical Systems (Title Unclassified) (Secret, Restricted Data) (September 15, 1960)
2-C	The Effect of Nuclear Radiation on Ceramic Materials (Title Unclassified) (Secret) (June 30, 1959), AD 157173
2-C (First Addendum)	The Effect of Nuclear Radiation on Ceramic Materials (Title Unclassified) (Secret, Restricted Data) (June 15, 1961)
4-C	The Effect of Nuclear Radiation on Electrical and Electronic Systems (Title Unclassified) (Secret, Restricted Data) (March 15, 1960).
6-C	The Effects of Nuclear Weapon Bursts and Simulated Bursts on Electronic Components (Title Unclassified) (Secret, Restricted Data) (May 31, 1961)

Unclassified Memoranda

Memorandum Number	Title
*9	The Effect of Nuclear Radiation on Glass (November 30, 1958), AD 207701
10	Format for Reporting Radiation Effects Data (May 15, 1959), AD 218251
*11	The Effect of Nuclear Radiation on Hydrocarbon Fuels (November 30, 1958), AD 207702
*15	The Effect of Nuclear Radiation on Hoses and Couplings (March 31, 1959), AD 225504
*16	The Effect of Nuclear Radiation on Refrigerants (June 30, 1959), AD 219510
*18	The Effect of Nuclear Radiation on the Performance of a Hydraulic Flight Control System (June 15, 1959), AD 219512
21	Space Radiation and Its Effects on Materials (June 30, 1961)
23	Radiation Dosimetry: An Annotated Bibliography (September 15, 1961), AD 265523

Classified Memoranda

Memorandum Number	Title
1-C	The Effects of Nuclear Radiation on Fluorolubes and Other Gyroscope Fluids (Title Unclassified) (Secret) (September 5, 1958), AD 302126
2-C	The Effect of Nuclear Radiation on Explosives and Solid Propellants (Title Unclassified) (Secret, Restricted Data) (June 15, 1959)

*Out of Print in REIC; Available only from ASTIA, Armed Services Technical Information Agency, Document Service Center, Arlington Hall Station, Arlington, Virginia.

Memorandum Number	Title
3-C	Dose-Rate Effects on Materials, Components, and Systems (Title Unclassified) (Secret, Restricted Data) (July 31, 1959)
10-C	Nuclear Radiation Effects Projects (Title Unclassified) (Confidential) (March 31, 1962)